To the Graduate Council:

I am submitting herewith a thesis written by K. K. Khan entitled "Effects of Postweld Heat Treatment on the Elevated Temperature Properties of 2 1/4Cr-1Mo Weldments." I have examined the final copy of this thesis for form and content and recommend that it be accepted in partial fulfillment of the requirement for the degree of Master of Science, with a major in Metallurgical Engineering.

Carl D. Lundin, Major Professor

We have read this thesis
and recommend its acceptance:

Charlie R. Brooks

Joseph C. Manko

Accepted for the Council

Vice Provost
and Dean of the Graduate School

EFFECTS OF POSTWELD HEAT TREATMENT ON THE ELEVATED TEMPERATURE PROPERTIES OF 2 1/4Cr-1Mo WELDMENTS

A Thesis

Presented for the

Master of Science

Degree

The University of Tennessee, Knoxville

K. K. Khan

December 1988

DEDICATION

This thesis is dedicated to my wife and parents.

ACKNOWLEDGEMENTS

The author would like to express his acknowledgement to his major advisor, Dr. Carl D. Lundin, for his patience and guidance throughout the course of this study. Deep gratitude is also extended to Dr. John Dunlap of the EM Facility for his kind help for the TEM/STEM study.

The author wishes to express his appreciation to the Pressure Vessel Research Committee of the Welding Research Council for financial support to conduct this investigation. Appreciation is also extended to Teledyne McKay for donating electrodes for this study.

Last but not the least, the author also wishes to thank his fellow graduate students of the Welding Research Group for their support and Mr. M. Neal, Mr. B. McGill, Mr. A. Carter and Mrs. A. Cagle, for their contribution to the success of this work.

ABSTRACT

2 1/4Cr-1Mo steels have been used in power and chemical plants for elevated temperature high pressure components since the 1930's. Recent concerns involving submerged arc (SA) and shielded metal arc (SMA) welded steam piping during service have resulted in the inception of this study. Since welded piping may be either annealed and tempered (A&T), normalized and tempered (N&T) or subcritically postweld heat treated (PWHT), the aim of this study was the determination of the elevated temperature properties of 2 1/4Cr-1Mo weldments subjected to these heat treatments after welding.

The SA weldment fabricated for this study had a difference of chromium content (0.62%) between the base metal (2.07%) and weld metal (2.69%). The significance of this chromium difference was investigated in addition to the determination of stress rupture properties in the different heat treated conditions. Another part of this study sought to evaluate the effect of the severity of tempering on the creep strength of SMA 2 1/4Cr-1Mo weld metal.

After heat treatment a "soft" carbon denuded ferritic region was found along the fusion line in the HAZ of the SA weldment because of carbon migration from the base metal to the weld metal driven by elemental differences (especially Cr) during heat treatment. This region was found to be widest for the A&T material followed by N&T and only a grain wide when PWHT(Cl.2). Hardness measurements on A&T specimens revealed a hardness approximately 35 DPH lower in the

"soft" zone compared to the adjacent enriched zone. The soft zone was found to be 15 DPH softer than base metal and 10 DPH softer than the weld metal remote from the fusion line.

SA weldment stress rupture and tensile tests conducted at 950 and 1050°F on all-weld metal specimens extracted parallel to the welding direction and composite specimens (base metal-HAZ-weld metal) extracted transverse to the welding direction revealed that none of the specimens ruptured in the "soft" zone. All transverse tensile specimens ruptured in the weld metal. Transverse creep specimens ruptured in the weld metal in N&T condition and in the base metal in the PWHT(Cl.2) condition. Transverse stress rupture specimens in the A&T condition ruptured in the weld metal at 950°F, base metal at 1050°F and in the weld metal at temperatures of 1150 and 1225°F. Creep rupture testing of specimens from the SA weldment reveals superior creep properties in N&T condition when tested at 950°F and in A&T condition when tested at 1050°F.

Stress rupture and tensile testing of the SMA weldment indicates that the strength decreases with an increase in the temper parameter. Characterization of microstructure using analytical techniques indicated that stability of M_2C type carbides in the various microconstituents (ferrite, bainite) dictate the elevated temperature properties of the weld metal. Microscopy of the "soft" ferrite band revealed presence of fine M_2C type carbides. This "soft" ferritic region is strengthened by fine acicular M_2C carbides along with interactive solid solution hardening effect of molybdenum in ferrite. In addition, adjacent regions which are stronger than

the soft zone exert a constraint effect thereby preventing rupture. Thus, the zone did not contribute to creep failure. A carbide evolution sequence in the weld metal due to tempering or service exposure has been determined from this study.

TABLE OF CONTENT

LIST OF FIGURES

FIGURE PAGE

FIGURE PAGE

FIGURE PAGE

LIST OF TABLES

CHAPTER 1

INTRODUCTION

1.1 HISTORY AND APPLICATIONS

For many years there has been a steady upward trend both in the operating pressures of vessels and in the material strength requirements for heavy equipment. A low alloy steel that fulfills these requirements is a ferritic steel with a nominal composition of 2.25% chromium, 1% molybdenum and 0.1% carbon. This steel has been in widespread use in fossil fired power plants, in the fabrication of pressure vessels and boiler piping since the 1930's.[1-7] This steel is also considered for liquid metal fast breeder reactors (LMFBR), steam generators and hydrocrackers.[1,6,7]

2 1/4Cr-1Mo steel is noted for its excellent high temperature strength (imparted by molybdenum), oxidation resistance (imparted by chromium) and microstructural stability in service. Therefore, it has been used for applications at elevated temperatures.[3] In addition, because of its resistance to hydrogen attack at elevated temperature, it has found application in hydrocrackers.[8] The excellent weldability is due to a low carbon content and this characteristic has enhanced its popularity because of the relative ease of fabrication and installation.[9]

1.2 MECHANICAL PROPERTIES

2 1/4Cr-1Mo steel is used in different heat treated conditions to meet various requirements of strength, ductility and fracture toughness. The nominal composition of 2 1/4Cr-1Mo steel is shown in Table 1. In the annealed(A) condition the tensile strength is typically about 75 KSI at room temperature and 40 KSI at about 1100°F.[10] The elongation is of the order of about 35 percent in a 2 inch gage length with the reduction in area about 65 percent at both room temperature and 1100°F. In the normalized and tempered(N&T) condition the tensile strength is typically 85 KSI at room temperature and 65 KSI at 1100°F. Creep rupture strength of the alloy is about 10 KSI at 1100°F for a rupture life of 100,000 hours.[10] Thus it can be seen that this alloy has excellent strength at elevated temperatures, second to austenitic stainless steels above 1050°F.

The properties of 2 1/4Cr-1Mo steel depend on the microstructure which is different for annealed and normalized and tempered treatments. The extremes in microstructural differences is such that the normalized steel may be entirely bainitic whereas the annealed steel will exhibit 75 to 80 percent proeutectoid ferrite and the balance bainite.[1] Therefore a wide range of properties can be obtained by choosing appropriate heat treatment. Currently, various ASTM specifications permit a range of room temperature tensile strengths from 60 to 135 KSI:[11]

A-387 Grade D (A) - 60 KSI min. tensile strength

A-387 Grade D (N&T) - 75 KSI min. tensile strength

Table 1. Nominal composition of 2 1/4Cr-1Mo steel as per ASTM specifications.

ELEMENTS	WEIGHT%
CARBON	0.15 MAX
SILICON	0.30-0.60
CHROMIUM	1.90-2.60
MOLYBDENUM	0.87-1.13
SULFUR	0.030 MAX
PHOSPHORUS	0.030 MAX

A-542 Class 4 - 85 KSI min. tensile strength

A-542 Class 3 - 95 KSI min. tensile strength

A-542 Class 1 - 105 KSI min. tensile strength

A-542 Class 2 - 115 KSI min. tensile strength

There exists a good correlation between the elevated temperature tensile strength and the room temperature tensile strength of this material as shown in figure 1. A similar correlation also exists for the creep rupture strength and is illustrated in Figures 2 and 3. However, it can be seen that the correlations tend to become less definitive at higher temperatures.[11]

1.3 CREEP PROPERTIES OF 2 1/4CR-1MO STEEL

"Creep" is the term given to a type of plastic flow, namely the continued change in dimensions as a function of time, that results from a particular condition of deformation, ie., under conditions of sustained stress (or load).[13] To understand creep in 2 1/4Cr-1Mo steel it is first necessary to comprehend creep mechanisms operating in polycrystalline materials.

Flow characteristics of a material under creep conditions will depend on three variables: the initial microstructural condition, the conditions of deformation and the entire thermal/mechanical history.[13] The requirements of a material entering elevated temperature service can be best described by the following features;[14,15,17]

(1) Deformation resistance,

(2) Fracture resistance,

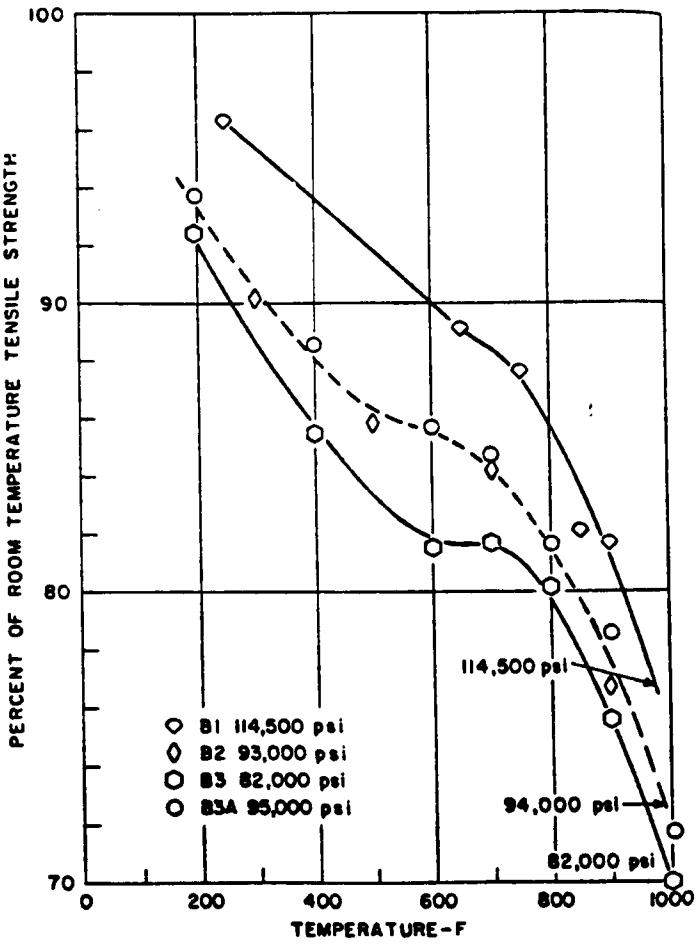

Figure 1. Change in tensile strength with temperature of 2 1/4Cr-1Mo steel as influenced by initial room temperature tensile strength.

Source: Emmanuel, G.N., Leyda, W.E. and Rozic, E.J., "Versatility of 2 1/4Cr1Mo as a Pressure Vessel Material," Symposium on 2-1/4 Chrome 1 Molybdenum Steel in Pressure Vessels and Piping, ASME-Mpc, Denver, CO, 1970, pp. 78 - 122.

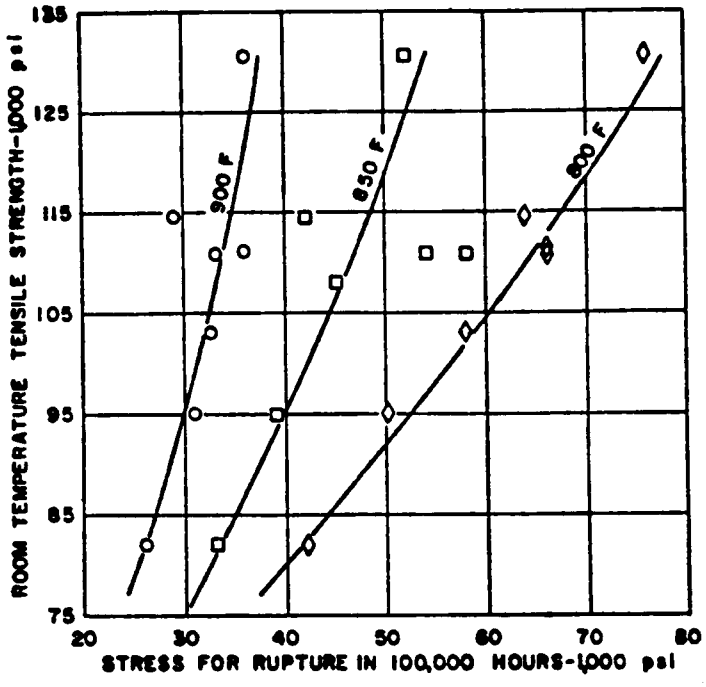

Figure 2. Effect of room temperature tensile strength of 2.25Cr-1Mo steel on stress to cause rupture in 100,000 hours.

Source: Emmanuel, G.N., Leyda, W.E. and Rozic, E.J., "Versatility of 2 1/4Cr1Mo as a Pressure Vessel Material," Symposium on 2-1/4 Chrome 1 Molybdenum Steel in Pressure Vessels and Piping, ASME-Mpc, Denver, CO, 1970, pp. 78 - 122.

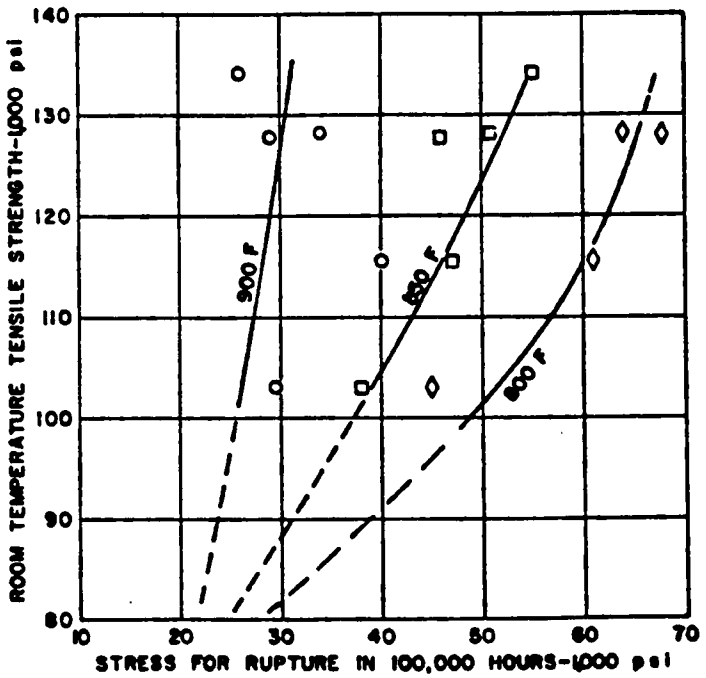

Figure 3. Effect of room temperature tensile strength of 2 1/4Cr-1Mo weld metal on the stress to cause rupture in 100,000 hours.

Source: Emmanuel, G.N., Leyda, W.E. and Rozic, E.J., "Versatility of 2 1/4Cr1Mo as a Pressure Vessel Material," Symposium on 2-1/4 Chrome 1 Molybdenum Steel in Pressure Vessels and Piping, ASME-Mpc, Denver, CO, 1970, pp. 78 - 122.

(3) Recovery resistance and

(4) Microstructural stability.

At elevated temperatures grain boundaries are less resistant to shear stresses. The sliding of grain boundaries permits relaxation of stresses within the grains. Suitable alloying by addition of solute elements which will be adsorbed or segregated at grain boundaries can overcome this. Also the grain boundary sliding can be prevented by the precipitation of particles which will "pin" the boundaries. It is important to do this in such a manner that the boundaries can flow locally to permit stress relaxation but that long range boundary shear is prevented. In addition to boundary sliding, boundary migration also plays an important part in creep. Migration of boundaries reduces strain hardening. This migration leads to softening and recovery and reduces the strength. A fine dispersion of particles within the grain can prevent migration of grain boundaries and the associated loss of strength.[14]

The creep resistance of material is also increased by solid solution strengthening of the grain interiors. The mechanisms which contribute to this effect are:

(1) Reduction in dislocation mobilities,

(2) "Pinning" of dislocations by solute "atmospheres" and

(3) The stabilization of dislocation arrays by inhibiting climb and recovery.

The strengthening process by the solid solution mechanism is limited by the extent of solid solubility. Also, small additions of solute elements is usually sufficient to decorate dislocations

completely by solute atmospheres. Addition of alloying elements above a critical value usually have little or no further effect on the strength.

As discussed earlier, grain boundary sliding and migration can be prevented by having a fine dispersion of particles at the grain boundaries and within the grains. Hence, the size, distribution, volume fraction as well as the degree of coherency of the particles or carbides, all effect the creep resistance of the material. In addition, at elevated temperatures the stability of the precipitates in terms of size, composition and distribution are affected. The control of structure to produce the highest creep resistance is hence, a matter of balancing the composition of both the precipitates and the matrix so that it is possible to obtain the optimum size and distribution of particles and the maximum degree of stability.

In 2 1/4Cr-1Mo steel the creep strength is obtained by solid solution strengthening effects of chromium and molybdenum and dispersion strengthening effects of carbide particles at grain boundaries as well as in the grains. Various types of metastable carbide phases are formed in 2 1/4Cr-1Mo steels and their stability is dictated by diffusion and strain controlled processes. The number and type of carbides as well as their size and distribution change with time as the alloy approaches equilibrium which is controlled by the diffusivity of the solute atoms.[14,15] Since the diffusivity of these large solute atoms is slow, the approach to the equilibrium phase is very slow. The identity of the individual phases found in 2

1/4Cr-1Mo steel and their effect on the creep strength of this alloy will be described in details in the following chapter.

1.4 STRENGTHENING MECHANISMS

In order to function at elevated temperature, alloys to be used in components and structures must be resistant to creep deformation in order to avoid failure. As described in the previous section, conditions must be created in the microstructure to resist deformation which occurs by dislocations motion.

Low alloy ferritic steels are strengthened essentially by carbide dispersion. The most important factor in the interaction between a carbide particle and a dislocation is the presence of stress field surrounding the precipitate particle. As proposed by Orowan[16] dislocations bend in the form of expanding loops around the precipitate particles. When adjacent loops intersect the particle from the other side they cancel leaving a dislocation ring surrounding the particle, the stress field of which increases the resistance to the motion of the next dislocation.

The microstructure of 2 1/4Cr-1Mo steel consists essentially of either a mixture of ferrite and bainite or is completely bainite. Baker and Nutting[18] have examined tempering reactions and found that a number of metastable carbides can be formed depending on the combination of time at temperature during postweld heat treatment or elevated temperature service. During normalizing or annealing heat treatments the reactions involving precipitation of carbides are incomplete and leave the ferrite matrix supersaturated with respect

to chromium and molybdenum concentrations. The presence of solutes, supersaturated in ferrite matrix, have a strong influence on both the tensile and creep strengths of 2 1/4Cr-1Mo steels. The solutes (Cr, Mo) have a strong affinity for carbon and forms M-C or M-C-M type solute atmospheres and decorate the dislocations, and this leads to an interactive type solid solution strengthening in these steels.

1.5 AVAILABILITY

2 1/4Cr-1Mo steel is available in a variety of shapes, strength level and prior heat treatment as per the ASTM specifications: A 213 Grade T22 for tubing; A 387 Grade D and A 542 for plate; A 336 Grade F22 for drum forgings; A 335 Grade P22 for pipe; A 356 Grade 10 and A 217 Grade WC9 for castings. 2 1/4Cr-1Mo steel is receiving widespread use in the power generation industry in normalized and tempered condition. For liquid metal fast breeder reactor steam generators this steel is used in annealed or isothermally annealed condition extensively because of its attractive properties at low cost.

1.6 SCOPE OF THIS WORK

Today, power plant design is based on achieving highest efficiency possible. Thermodynamically, the efficiency depends on the differences between the operating temperature and the ambient temperature. So, it is always attractive to operate at the highest temperature possible. Since 1930, when the all welded steam drum was successfully manufactured, welding has been the principle means of

fabricating critical pressure parts for service at elevated temperatures and pressures. This ability to economically create sound metallurgical bonds between thick-walled pressure vessel plates has permitted design and operation of boilers and other pressure parts at increasingly higher temperatures and pressures, thereby dramatically improving the efficiency of energy systems.

Traditionally, designers of welded power plant equipments and pressure vessels have assumed weld metals to possess properties similar to those of the respective wrought, forged or cast material it was being used to join. This assumption has been given implicit expression in the ASME Boiler Code, in which there is no demonstration of the adequacy of welded joints for high temperature service. This has resulted in no systematic efforts to evaluate the long term properties of weld metals, especially, the influence of important factors such as process and postweld heat treatment(PWHT). Until recently, the integrity of seam welded joints performing at elevated temperatures in the creep regime has been exemplary, and the absence of comprehensive study of the high temperature properties of weldments has not been viewed as a significant deficiency.

Particularly, this assumption has been put to question after two highly publicized steamline failures in U.S. power plants. Both the failures have occurred along the edge of the longitudinal seam weld. Although the results of the metallurgical analysis of these two failures have not been made public due to pending litigation, certain conclusions have emerged regarding the failures. Extensive inspection programs undertaken by a number of utilities to evaluate

high temperature welded components have uncovered evidence of many weld related problems. Careful analyses have shown improper design, fabrication defects and/or off nominal operating conditions. In many cases, however, the test results have indicated inferiority of elevated temperature properties of weld metals compared to their respective base metals.

The project undertaken has been to evaluate the high temperature properties of weldments in an effort to explain the apparently anomalous behavior of welds in elevated temperature service. Most of the welds in service are deposited by either submerged arc(SA) or shielded metal arc(SMA) processes. Subsequent heat treatment prior to installation is usually anneal and temper, or normalize and temper or a subcritical stress relief heat treatment. So, the effect of these heat treatments on the elevated temperature strength has been examined. Extensive metallography to understand the behavior of the weldments has been performed to correlate the properties with the microstructure.

CHAPTER 2

LITERATURE REVIEW

2.1 GENERAL MICROSTRUCTURE

The microstructure of 2 1/4Cr-1Mo steel depends essentially on the heat treatment and the alloying elements present. The continuous cooling transformation diagram for a 0.1%C, 2 1/4Cr-1Mo steel is given in figure 4.[20] From this figure it can be seen that there is an extensive range of cooling rates over which the microstructure will be bainitic. Slower cooling rates than the critical cooling rate would result in microstructures containing mixture of proeutectoid ferrite and bainite.

Usually most of the applications for this steel require a 100% bainitic structure and this requires high hardenability especially for thick plates. This is accomplished by the addition of alloying elements which have different effects on the critical cooling rate either individually or in combination with other elements. Such alloying elements added to the nominal composition of 2 1/4Cr-1Mo steel are vanadium, titanium, boron, nickel and niobium. The effects of these elements will be discussed in detail in subsequent sections.

Austenitizing temperature effects the prior austenite grain size and also the cooling rate. Plates of large section thickness (especially the center) cools very slow and this may result in different microstructures at the surface and center. With proper austenitizing temperature and alloying elements it is possible to

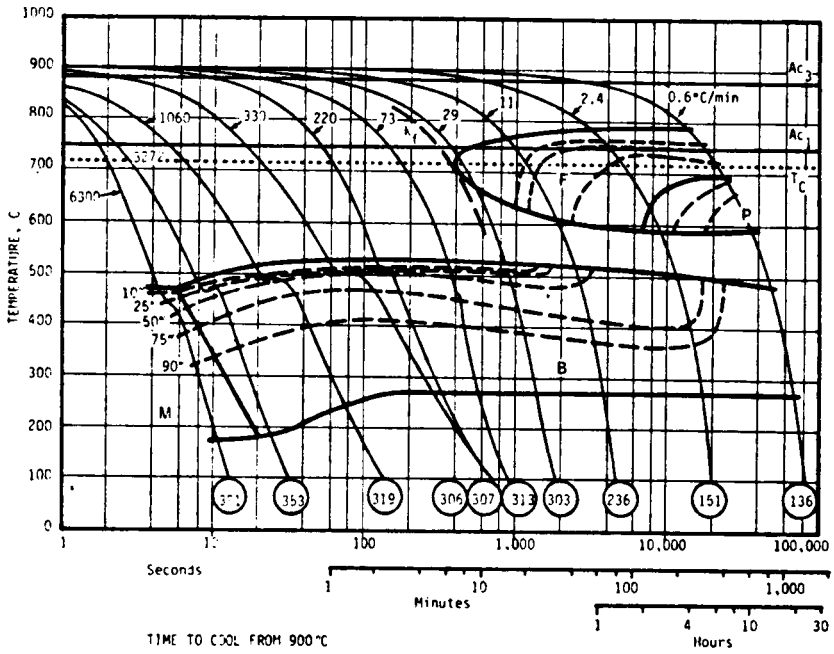

Figure 4. Continuous cooling transformation diagram of 0.1%C, 2 1/4Cr-1Mo steel.

Source: Wada, T. and Eldis, G.T., "Transformation Characteristics of 2 1/4Cr-1Mo Steel," Applications of 2 1/4Cr-1Mo Steel for Thick-Wall Pressure Vessels, ASTM STP 755, G.S. Sangdahl and M. Semchyshen, Eds., ASTM, 1982, pp. 255 - 274.

attain 100% bainitic microstructures even in 16 inch thick plate, the center of which cools at the rate of about 2.8 C^{o}/min.

With most of the welding processes the deposited weld metal cools much faster and also has an essentially 100 percent bainitic microstructure.[4] High heat input processes, create a wide heat affected zone with a coarse prior austenite grain size. During subsequent postweld heat treatment this zone is susceptible to postweld heat treatment cracking which is overcome by using proper composition and by modification of inclusion morphology in the base metal through proper deoxidation and desulfurization practices such as calcium treatment.[21]

Sims and Fuchs[22] studied the weld metal microstructure and mechanical properties employing different welding processes. Electroslag welding is usually completed in one pass. So the resulting microstructure is coarse in both the weld metal and heat affected zone. For this reason, as per the ASME Boiler and Pressure Vessel Code, Section VIII Paragraph UCS56a requires that electroslag welds in ferritic material over 1 1/2 inch in thickness be given a grain refining (austenitizing) heat treatment.

The submerged arc process can be used with a wide range of heat inputs. Hence, the subsequent postweld heat treatment usually depends on the heat input; being a subcritical stress relief for a low heat input processes or an austenitizing heat treatment for a high heat input process. For weld made with the shielded metal arc welding process (usually a low heat input process) the subsequent heat treatment is normally subcritical.

Welding processes like electron beam welding and laser beam welding use very concentrated heat sources which induces very fast cooling rates in the weld metal and the heat affected zone and the resulting microstructure has been reported to be lath type martensite in the weld metal and heat affected zone.[22] Subsequent subcritical postweld heat treatment result in excellent toughness in the weld metal and heat affected zone comparable (usually better) than the base metal.

Clark[23-25] has modeled the shielded metal arc process with respect to process parameters and has explained the dimensions of weld bead and heat affected zone for single pass and multipass welds. He has also described two layer heat affected zone refinement technique under shop floor conditions. His study shows that depositing a layer of weld beads on the parent material with a low heat input, followed by a second layer of beads superimposed so as to retransform the areas of coarse grained bainite left by the first layer, reduces the susceptibility of the parent weldment to postweld heat treatment cracking.

To describe the morphology of constituents in weld metal microstructures, especially ferrite, has been the subject of controversy and confusion. The IIW has published guidelines for classification of ferritic steel weld metal microstructures.[26,27] As per these guidelines primary ferrite has been classified separately as grain boundary ferrite and intragranular polygonal ferrite. Other ferritic constituents have been classified as acicular ferrite for small aligned ferrite grains within prior austenite grains, and

ferrite with second phase for ferrite with martensite or bainite which may be further classified as upper bainite or lower bainite. Ferrite carbide aggregate is the recommended term to be used for fine ferrite/carbide structures including ferrite with interphase carbides and pearlite. M-A constituent have been classified to include lath and twinned martensite and retained austenite. Sometimes lower bainite and autotempered martensite, especially in low carbon steels are difficult to differentiate. M-A constitute is hence used to classify a wide range of such microstructures. Usually in 2 1/4Cr-1Mo weld metal microstructures, all of the above are found depending upon the welding process used and postweld heat treatment employed.

The microstructure of 2 1/4Cr-1Mo steel and weld metal is mainly bainitic and the morphology of bainite depends upon the alloying elements, carbon content and the rate of cooling or the temperature of isothermal transformation. Bainite in low carbon steels have been characterized as upper and lower bainite.[28,29,30] In addition two more types of bainite are found in literature termed as granular bainite and massive bainite.[4] Bainite has a feathery appearance or acicular appearance depending upon the temperature of transformation. The transformation of austenite to bainite is by nucleation and growth process with the growth direction approximately perpendicular to the <111> direction of the parent austenite.

The microstructure of bainite is essentially an aggregate of carbides in the form of very small particles in ferrite, the size and distribution of which depends on the temperature of transformation for a particular alloy system. Hence, the formation of bainite is

dependent on the diffusion-controlled partitioning of carbon between ferrite and carbides. The ferrite of bainite is in the form of laths or plates containing a dislocation structure and to some extent therefore, the mechanism of bainite formation involves shear as well as diffusion. The strength of bainite is due to the carbide size and distribution, ferrite grain or subgrain size, dislocation structure and of course the carbon content which dictates the volume fraction of carbides. The ferrite in bainite is usually supersaturated with respect to both carbon content and alloying elements and this also makes a major contribution to the total strength of the alloy.

2.2 CARBIDES

The elevated temperature properties of 2 1/4Cr-1Mo steel depends primarily on the type, size, morphology and distribution of the carbides in the microstructure. Baker and Nutting[18] have studied the sequence of evolution of carbides during tempering of 2 1/4Cr-1Mo steel in the quenched and normalized conditions. The types of carbides present in 2 1/4Cr-1Mo system are MC, ϵ-carbide, M_3C, M_2C, M_7C_3, $M_{23}C_6$ and M_6C.

MC type:

MC carbides have a NaCl type cubic structure and in 2 1/4Cr-1Mo type steel are usually not found unless there are alloying elements like vanadium, titanium or niobium in which case they occur as VC, TC or NbC respectively. There is some solubility of iron, chromium and molybdenum in MC carbides.[31] Another variety of MC type carbides are

MoC and WC type which have a hexagonal structure compared to NaCl type cubic structure described above. Also they are not normally found in 2 1/4Cr-1Mo steel because of the stabilization of other phases by solution effects, eg $M_{23}C_6$ is stabilized by Cr and M_2C by Mo and Cr.[31] The MC types are usually very fine and stable.[18] Being stable carbides they increase the resistance of 2 1/4Cr-1Mo steel to hydrogen attack at elevated temperature. However, they also promote hydrogen assisted cracking during welding because the elements associated with these carbides result in increasing the hardenability of HAZ and so a proper balance must be achieved depending upon the application.

M_3C type:

This is a iron rich carbide having the orthorhombic structure of cementite.[31] M_3C type carbide has considerable solubility for other alloying elements and is completely isomorphos with Mn_3C. Chromium and molybdenum have a limited solubility in M_3C. During formation there is usually no further nucleation in the matrix and no further change in the particle shape except for the slow coarsening of the particles. This is usually very unstable in alloy steels and transform to more stable forms on tempering.

M_2C type:

This carbide is usually molybdenum-rich with a face centered cubic structure.[31] Considerable solubility of chromium and vanadium is seen in this phase. In 2 1/4Cr-1Mo steel this carbide also shows

solubility for nitrogen and is seen to occur as $(Cr,Mo,V)_2(C,N)$, especially in weld metal.

M_2C carbides are typically acicular and very fine, occurring intergranularly. They are also found to be slightly globular, specially at grain boundaries or at lath boundaries. M_2C is precipitated after tempering in both quenched and normalized steels, in each case by separate nucleation in ferrite. At the onset, the precipitate is coherent with the matrix but soon looses its coherency and grows into well defined flattened needles.[18] The creep resistance of the 2 1/4Cr-1Mo steel has been attributed to the stability of this metastable carbide.

$\underline{M_7C_3 \text{ type}}$:

This is a chromium rich carbide with a rhombohedral structure[31]. It has high solubility of iron and manganese. Molybdenum and vanadium are soluble but to a much lower extent. It is also found in an acicular shape in the matrix and in a globular shape in the grain boundaries. The nucleation event is in the vicinity of M_3C, either within M_3C or in the interface between the carbide and ferrite. The chromium content of M_3C increases before M_7C_3 forms.[18]

$\underline{M_{23}C_6 \text{ type}}$:

$M_{23}C_6$ type carbide is again a chromium rich carbide with a complex face centered cubic structure. They have a high solubility for iron and manganese upto a metal atom ratio of 0.4.[31] $M_{23}C_6$ forms

throughout the matrix of quenched and tempered steel but only in the bainitic regions of normalized and tempered steel. They form in the interior of the bainite in the regions containing M_3C and Mo_2C and grows at the expense of these carbides. They nucleate either within the M_3C particles or at the ferrite/M_3C interface.[18]

M_6C type:

M_6C type carbides are essentially ternary carbides of iron and molybdenum and show appreciable solubility for other elements.[31] This carbide also shows a relatively high silicon content.[33] Usually globular in shape, M_6C, is the equilibrium type carbide in 2 1/4Cr-1Mo steel.[18] These particles usually form at the grain boundaries and grow very rapidly at the expense of all the surrounding carbides. Nucleation of these carbides take place between existing carbides and the matrix for both normalized and tempered and quenched and tempered steels.[18]

The sequence of carbide formation in 2 1/4Cr-1Mo steels is as follows:[18]

in bainite:

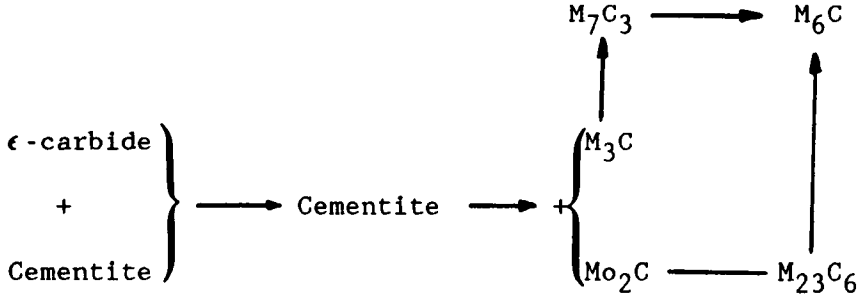

in ferrite:

$$M_2C \longrightarrow M_6C$$

M_2C or Mo_2C is the type of carbide responsible for the excellent creep strength of 2 1/4Cr-1Mo steel. It occurs in both the bainitic and ferritic regions. Baker and Nutting[18] suggested that the creep strength of 2 1/4Cr-1Mo steel depends on the stability of the M_2C carbides. In normalized and tempered steel, M_2C is stable for a longer period than in quenched and tempered steel and thereby the creep properties of normalized and tempered steels are superior to quenched and tempered steels. The isothermal diagram showing the sequence of carbide formation on tempering in quenched and normalized steels is given in figures 5 and 6 to illustrate this point.[18] The matrix of both proeutectoid ferrite and bainite is a ferritic solid solution. In proeutectoid ferrite a high density of needle or platelike Mo_2C precipitates. This unstable precipitate is eventually replaced by M_6C. Bainite, on the other hand, contains a high density of M_3C precipitates. Upon tempering M_2C forms first and subsequently on further elevated temperature exposure M_3C and Mo_2C are replaced by M_7C_3, $M_{23}C_6$ and finally by M_6C. However, in bainite, transformation to M_6C is faster than in proeutectoid ferrite. This is due to the fact that bainitic regions have more boundaries along which the diffusion of solute elements can occur more rapidly. Thus, at elevated temperatures, the properties of bainite change more rapidly than those of the proeutectoid containing steel (the hardening effect

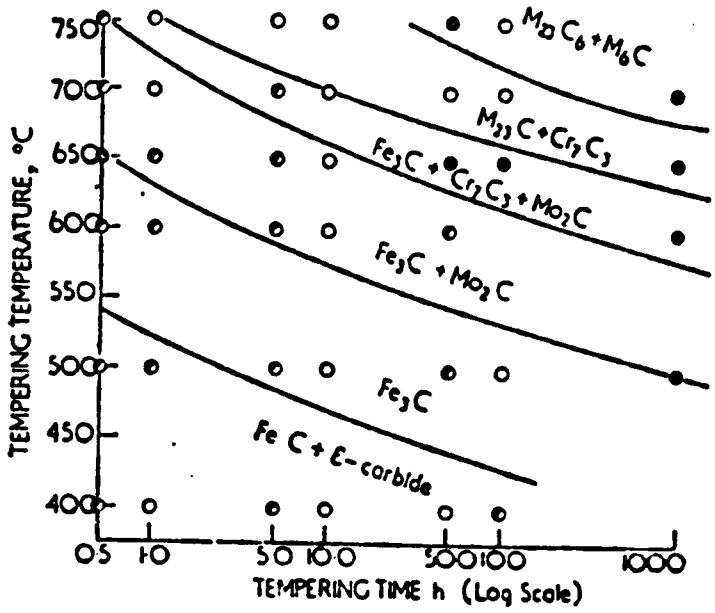

Figure 5. Isothermal diagram showing the sequence of carbide formation on tempering of quenched 2 1/4Cr-1Mo steel.

Source: Baker, R.G. and Nutting, J., "The Tempering of 2 1/4Cr-1Mo Steel after Quenching and Normalizing," JISI, 192(7), 1959, pp. 257 - 268.

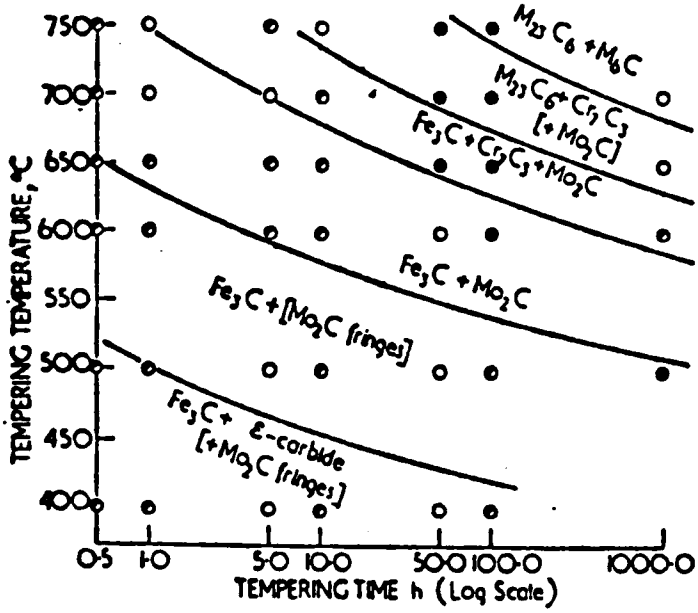

Figure 6. Isothermal diagram showing the sequence of carbide formation on tempering of normalized 2 1/4Cr-1Mo steel.

Source: Baker, R.G. and Nutting, J., "The Tempering of 2 1/4Cr-1Mo Steel after Quenching and Normalizing," JISI, 192(7), 1959, pp. 257 - 268.

of Mo_2C extends over a longer period of time in a ferritic microstructure as described earlier). Also, in ferrite, due to interaction solid solution strengthening the dislocation motion during creep is hindered by the interaction of dislocations with molybdenum and carbon atoms or atom clusters.[1]

As described by Klueh,[1] the creep strength of 2 1/4Cr-1Mo steel will depend on the test temperature and prior heat treatment. At low temperatures (<500°C or 932°F), the normalized and tempered steel (containing 100% bainite) is slightly stronger. Between 500 and 600°C (932 and 1112°F) only for lower rupture times (approximately 1000 to 10,000 hours) normalized and tempered steel is stronger than annealed steel. Above 600°C(1112°F), the annealed steel is stronger than the normalized and tempered steel. The creep strength of the weld metal and heat affected zone can also be explained in a similar manner. Roy and Lauritzen[32] have explained the rupture of composite creep specimens in heat affected zone using the same analogy.

2.3 TECHNIQUES OF CARBIDE ANALYSIS

Woodhead and Quarrel[31] have indicated that it is unwise to attempt to identify carbides from their shape and distribution. Selected area electron diffraction is essential for the identification of carbides. Several cases in which different morphologies of the same type of carbides occurring in the same steel have been cited by the authors to illustrate this point.

Extraction of carbides or particles for analysis is usually accomplished by two techniques: anodic dissolution and carbon

extraction replica. These techniques are used to determine composition, volume or weight percent, size, distribution and type of carbide in steels. Each technique has its own advantages and limitations.

Klueh and Leitnaker[34] have used electrolytic extraction by anodic dissolution of the matrix to determine the overall weight fraction of carbides and other second phase precipitates in low alloy ferritic steels. The solution usually used is 10 percent HCl in methanol and the precipitates are collected and subsequently washed and dried. The extracted samples may then be examined using X-ray diffraction procedures. This method involves the comparison of intensities of X-ray diffraction peaks from phases in the sample with a peak from a standard substance (mixed with the substance in known proportion). The limitations of this method are manifold. The precipitates obtained are essentially very fine. The collection, washing and subsequent handling is difficult and should be done very carefully so that nothing is lost in the process. The addition of standard introduces diffraction peaks into a multicomponent system where peak overlapping may already be a problem. It is necessary to prepare calibrations of the standard substance against each phase, which involves first obtaining pure samples of each phase in isolation. This frequently requires using different steels, or different heat treatment procedures, to produce single carbide systems. The resulting precipitation may therefore differ in chemical composition, and hence in intensity of X-ray diffraction peaks. However, techniques for isolation of carbides from

multicomponent systems have been studied by Stevens and Lonsdale[34] which makes this type of study slightly easier and less confusing.

Another technique utilized is by STEM and electron diffraction analysis of carbides extracted on a carbon film.[35-38] The carbides can be identified by chemical composition, morphology and electron diffraction patterns.

Electron diffraction patterns, in most cases, have been found to suffer interference from the adjacent carbides. Identification of carbides based on EDAX and the microanalysis from the EDAX spectra thus obtained have been done by Shaw[38]. He indicates that the several types of carbides occuring in 2 1/4Cr-1Mo system can be distinguised easily based on EDAX spectra and microanalysis. Typical EDAX spectra for the carbides observed on tempering a normalized 2 1/4Cr-1Mo steel are shown in figure 7. It can be seen that the spectra are characteristic and easily distinguishable and comparision would result in the identification of carbides. This method however, suffers from the limitation that the volume fraction or weight fraction of particles in the steel cannot be determined accurately.

2.4 TEMPERING AND POSTWELD HEAT TREATMENT

Excellent stress rupture properties of 2 1/4Cr-1Mo steel is due to the presence of M_2C type carbides, the stability of which depends on the diffusivity of the substitutional alloying elements. At higher temperatures Mo_2C transforms rapidly into more equilibrium type carbides which are detrimental to the overall creep resistance. So, the highest creep strengths can be obtained in steels that have

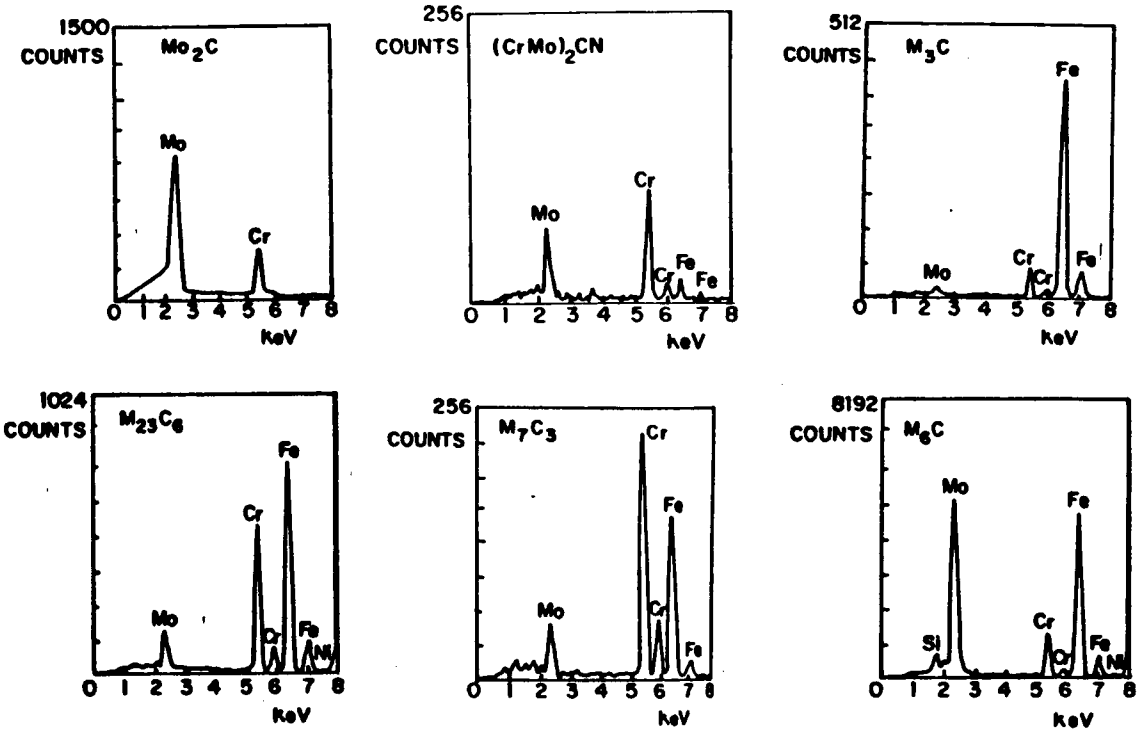

Figure 7. Typical EDAX spectra for the carbides observed on tempering of 3Cr-1 1/2Mo steel.

Source: Todd, J.A., "The Early Stages of Tempering in a 3Cr-1.5Mo Steel," Scripta Metallurgica, 20, 1986, pp. 269 - 274.

been tempered at a low temperature for a short time. Unfortunately the microstructure derived in this manner is less stable and so the advantages derived is only for a very short time.

Planning and execution of heat treatment of a 2 1/4Cr-1Mo vessel is hence a crucial step in the fabrication plan. As per the ASME code for P-5 material (2 1/4Cr-1Mo) postweld heat treatment of 1 hour per inch of thickness for the first 5 inches of vessel wall thickness is required. For each additional inch an additional 15 minutes of postweld heat treatment is required. So it can be seen that for a vessel of about 8 inch section thickness requires 6 hours of postweld heat treatment time.[22] Additionally, some postweld heat treatment is required if the welds need repair. So this becomes a very important criteria for determining if the mechanical properties have been met.[39]

2.5 EFFECT OF ALLOYING ELEMENTS

The strength of iron is increased by the addition of alloying elements and significant work has been carried out to investigate the effect of various alloying elements individually as well as in the presence of other elements. In this part of the review the effect of elements that are commercially added to 2 1/4Cr-1Mo steel to enhance its properties will be discussed. The influence of impurities or trace elements will also be described. Figure 8 shows the effect of the important alloying elements on the creep properties of steel.

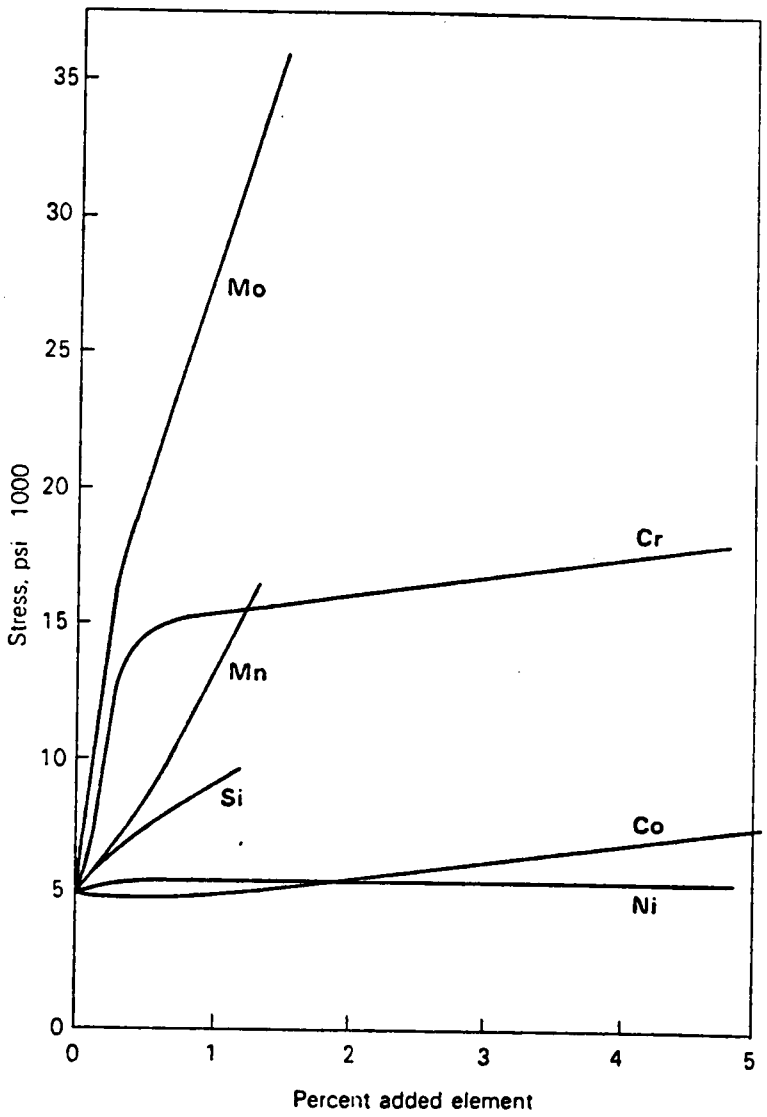

Figure 8. Stresses necessary to cause 0.1% creep per 1000 hours at 425°C(797°F) for each element investigated.

Source: Austin, C.R., St. John, C.R. and Lindsay, R.W., Trans. AIME, 162, 1945, pp. 84 - 105.

Chromium

The presence of chromium affects the creep properties of 2 1/4Cr-1Mo steels in the following manner:

(a) as a solid solution strengthener,

(b) as a carbide former and

(c) it imparts moderate corrosion resistance to the alloy at elevated temperatures.

The interaction energy of chromium with dislocations, though, is smaller in magnitude, but its interaction parameter with carbon in ferrite is high and this leads to the formation of chromium-carbon pairs which interact with the dislocations thereby restricting their motion.[40] Chromium carbides $M_{23}C_6$ and M_7C_3 improve creep strength of the steel significantly at temperatures below 500°C(932°F) but this beneficial effect is limited above 600°C(1112°F) because carbides coarsen rapidly to a size where interparticle spacing becomes greater than the elements of the three dimensional dislocation network.

The increase in chromium concentration in fact has been seen to reduce the creep strength.[37,41] Shaw's work has shown that increasing chromium reduces the amount of Mo_2C and enhances the formation of M_6C. High chromium is sometimes attractive in a way that more stable carbides are formed and they offer greater resistance to hydrogen attack.[27] Klueh and Swindeman[42] have shown that addition of chromium beyond 2.25 percent has no marked strengthening effect. The only effect of increased chromium is towards the improvement of oxidation and corrosion resistance and hardenability of the steel.

Molybdenum

As shown in figure 8, molybdenum increases the creep resistance of low alloy ferritic steels more than any other alloying element. Molybdenum is not a particularly strong carbide former but is an effective solid solution strengthening element which saturates the dislocation network. It is reported that additions of about 1% molybdenum saturates the dislocation network but higher concentrations do not lead to further increase in strength.[40]

The precipitation of molybdenum carbides may increase the stress rupture strength, despite its negative effect on solid solution strengthening. The carbide which is most effective in this regard is Mo_2C, particularly when present as a fine dispersion of acicular precipitates.[43] This morphology has been observed in both bainite and ferrite in 2 1/4Cr-1Mo steel, with the Mo_2C being much more stable in ferrite at elevated temperatures than in bainite.

Carbon

Carbon acts as a strengthening element which distinguishes steel from iron. The strengthening effect can be attributed to one or more of the following:

(a) its combination with other elements in the steel to produce carbide precipitates,

(b) its effect on the transformation kinetics of austenite to lower temperature microconstituents thus

determining the microconstituents present for a given heat treatment, and

(c) its interaction while in solution with other alloying elements and dislocations.

Carbon readily combines with several alloying elements to form carbides. Carbide formers like chromium, molybdenum, vanadium, titanium, and niobium are added to the ferritic steels to impart creep resistance. The amount, type, size and distribution of the carbide precipitates are controlled by the concentration of carbon and alloying elements added to the steel in addition to the heat treatment time and temperature. Because of the strength loss associated with increased precipitate spacing, it is desirable to produce a large volume fraction of precipitates in the microstructure. Thus when the carbides grow at elevated temperatures, the interparticle spacing increases at a slower rate. This argument leads to the conclusion that higher carbon steels should be used to increase the volume fraction of carbides. Analyses have indicated that optimum creep properties are obtained for carbon levels in the range of 0.1-0.2 weight percent.[31] However, such a practice may lead to a steel with unacceptable ductility, weldability and impact toughness.

Because the carbon level in a steel has a pronounced effect on hardenability it is at least partly responsible for determining the microconstituents present as a function of cooling rate and thus indirectly affects the creep behavior of the steel. In 2 1/4Cr-1Mo steel, the microconstituents observed include ferrite and bainite.

Martensite is attainable at very high cooling rates and may occur in quenched and tempered steel, depending on the section thickness. 2 1/4Cr-1Mo weld metal deposited with the shielded metal arc or submerged arc process may be fully bainitic or a bainite/ferrite mix depending on such factors as carbon content, preheat/interpass temperature and energy input. Kotecki[44] reports that for submerged arc welds using 2 1/4Cr-1Mo filler metal with a manganese content below about 0.7% and a preheat/interpass temperature of 400°F, some polygonal ferrite may form when the weld metal carbon content is below 0.08-0.10%. A similar effect is observed for shielded metal arc welds. However, due to lower energy inputs characteristic of this welding process, the carbon level below which polygonal ferrite is observed in the microstructure is somewhat lower.

Carbon plays a major role in "interaction" solid solution hardening.[40,41] Associating with certain alloying elements carbon forms substitutional/interstitial clusters which can impede dislocation movement. In creep resistant ferritic steels with low carbon content, carbon can be tied up in the form of alloy carbides and still leave sufficient quantities of carbide forming substitutional alloying elements in solution to contribute to this strengthening effect.

The effect of carbon content on the stress rupture strength also depends on the test temperature.[45,46] Klueh and Canonico[45,46] found that at 1050°F, the rupture strength of the low (0.003%C) and medium carbon (0.035%) steels were similar, while that of the higher carbon (0.12%) steel was much greater. However, at 850°F and 950°F,

the stress rupture strength of the high and medium carbon steels were similar, while the low carbon steel was considerably weaker than both.[46] The low strength of the low carbon material can be explained by the fact that it obtains little precipitate strengthening from the large, widely scattered carbides present in its microstructure. Campbell[47] during his stress rupture testing of 2 1/4Cr-1Mo weld metal with wide range of carbon content found that above 0.4% C there is no furthur effect of carbon on the stress rupture properties of weld metal. However, his tests were carried out at relatively higher temperatures (1050 to 1200°F). So it can be concluded that carbon is less effective at temperatures exceeding 1000°F. Zeisloft, Leyda and Domian[7] found that between (0.08 to 0.14% C) there is no further increase in the stress rupture strength of 2 1/4Cr-1Mo steel.

Manganese and Silicon

Manganese and silicon both act as substitutional alloying elements in ferrite. However, manganese has almost the same atomic diameter as iron and hence does not contribute substantially to the solid solution hardening. Shaw[37,38] reported that both manganese and silicon enhance the formation of M_6C and hence may be considered to be detrimental to elevated temperature properties. Increasing silicon also reduces the amount of Mo_2C.

Dittrich et al.[49] have found that manganese and silicon act as cosegregates. Manganese in weld metal acts in a way helping formation of acicular ferrite in the primary microstructure which results in an improvement of the toughness properties. In weld

metal, silicon is needed for deoxidation purposes without which it will be impossible to get weld deposits free of porosity. Silicon in the base metal however, is not desirable because it increases susceptibility to temper embrittlement and decreases stress rupture strength.[50,52]

Vanadium

Vanadium addition increases the hardenability, tensile strength and creep rupture strength of 2 1/4Cr-1Mo steel. However, its addition is usually limited to 0.25% because of its adverse effect on the postweld heat treatment cracking susceptibility.[53] Vanadium is a strong carbide former.[31,43] The carbide formed is V_4C_3 type and is very fine and thus is responsible for the strengthening effect. However, V_4C_3 is relatively stable at lower temperatures but coarsens rapidly above 600°C (1112°F).[40] Wagner and Seth[53] investigated the effect of vanadium on shielded metal arc and submerged arc welds. They found that vanadium has no effect on the stress rupture properties of weld metal. However, it is to be noted that their creep testing was conducted at 1100°F.

Another effect of vanadium is that it has higher affinity for carbon than molybdenum. So in the presence of vanadium, carbon is usually tied up with vanadium thereby leaving molybdenum in solid solution to strengthen the matrix.

Titanium

Titanium is added in steels as a strengthener (particularly for elevated temperature), a stabilizer and/or a deoxidizer.[54-56] Strengthening by titanium additions results from the formation of fine TiC precipitates in the matrix. These carbides are very stable and resist coarsening during elevated temperature service.

Titanium in steel is believed to act in a manner intermediate to that of niobium and vanadium[47] with the ratio of strengthening by grain refining to that by carbide precipitation, being dependent upon the austenitizing temperature. Pilling et al[47] have found that titanium additions of 0.04 wt% to 2 1/4Cr-1Mo steel markedly increased its creep strength. Titanium carbides are very stable and so to dissolve them while austenitizing it is necessary to austenitize the steel at a higher temperature than usual depending upon the carbon content of the steel. Subsequent morphology of TiC precipitate upon tempering is fine (50-100A^{o}) and they resist microstructural degradation during creep and thus contribute, through microstructural stability to the observed increase in creep resistance. Moreover, the extent of strengthening, derived from the presence of very small titanium rich precipitates in 2 1/4Cr-1Mo steel is further enhanced by leaving the molybdenum in solid solution especially at low carbon levels. The improvement in the rupture life and minimum creep rate of 2 1/4Cr-1Mo steel with the addition of titanium is shown in figure 9. The effect of minimum creep rate as a function of carbon content in the presence of 0.04% titanium is shown in figure 10. It is seen that titanium is more effective at low

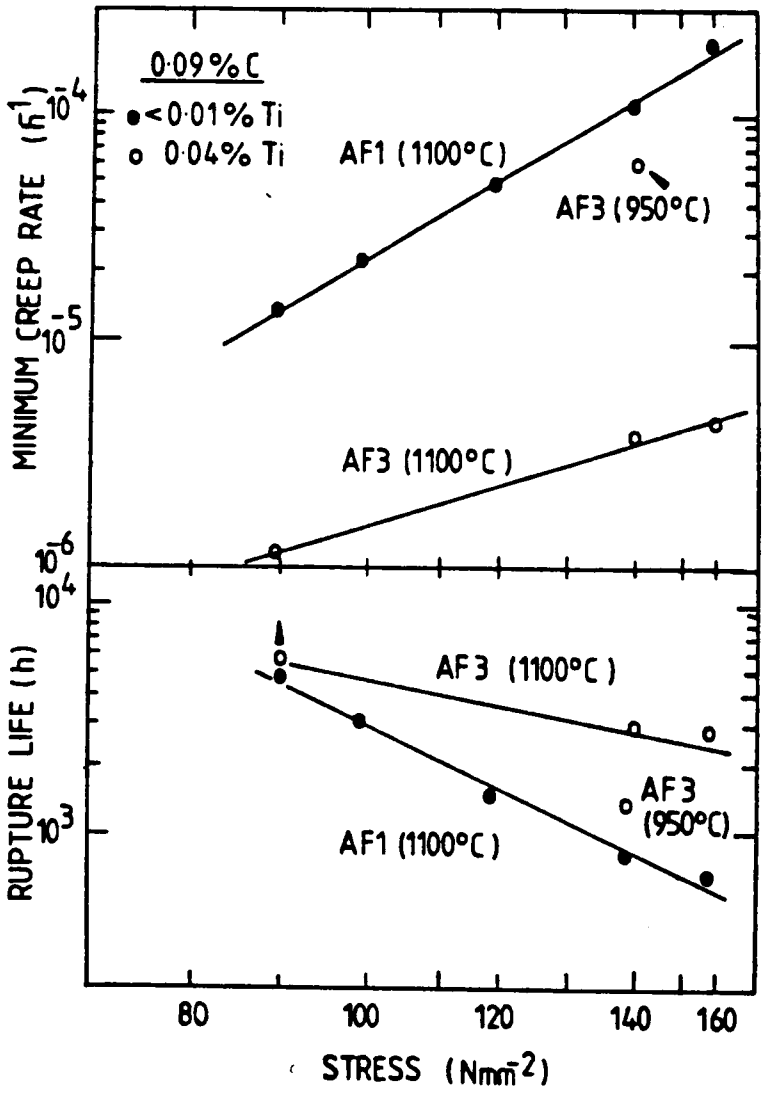

Figure 9. Rupture life and minimum creep rate of 2 1/4Cr-1Mo steel with and without addition of titanium.

Source: Pilling, J., Ridley, N. and Gooch, D.J., "The Effect of Titanium on Creep Strength in 2.25 Pct Cr-1 Pct Mo Steels," Met. Trans. A, 14A(7), 1983, pp. 1443 - 1449.

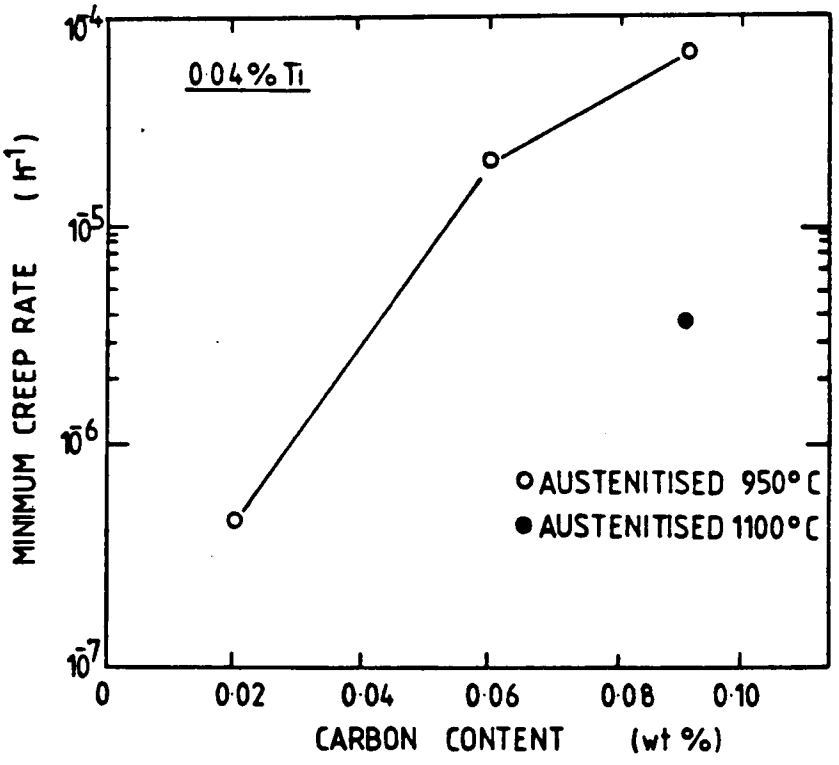

Figure 10. The variation of minimum creep rate of 2 1/4Cr-1Mo steel with titanium addition with carbon content and austenitizing temperature.

Source: Pilling, J., Ridley, N. and Gooch, D.J., "The Effect of Titanium on Creep Strength in 2.25 Pct Cr-1 Pct Mo Steels," Met. Trans. A, 14A(7), 1983, pp. 1443 - 1449.

carbon levels and higher austenitizing temperature than at higher carbon levels and lower austenitizing temperatures.

Viswanathan[56] has looked into the effects of titanium in 1 1/2Cr-1/2Mo steels at 538°C in the presence of other impurity elements and found that titanium additions reduced the tensile, stress rupture and creep strengths if phosphorus is the only major impurity, but improves creep properties markedly when large amounts of phosphorus, antimony and tin are present. Also in the presence of boron, titanium additions appreciably improve the tensile and creep strengths. However, titanium addition improves the rupture ductilities irrespective of the presence of boron. Gooch[55] has found that titanium distribution between inclusions, carbides and solid solution depends on the steel melting practice. In weld metal, which has lot of inclusions, titanium is found preferentially in inclusions, than in carbides or in solid solution.

Niobium

Relative to vanadium and titanium, niobium carbides are more stable and resists degradation at elevated temperatures. For niobium containing steels it is necessary to austenitize at a relatively higher temperature in order to be certain that all the niobium has been taken into solution. This temperature depends on the carbon and niobium concentration and is of the order of about 2370°F (1399°C). Niobium containing steels resist decarburization in liquid sodium environment because of the presence of stable carbides. So, 2 1/4Cr-1Mo steel containing niobium is superior in high pressure hydrogen

atmosphere at elevated temperatures.[57,58] Niobium also has a high affinity for nitrogen and oxygen and so the creep strength is primarily due to fine precipitation of niobium carbonitrides (seen both in base metal and in weld metal).[58] Husslage and Dortland[58] have also reported the presence of large amounts of very fine Laves phase (Fe_2Nb) in 2 1/4Cr-1Mo steels containing 0.5 to 0.8% niobium. These precipitates also add to the creep strength of the steel but is not very stable and coarsens at elevated temperatures.

Boron

Boron is added to steels to increase their hardenability by retarding the transformation of austenite to ferrite and pearlite.[52] Figure 11 shows the shift in the continuous cooling transformation diagram of 2 1/4Cr-1Mo steel to the right when boron is added. From the figure it is clear that addition of boron can result in 100% bainitic microstructure even at the center of 500mm (~ 20 inch) thick plate when cooled in air. Thomas and Chen[59] observed that 2 1/4Cr-1Mo steel containing 0.0016% boron showed less retained austenite films at the bainite lath boundaries. Boron containing steels show higher tensile strengths but have lower impact strengths than boron free steels. Boron has also been found to improve creep strength and ductility of creep resisting steels. However, the effects of boron on hardenability is seen only at low austenitizing temperatures because the effect of boron on hardenability is evident only when it segregates at the prior austenite grain boundaries and not when it is evenly distributed throughout the matrix. Boron has been found to

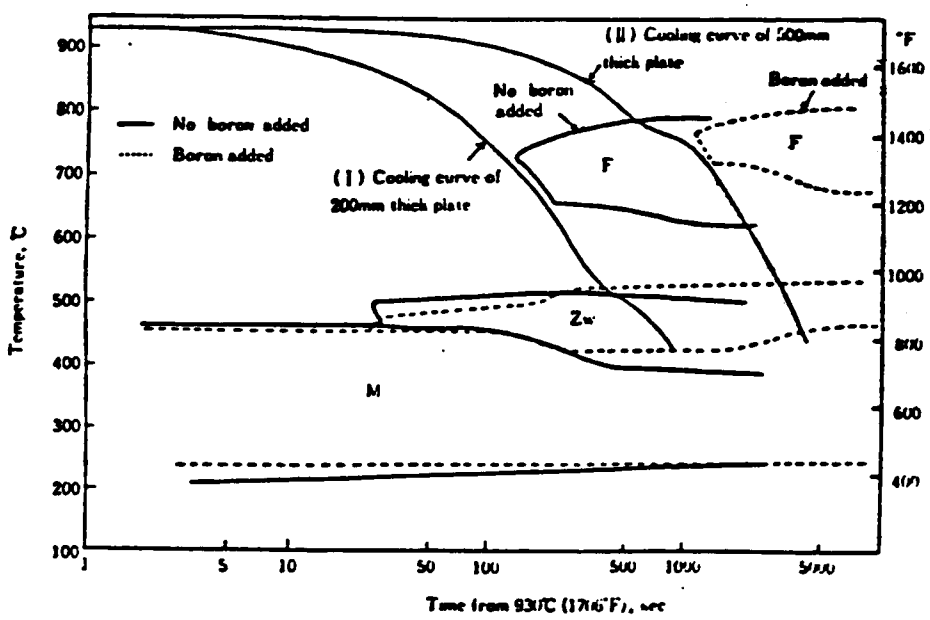

Figure 11. Changes in the continuous cooling transformation diagram of 2 1/4Cr-1Mo steel by addition of boron.

Source: "Improvement in High Temperature Properties of Heavy Section 2 1/4Cr-1Mo Steel," Kawasaki Steel Corporation, January 1982.

have no effect on the martensite or bainite transformation temperature of 2 1/4Cr-1Mo steel. Viswanathan[60] has investigated the effects of boron additions in the presence of other impurities like antimony, tin and phosphorus and found that boron additions leads to strengthening effect or weakening effect depending on the presence of other impurities. B+Sn exhibits consistently higher creep strength whereas steels containing B+Sn+P+Sb exhibit lower creep strength than steel containing similar amounts of Sn+P+Sb and no boron. However, he also found out that regardless of other impurities boron containing steel invariably shows lower creep ductility than boron free steel.

Phosphorus, Antimony and Tin

Phosphorus, antimony and tin are impurity elements in low alloy ferritic steels and it is always desirable to keep their levels as low as possible. Pilling et al.[64] have seen that the increase in phosphorus in 2 1/4Cr-1Mo results in an increase in the minimum creep rate of a given steel and this effect is even more pronounced in case of higher carbon steel (0.09%). However, they found no distinct effect of phosphorus on rupture life and rupture ductility. Phosphorus is usually seen to segregate at the prior austenite grain boundaries. Phosphorus in alloy steels at elevated temperatures causes a strain induced segregation of molybdenum to the prior austenite grain boundaries, causing dissolution of Mo_2C type carbides and hence resulting in loss of strength.[55,64]

In combination, the elements, tin, phosphorus and antimony can influence the action of other strengthening additions. Viswanathan[60] has indicated that the combined additions of large amounts of these three elements to 1 1/2Cr-1/2Mo steel does not effect the short time creep strength or ductility of the material measured at 1100°F (538°C). However, the relative amounts of these impurities can determine whether the addition of boron has a beneficial effect or detrimental effect on the creep properties. In another paper Viswanathan[56] states that similar interaction between impurity and strengthening alloying elements occur for titanium and titanium and boron.

2.6 SERVICE EXPOSURE AND LIFETIME PREDICTION

According to industry estimates, by the year 1990, 15% of the total capacity and 75% of the reserve capacity of the electric power in the United States will be supplied by units which are over 30 years old.[69] Current procedures for life assessment, are based on overly conservative assumptions and a large number of boilers will probably have to be replaced at the end of 30 years of service unless more accurate life assessment procedures are applied which may enable extension of their useful life by 20 to 30 years and also result in an increase of their service availability. Moreover, remaining life of aged components is required to safely operate and to avoid costly forced outages even when the plant is running within its designed lifetime. In this context the "useful lifetime" of a component has been defined by Viswanathan[69] as the period during which the

component can perform its intended function safely, reliably and economically.

In spite of the safety margins provided by design, premature failures of components do occur in practice, mainly because of operational, environmental and metallurgical factors outside the scope of the original design. Significant amongst them are unanticipated residual and system stresses, stress concentrations, excessive temperature and cycling, corrosion, oxidation and long term material degradation. In addition, welds and adjoining heat affected zones are sometimes weaker than the base material. Numerous creep damages in welded hot steam components like boilers, headers, superheaters, reheat pipings etc. have shown that under certain circumstances welds can be a weak point.[70]

To predict the residual life of an aged component it is first necessary to recognize and understand the microstructural changes taking place in a steel at elevated temperatures. These changes in microstructure can be broadly categorized into two separate groups.

(a) It is associated with the type, size and morphology of the carbides and thereby affecting the composition of the matrix (which gets depleted of carbon and other substitutional alloying elements due to the precipitation and growth of carbides), and

(b) it is the formation of intergranular creep voids leading to aligned cavities and microcracks which eventually join to form macrocracks and finally lead to rupture or failure.

The loss of strength in 2 1/4Cr-1Mo steel during service exposure has been investigated extensively by Wada and Biss[73,74]

Murphy and Branch[76] and D'Angelo et al.[79] These studies reveal that loss of creep strength is mainly due to two factors:

(1) the change in the carbide morphology occurring during tempering or postweld heat treatment, and

(2) reduction of carbon and alloying elements especially molybdenum, in the ferrite matrix thereby causing loss of the interactive solid solution type strengthening.

The latter factor becomes more pronounced during long periods of exposure as encountered in service because of the precipitation of molybdenum containing carbides or carbonitrides thus leading to a progressively decreasing concentration of both molybdenum and carbon in the matrix. The strength loss due to the change in carbide morphology follows the precipitation sequence outlined by Baker and Nutting.[18] This results in dissolution of acicular M_2C type carbides in both bainite and ferrite and leads to the formation of globular M_6C type precipitates. These changes in carbide morphologies are associated with rapid coarsening causing the interparticle distances to increase and results in the formation of precipitate free zones where the creep voids or cavities nucleate.

Material degradation by plastic deformation under the combined influence of high temperature and stress results in the formation of creep voids or cavities. Svensson and Dunlop[80] have reviewed the status of theory and experiment concerning the growth of intergranular cavities during high temperature service. The creep-fracture process can be divided into the following stages but it should be realized that these are not mutually exclusive. In many

cases these can occur simultaneously. The stages consist of nucleation of cavities, their growth and interlinkage followed by crack propagation and fracture.

The theory concerning the growth of intergranular cavities during creep considers that cavity volume increases either by the accumulation of vacancies at the cavity surfaces, or by plastic void growth because of the deformation of the material surrounding the cavity. The rate of growth of cavity by vacancy condensation is enhanced by creep deformation of the surrounding material.

Various methods are now in use to determine the extent of accumulation of damage in the material. Some of them are non destructive in nature whereas some of them requires small amount of material to be removed from the component in service to determine the extent of damage or degradation of the material. Some of these methods are quantitative in nature but most are qualitative. Another very important aspect of these evaluations is to assess whether the component will leak or rupture when in extended use. In this review some of the creep damage assessment methods will be presented. Various techniques which may be applied for these evaluations are:[81]

(a) Isothermal creep testing,

(b) Tensile testing at room and elevated temperature,

(c) Macro and micro hardness measurements,

(d) Optical microscopy,

(e) Transmission electron microscopy,

(f) Cavitation analysis,

(g) Density measurements,

(h) Coercive field measurements,

(i) Barkhausen effect and

(j) Short time isostress creep testing.

Witte and Stubbe[81] from their study on different life time prediction methods conclude that except isostress creep testing, none of the other methods are capable for making quantitative or even qualitative residual life determination. However, the following techniques can be used for estimating residual life of a component.

- Replica technique for detection of creep cavitation in material. By this method it is possible to estimate qualitatively or sometimes semi-quantitatively the remanent life of a component. The main advantage of this method is that it is non destructive, inexpensive and can be done very quickly.
- Creep deformation assessment is another very useful method but utilizes very accurate instrumentation. It is indeed very useful to follow the real creep deformation behavior in service in term of total deformation or creep rate.
- Creep tests on the material removed from the component in service is probably the easiest in terms of quantification of the remaining life time prediction. Isostress and isothermal creep tests allow evaluation of the deformation behavior giving indications about the creep mechanisms.
- Density measurements could be a useful technique to quantify the cavitation damage. However, the practical interest in this area is not seen.

Bendick and Weber[82] state that the uncertainty of prediction of the lifetime of components is because of the scatter in the properties of the as-received materials, insufficient knowledge about the service parameters (stress and temperature) and lack of satisfactory numerical methods and models for accurate assessment. They also state that isostress creep test is the only method which provides a far better insight into the lifetime situation. However, main disadvantage of this method is that long term tests at low stresses are necessary and material has to be removed from the component in service. Moreover, the data obtained from a sample may not be representative of the damage at other locations where deterioration may be more extensive.

Kimura et. al.[84] have conducted investigations on a rotor which was taken out of service after 130,000 hours of operation. They reported that correlation is possible between the hardness and creep properties. Various parts of the rotor had experienced different temperatures and high temperature portion of this rotor has shown severe service degradation caused by softening of the material due to carbide coarsening and recovery of the dislocation structure. The authors have proposed techniques of restlife estimation by hardness measurements. The relations proposed through various equations seem to fit the experimental data very well. However, the suitability of this method needs more extensive research.

Hildebrandt et. al.[83] have proposed some more non destructive testing (NDT) methods for restlife estimation. However, they state that the optimum combination of methods still requires thorough

microstructural investigations. The various methods suggested use the changes in property of the material by service exposure measured by ultrasonic techniques, acoustic microscopy techniques, micromagnetic property measurement techniques and electrical conductivity methods. The authors also present the effect of aging, dislocations and vacancy agglomeration and internal crack and surface crack formation on the various parameters measured using the above techniques.

Among the techniques being used extensively for the estimation of accumulation of damage is the in-situ metallographic replication techniques.[85-89] This technique essentially consists of polishing the surface of the component to metallographic quality followed by etching by a suitable etchant and taking the impression of the surface on a soluble acetate film followed by metallographic examination by both optical and scanning electron microscopy. Neubauer[87] states that creep microcracks and cavities of approximately 1 micron in size can be detected successfully by using this technique.

Sklenicka and Cadek[85] have studied the formation and growth of creep cavitation as a function of the crossection of specimens. They state that the extent of cavitation at the crossection varies - the highest being at the specimen surface which gradually decreases towards the specimen interior. Under a threshold stress, the process of cavity nucleation is characterized by an incubation time and that the process of nucleation of cavities is rather a continuous process and not a spontaneous process. Needham and Cane[88] also studied the

process of nucleation and growth of creep cavities in base metal, weld metal and heat affected zone in low-alloy ferritic steels leading to failure of a component. They found that the cavitation was most extensive in weld metals in most cases. Their study shows that the damage accumulation at weldments can give an indication of the life usage in regions remote from the welds. Their observations predominantly show that the nucleation of cavities occur at inclusions like MnS and has been also seen to occur at the carbides. The growth of cavities mainly occur by grain boundary vacancy diffusion process and also by plastic deformation around the cavities due to imposed stress.

Neubauer[86,89] has quantified the process of cavitation leading to final rupture of the material by assigning damage parameter by in-situ replication techniques. The various stages leading to fracture has been given as:

1. Coagulation of carbides, recrystallization, etc.
2. Pinning of dislocations by fine dispersed carbide
3. Dissolution and redistribution of various types of carbides
4. Accumulation of carbide forming elements in the carbides
5. Formation of isolated cavities
6. Linkup of these cavities to form microcracks
7. Final creep fracture of the component by macrocrack formation

As shown in figure 12 Neubauer and Wedel[86] have assigned different damage parameters and actions to be taken based on observation of replicas. Stage A shows isolated cavities; Stage B is the transition from secondary creep to tertiary creep and the creep

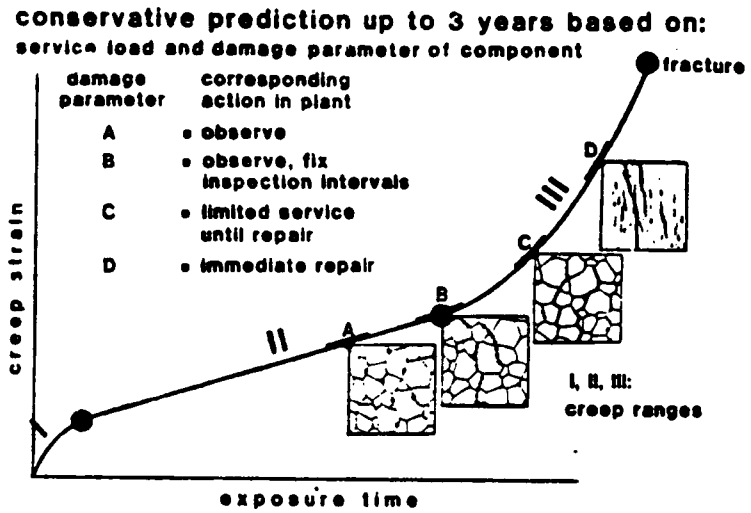

Figure 12. The creep damage measured by replica technique classified into four damage parameters.

Source: Neubauer, B. and Wedel, U., "Restlife Estimation of Creeping Components by Means of Replicas," ASME International Conference on Advances in Life Prediction Methods, April 18-20, 1983, pp. 307 - 313.

cavities are oriented; Stage C shows linkup of the cavities and formation of microcracks and stage D shows macrocracks. They also point out that welds are weak points in creep loaded tubing systems. This is due to metallurgical reasons and also some fabrication defects which are not detected by conventional NDT. So creep damage is usually concentrated in this region (weld metal and heat affected zone). They also have observed that the creep cracks perpendicular to weld grows slowly than parallel to the weld. Also crack depths upto 10% of the wall thickness is not harmful for extended operation depending upon the service conditions and the orientation and morphology of the crack. They have also suggested about the locations where most of the creep damage can be expected and these areas should be closely observed for creep damage and restlife assessment.

2.7 STRESS RUPTURE TESTING AND DATA ANALYSIS

The objective of stress rupture testing is to collect data on rupture time as a function of applied stress and test temperature for a particular material. The goal is to characterize its behavior sufficiently so as to permit determination of allowable stress levels for design purposes. Structures and components to be used at elevated temperatures are generally expected to operate for a minimum of 100,000+ hours. Since it is impractical to test material for such long periods to determine the stresses associated with that life, data are collected for shorter rupture times and analyzed to determine the relationship between stress and rupture time.

Extrapolations to 100,000+ hours are then made and the stresses thus obtained are used to develop design criteria.

Standard practice for conducting creep, creep-rupture and stress rupture testing of metallic materials is given in ASTM E139-83. But there exists no universal method for data analysis. Several methods are used for analysis of data obtained using linear or nonlinear regression methods. The dependant variable varies with the type of material, test temperature and applied stress level. Various parametric type analysis are also used which combines two or more of the variables into a single parameter and then regression is performed to get the best fit. Some of the testing and data analysis techniques will be discussed in this review.

Log Stress/Log Rupture Time

This is the simplest technique and involves plotting log stress vs. log rupture time. This method takes advantage of the fact that the data plotted in this manner generally falls on a straight line. Linear regression analysis techniques are applied and the coefficients are derived which define the equation of the best fit straight line. It is then very simple to extrapolate the straight line to determine the stress which will cause rupture in 100,000 hours. However, this technique assumes that the behavior is linear to 100,000 hours. Unfortunately, at elevated temperatures, many metallurgical systems are not microstructurally stable. Significant microstructural changes alter the straight line behavior and changes the slope of the log stress/log rupture time plot. Relatively, rapid

changes such as recrystallization, produce an abrupt change in slope, replacing the expected straight line with two straight line segments with different slopes. Gradual changes such as oxidation, grain growth, or precipitate growth/evolution procedure produce a gradual slope change causing the line to become concave downwards. These instabilities are more pronounced at higher temperatures and stress levels.

Time-Temperature Parameters

Another data analysis technique involves the use of time/temperature parameters. These parameters are based on an Arrhenius relation implying that creep to rupture is a thermally activated process governed by a single mechanism. However, as shown by Coffin and Goldhoff[91] there are many deformation mechanisms at work during creep rupture. Thus the basis for the parametric approach is not theoretically rigorous. Despite this fact, parameters are widely used in the analysis of rupture data and can be quite useful. The technique has an advantage that all of the data for a given heat of material taken at various temperatures can be depicted on a single master curve. The most commonly used parameter is the Larson-Miller parameter (LMP) and is defined as:

$$LMP = (T + 460)\ (C + \text{Log}\ t_R)$$

where,

T is the test temperature in ^{o}F,

C is constant, usually taken as 20,

t_R is the time to rupture in hours.

The data is then plotted as log stress/LMP and nonlinear regression analysis is carried out to get the best fit. Another advantage of this technique is that the stress to produce rupture time of 100,000+ hours is interpolated and not extrapolated and so the accuracy obtained is usually higher than obtained by log stress/log rupture time type of analysis.

The latest data analysis techniques make extensive use of computers and are not as rigid in assigning a prior relationship between stress, rupture time and temperature. Among others, Prager[92], Booker and Booker[93] currently active in this area utilizes a computer program which requires an input consisting of a list of possible terms to be used to construct a parametric relation with the stress rupture data. The program combines the terms to be used to generate a multiplicity of parametric equations, fits the data to each, then outputs a ranked list of the models which gives the best fit. It is then upto the analyst to choose the fit which not only describes the data well but also predicts reasonable behavior for the material upon extrapolation.

Isostress Creep Testing

Isostress creep testing has gained popularity because of the ease of prediction of remaining lifetime of components operating at elevated temperatures. Isostress creep testing is essentially creep testing of the material at the service stress but at temperatures higher than the operating temperature. The data are plotted as log rupture time vs. temperature and a straight line fit is extrapolated

to the operating temperature to determine the life remaining at operating temperature. Researchers working in this area have found a straight line relationship between log rupture time and temperature.[95-101] This method however, suffers from a disadvantage that the estimation of design stress for a material is not possible. In such cases testing at different stress levels are required and this leads to testing of a lot of specimens involving higher cost and longer time.

Environmental Effects on Creep Testing

The performance of high temperature materials in service is usually judged on the basis of either corrosion resistance or mechanical properties. Possible interactions between corrosion and mechanical behavior are not taken into account. Thus investigations on the interaction of corrosion process and material creep properties is required in order to provide a quantitative understanding of the material behavior and to enable supply of reliable design data.[104]

The accuracy of extrapolated long-term creep strength values based on short-term creep tests depends highly on reliable creep results. There are two main sources for introducing erroneous creep rupture data for high temperature steels: specimen surface effects and structural instability during testing.[103] The surface effects are more pronounced when the specimen size is made smaller and smaller.[96,103] Borggreen and Huntley[96,103] have designed a model for correction of rupture times and residual lifetimes due to oxidation based on isostress testing in air and helium. However, their model

was developed and tested for 0.5Cr-0.5Mo-0.25V steel but for other materials this model needs to be modified depending on their high temperature oxidation resistance. Their study concludes that the extrapolation of creep rupture data should be done with caution because of oxidation effects. However, without correction the estimations will be conservative leading to conservative life estimation.

2.8 SUMMARY

The preceding literature review has discussed, in detail, the microstructures of 2 1/4Cr-1Mo steel (base metal, weld metal and heat affected zone) and their effects on stress rupture properties. In addition, the effects of elevated temperature exposure (postweld heat treatment, tempering and service exposure) and chemical composition on the stress rupture properties have also been addressed. Finally, a brief discussion of some of the analytical techniques currently used for lifetime prediction and characterization of stress rupture behavior of materials based on data collected during rupture testing has been presented.

The important points concerning the microstructures of 2 1/4Cr-1Mo steel are summarized:

(a) Depending on the cooling rate from temperature above A_3 during welding or heat treatment, the microstructure obtained is typically bainitic or ferritic/bainitic. Cooling rate is controlled by the cooling method employed, the weld energy input, the preheat/interpass temperature, and the size and

thickness of the member. The amount of ferrite formed can also be influenced by the carbon content of the material. Under extremely rapid cooling conditions, martensite may also form.

(b) The alloy carbides in the microstructure evolve according to a scheme determined by Baker and Nutting.[18] The details of the scheme are similar for martensitic or bainitic microstructures but differ significantly for ferritic microstructure.

(c) The evolution of carbides in 2 1/4Cr-1Mo weld metal appears to be slowed by increase in carbon content.

The influence of microstructure on stress rupture strength may be summarized as follows:

(a) The primary strengthening alloy carbide in 2 1/4Cr-1Mo steel is M_2C. This precipitate can form in any of the microconstituents found in 2 1/4Cr-1Mo steel (martensite, bainite, ferrite) but persists for a much longer time in ferrite during tempering or elevated temperature service exposure.

(b) Prolonged exposure at elevated temperatures results in a continuous decrease in stress rupture strength as a result of carbide evolution, coarsening, spherodization, and agglomeration.

(c) The loss of strength described in "b" above may be significantly slowed by addition of strong carbide formers such as titanium, vanadium or niobium which precipitate as relatively stable MC carbides.

(d) Mild tempering or postweld heat treatment of 2 1/4Cr-1Mo steel or weldment results in a significant increase in room

temperature tensile strength. However, the strength advantage thus obtained decreases with increasing service temperature and is insignificant above about 900°F.

(e) The strength of all 2 1/4Cr-1Mo steel, however heat treated, approaches a common value given sufficient time at temperature as the microstructure evolves to one of overaged equilibrium carbides in a ferrite matrix.

(f) The rupture strength of 2 1/4Cr-1Mo steel is a function of microstructure and test temperature. At higher test temperatures a ferritic microstructure is superior because of higher stability of M_2C carbides in ferrite.

(g) Interactive type solid solution strengthening plays an important role in conferring stress rupture strength to 2 1/4Cr-1Mo steel. Interactions between substitutional (Cr, Mo) and intersticial (C, N) atoms are described.

The effects of individual alloying elements may be summarized as follows:

(a) Increasing levels of chromium, silicon, aluminum and manganese decreases rupture strength.

(b) Increasing levels of molybdenum, vanadium, titanium and niobium improves rupture strength.

(c) Stress rupture strength increases as the carbon content is increased. However, the effect is only significant for carbon levels below about 0.04%. Furthermore, as the temperature increases, the strengthening effect decreases until 1000°F, after which the strength advantage becomes insignificant.

(d) The influence of boron additions on rupture strength is not clear except for the fact that boron additions decreases creep ductility. The effect of boron on rupture strength appears to depend on the levels of other elements present including titanium, phosphorous, tin and antimony.

(e) Tin and phosphorus appear to increase the creep rate with the latter also increasing the creep ductility. The influence of phosphorus is further bolstered by increasing the carbon content.

(f) At levels upto 1.0%, increasing the nickel concentration does not affect the rupture strength.

The discussion of the effects of service exposure and lifetime prediction methods may be summarized as follows:

(a) The loss of strength during service is due to changes in the carbide type, size and morphology and depletion of the matrix of the solute elements thereby resulting in an increase in the interparticle spacing where creep cavities can easily nucleate.

(b) Among the various methods available for remaining lifetime prediction, isostress creep testing is the only method which is somewhat quantitative. In-situ replication technique is however, the most popular technique because of its non-destructive nature.

(c) Some of the other methods utilizes measuring changes in the acoustic, ultrasonic and micromagnetic properties of material due to service exposure for lifetime prediction. These methods, however, are relatively new and need more research.

The discussion of the analysis of stress rupture data may be summarized as follows:

(a) The objective of the stress rupture testing is to gather data on rupture time as a function of applied stress and test temperature for a particular material. The ultimate goal is to characterize the behavior of the material sufficiently so that establishment of allowable stress levels for design purposes is possible.

(b) Some of the analytical techniques currently employed in rupture data analysis include the log stress/log rupture time method and various time/temperature parameter methods.

CHAPTER 3

MATERIALS AND EXPERIMENTAL PROCEDURE

The goal of this program was to investigate the effect of heat treatments on the stress rupture strength of 2 1/4Cr-1Mo weldments. 2 1/4Cr-1Mo steel has been used extensively for the fabrication of power plant and chemical processing plant and elevated temperature, high pressure piping and other components. After welding various heat treatment practices have been used by the industries to relieve the residual stresses and to increase the toughness of the weld metal. These heat treatments are annealing and tempering (A&T) or normalizing and tempering (N&T) or subcritical stress relief heat treatment. This study was essentially divided into two parts to probe into the long time stress rupture behavior of 2 1/4Cr-1Mo weldments heat treated to different conditions. First, the effect of annealing and tempering, normalizing and tempering, and subcritical postweld heat treatment have been studied. Secondly, the effect of severity of subcritical postweld heat treatment, which is in fact more popular, has been studied to establish its effect on the long time rupture behavior.

In order to establish the effect of heat treatment, rupture tests were conducted on all weld metal and transverse composite (weld metal, heat affected zone and base metal) creep specimens. For the first phase of the study, a submerged arc weldment was fabricated. Pieces from the weldment were annealed and tempered, normalized and

tempered and subcritically postweld heat treated. Both, longitudinal all-weld metal and transverse composite specimens were tested. For the second phase of the study a shielded metal arc weldment was used to determine the effect of severity of postweld heat treatment on the rupture strength of the weld metal. Sections of this weldment were given a range of subcritical postweld heat treatments (seven temper parameters from 32.3 to 38.7). 100 percent weld metal specimens were extracted longitudinal to the welding direction from the postweld heat treated blocks and rupture tested in this phase of the study.

To support the rupture testing effort, extensive microstructural examination of the above weldments in the as welded, heat treated and rupture tested condition was performed using the SEM and STEM. This microstructural work was aimed at characterizing the microstructure as a function of heat treatment with an ultimate goal of correlating the microstructure with the stress rupture properties. SEM examination revealed the dependence of microconstituent morphology on prior heat treatment history. Furthermore, STEM examination of carbide extraction replicas was also conducted to obtain information on the type, size, morphology, distribution and composition of the alloy carbides present.

3.1 MATERIALS

Two 2 1/4Cr-1Mo weldments were fabricated for this study using two different welding processes. A submerged arc weldment was used to study the effect of anneal and temper, normalize and temper and

subcritical postweld heat treatments on the rupture strength. The shielded metal arc weldment was used for the temper parameter study. The chemical composition of the base metal and the two different weld metals are shown in table 2.

All weld metal stress rupture specimens were extracted longitudinal to the welding direction. Transverse creep specimens were extracted transverse to the welding direction in such a manner so that the heat affected zone was at the center of the sample (see figure 13). The weldments were fabricated in 2 1/2 inch thick SA 387 Grade 22 plate using a single V-groove preparation employing a backing bar. In addition a thick backing plate was welded to avoid the weldment from bending due to solidification stresses.

Welding was conducted using good low hydrogen practice and a preheat/interpass temperature of 300/375^{o}F was maintained untill welding was completed. Subsequent to the completion of welding and before dropping preheat, the weldment was postheated at 500^{o}F for 12 hours and then cooled to room temperature. After cutting the run off tabs the welds were sectioned and the pieces were heat treated.

From the submerged arc weldment three pieces were cut and heat treated as per the schedule shown in table 3. External thermocouples were placed below the specimen for accurate temperature control. The shielded metal arc weldment was sectioned into seven pieces and the sections were postweld heat treated and aged. The temperatures, times and the resulting temper parameters are shown in table 4. The temper parameter (TP) was calculated using the equation,

$$TP = (T+460)\ (20+\log t)\ X\ 10^{-3}$$

Table 2. Chemical composition of base metal and weld metals employed in this study.

Element	Base Metal	SAW Weld Metal	SMAW Weld Metal	AWS A5.5-81
C	0.11	0.07	0.081	0.05-0.12
Mn	0.38	0.54	0.55	0.90 max
P	0.011	0.010	0.012	0.03 max
S	0.022	0.006	0.009	0.04 max
Si	0.29	0.22	0.36	0.80 max
Cu	0.15	0.28	0.04	-
Ni	0.15	0.19	0.03	-
Cr	2.07	2.69	2.15	2.00-2.50
Mo	0.88	0.97	1.15	0.90-1.20
V	<0.004	<0.004	0.005	-
As	0.007	0.012	0.007	-
Sb	0.009	0.009	<0.001	-
Bi	<0.005	<0.002	ND	-
Sn	0.012	0.006	0.004	-
Pb	<0.001	<0.012	ND	-
Ti	<0.006	<0.006	0.009	-
Al	0.008	0.024	<0.001	-
Nb	ND*	0.005	0.003	-
B	0.0003	0.0004	<0.001	-
Zr	ND	0.004	<0.001	-
Co	ND	0.017	0.007	-
Te	ND	0.004	ND	-

*ND - Not Determined

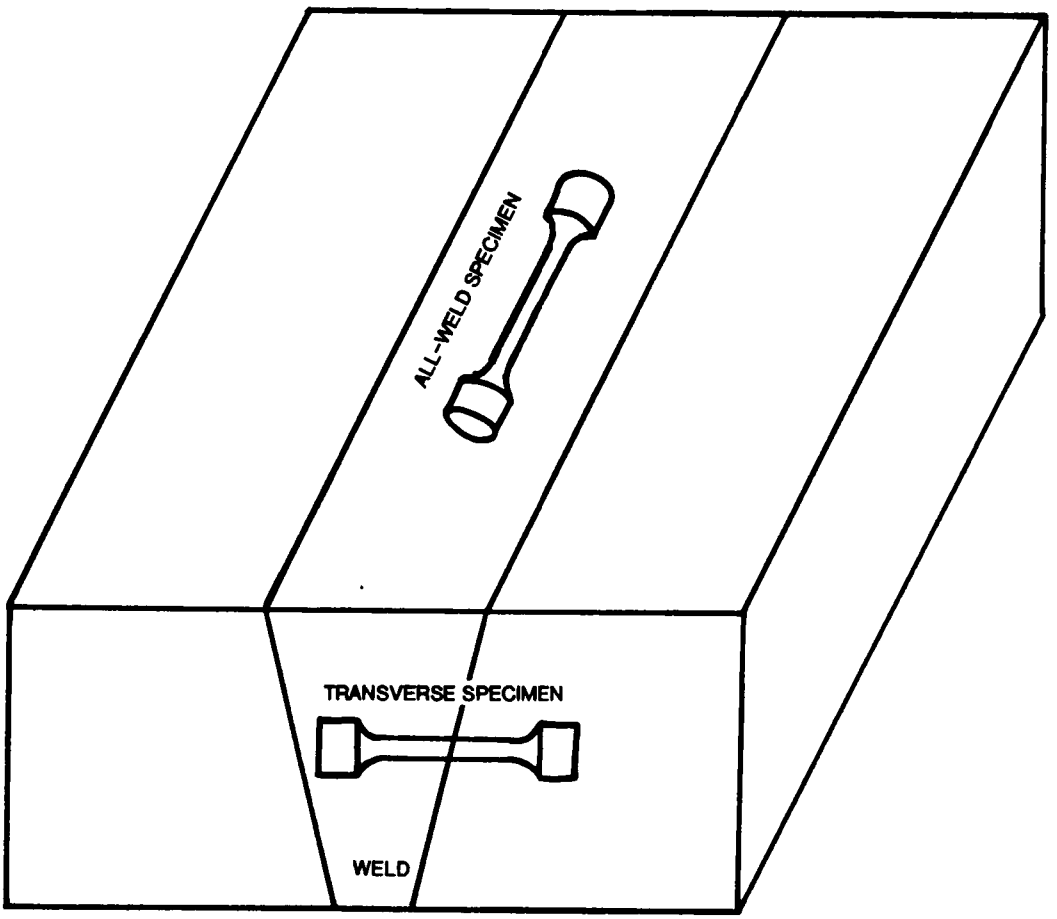

Figure 13. Orientation of all-weld metal longitudinal and composite transverse specimens.

Table 3. Schedule for heat treatment of the submerged arc weldment.

HEAT TREATMENT		TEMPERATURE/TIME
A&T	Annealed and Tempered	Austenitized 1700°F (926°C) Tempered 1300°F (704°C) for 2 hours
N&T	Normalized and Tempered	Austenitized 1700°F (926°C) Tempered 1300°F (704°C) for 2 hours
PWHT	Postweld Heat treated (Cl.2)	1300°F (704°C) for 25 hours

Table 4. Schedule for postweld heat treatment of the shielded metal arc weldment.

POST WELD HEAT TREATMENT	TEMPER PARAMETER
1050°F (565°C), 25 hours	32.3
1100°F (593°C), 25 hours	33.4
1150°F (621°C), 25 hours	34.4
1100°F (621°C), 25 hours Aged 1193°F (645°), 21.5 hours	35.3
1250°F (677°C), 25 hours	36.6
1300°F (704°C), 25 Aged 1193°F (645°C), 21.5 hours	37.7
1350°F (704°C), 25 hours	38.7

where "T" is the temperature in ^{o}F and "t" is the time in hours at the postweld heat treatment temperature. In case of aging the time at the aging temperature has been converted to an equivalent time at postweld heat treatment temperature using the above relation and the resulting temper parameter calculated. For the temper parameter study only longitudinal all-weld-metal samples were extracted for stress rupture testing.

3.2 STRESS RUPTURE TESTING

To determine the effect of heat treatment on the stress rupture strength, rupture testing of the 2 1/4Cr-1Mo weldment was conducted in three phases. In the first phase all weld metal longitudinal specimens from the submerged arc weldment with different heat treatments (annealed and tempered, normalized and tempered and postweld heat treated (class 2)) were rupture tested at 950 and $1050^{o}F$. The temperature selected is representative of the current and anticipated operating range of 2 1/4Cr-1Mo pressure vessels.

Next, transverse composite specimens from the submerged arc weldment in annealed and tempered, normalized and tempered and postweld heat treated (class 2) were rupture tested at 950 and $1050^{o}F$. The composite specimens were machined so that the heat affected zone is approximately at the center of the specimen gage length. In addition, isostress testing of transverse specimens in annealed and tempered condition was also conducted at 11 KSI. The stress level of 11 KSI was selected for isostress rupture testing

based on the maximum allowable stress at 950°F as per the ASME Boiler and Pressure Vessel Code, Section VIII, Division 2.

From the shielded metal arc weldment subcritically postweld heat treated and aged to a range of temper parameters (32.3 to 38.7), 100 percent weld metal rupture specimens were fabricated with their longitudinal axis parallel to the welding direction . The specimens were rupture tested at 950°F at different stress levels to achieve rupture times ranging from about hundred hours to several thousand hours. Additional isostress testing was conducted for four selected temper parameters (32.3, 34.4, 36.6, and 37.7) at 16.5 KSI. The stress level for isostress testing was selected to be 16.5 KSI since ASME Boiler and Pressure Vessel Code specifies the maximum allowable stress at 950°F to be 11 KSI (based on the assumption that the allowable stress is 2/3 the stress to cause rupture in 100,000 hours ie. 16.5KSI).

Stress rupture test specimens used for this program were of two different types as shown in figure 14. The threaded test specimens were used for testing at 950 and 1050°F. For testing at higher temperatures specimens without threads were used with a slit type holder on the creep frame. The reason for the use of rupture test specimens without threads is for the ease of removal of the specimen from the holder after testing. The threaded test specimens are relatively difficult to remove from the holders after testing due to oxidation, especially for tests at higher temperature and longer times. In each case the specimen gage length is 1.125 inch with a gage diameter of 0.125 inch. The small size rupture specimen not

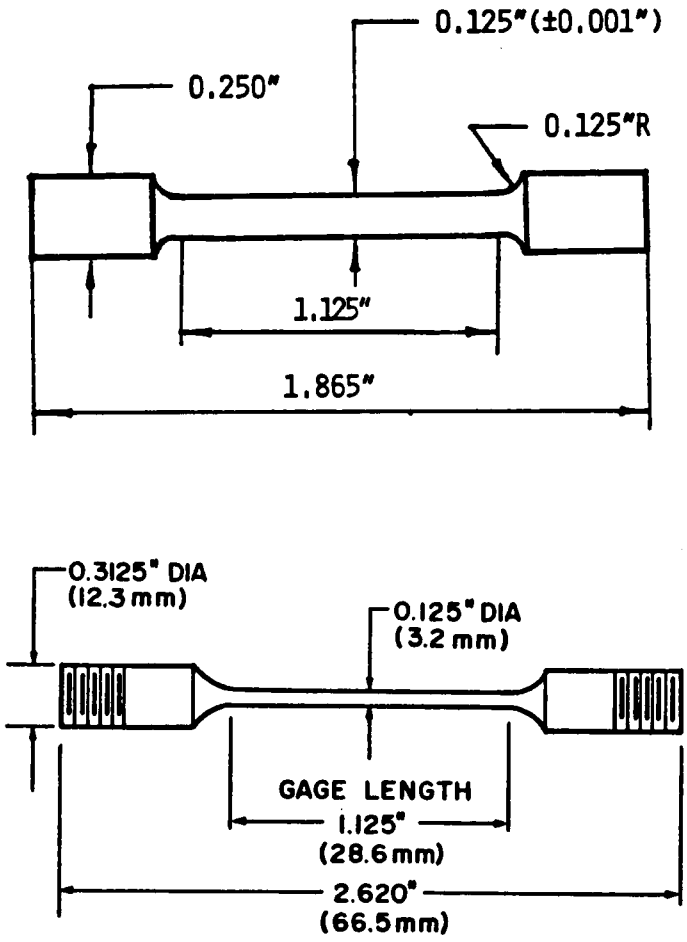

Figure 14. Stress rupture test specimens.

only increased the number of specimens which could be fabricated from a given length of weldment, but also kept the load requirements in necessary bounds so as to obtain rupture times in the range of ten to several thousand hours and allow operations within the capabilities of the testing apparatus.

Rupture testing was conducted on eight constant load, dead-weight creep frames. Each frame contains a three-zone furnace with the power level of each zone independently adjustable. Each furnace is controlled by a Leeds and Northrup Electromax III controller which utilizes a chromel-alumel thermocouple to monitor the temperature at the center of the middle zone. All furnaces were profiled and the zone controls used to obtain a constant temperature profile over the specimen gage length ($\pm 1F^{o}$).

Each specimen was mounted in a testing frame and suspended within the furnace. Figure 15 shows a schematic view of the test geometry. A chromel-alumel thermocouple wired to the center of the specimen gage length was connected to a digital temperature readout which, in turn, was used to monitor the temperature of the specimen during testing. To minimize convection through the furnace, both the top and bottom openings of the furnace were packed with ceramic wool. At the beginning of each test, the specimens were heated to the desired temperature and stabilized there prior to loading. Loading was in uniaxial tension and maintained constant throughout the test. In addition to the temperature, specimen extension measured by a dial gauge attached to the testing frame, was also recorded as a function of time.

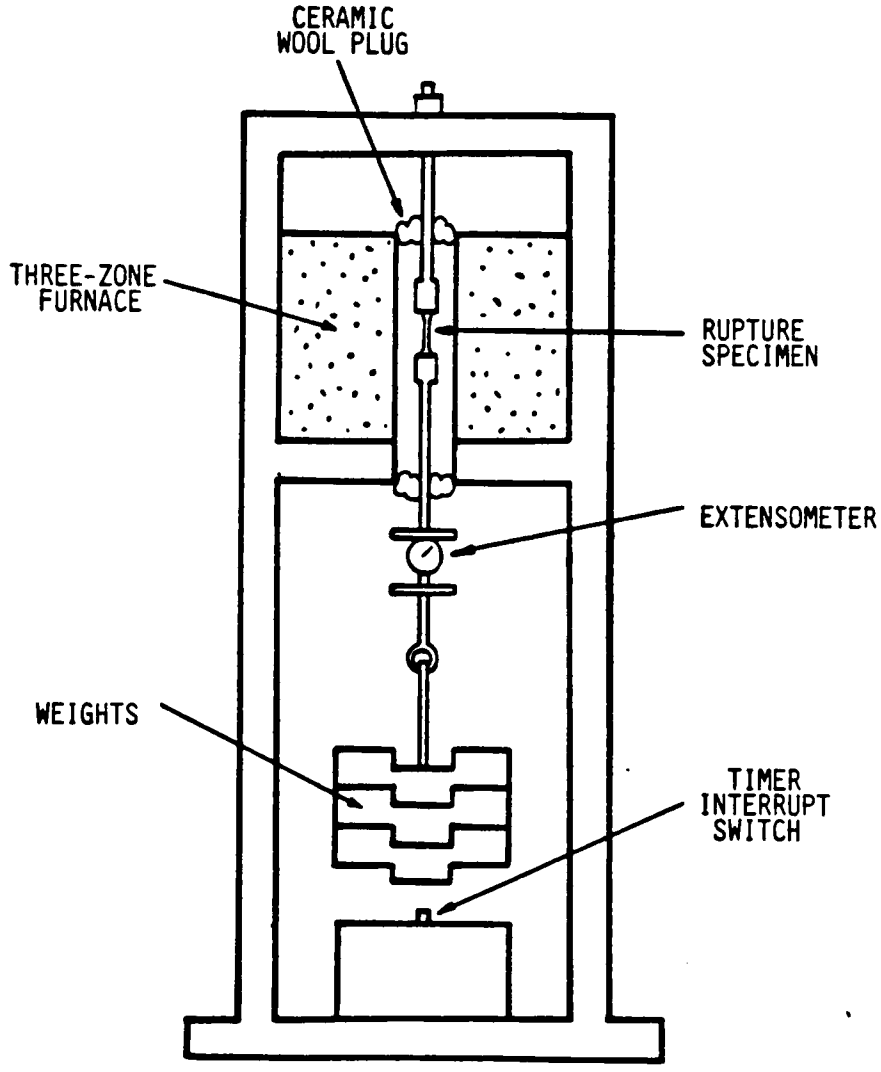

Figure 15. Schematic representation of a creep frame with specimen.

The rupture data obtained were analyzed using the following two techniques to determine the effect of heat treatment on the stress rupture strength:

(a) the log stress/log rupture time method, and

(b) the Larson-Miller parameter method.

Comparison of the 100,000 hour stress predictions derived using each method were also made.

For analysis of rupture data using the log stress/log rupture time approach, a model for stress as a function of rupture time given by

$$\log(s) = A + B \log(t_R)$$

was assumed, where, "s" is stress in KSI, "t_R" is the rupture time in hours and "A" and "B" are the regression constants. Using linear regression analysis, the best fit was calculated. Stress for 100,000 hour rupture time was also obtained by extrapolation. Because this model does not include a temperature term, the above analysis had to be performed for each temperature at which data were available.

Analysis of rupture data using the Larson-Miller parameter was also conducted. A parameter value for each data point was calculated using the equation

$$LMP = (T + 460)\ (C + \log t_R)\ X\ 10^{-3}$$

where, "T" is the test temperature in ^{o}F, "C" is a constant, and "t_R" is the rupture time in hours. A value of 20 was used for "C" for all analyses and is generally accepted as a average value applicable in most cases. After plotting the data on a log stress vs. Larson-Miller parameter graph, curves were fitted to the data using

regression analysis techniques. In a majority of cases, a quadratic equation of the form

$$\log(s) = A + B\ (LMP) + D\ (LMP)^2$$

was used in the analysis where "s" is the stress in KSI, "LMP" is the Larson-Miller parameter, and "A", "B", and "D" are regression constants. The resulting curves provided a reasonable data fit except where only a few data points were available. In such cases, application of a quadratic fit sometimes resulted in a curve which was concave upwards. As an alternative, in such cases, regression was performed using a linear fit of the form,

$$\log(s) = A + B\ (LMP)$$

The curve fits were used to calculate stress for 100,000 hour rupture.

For isostress testing the data were plotted as log rupture time vs. test temperature and linear regression analysis were carried out to fit the data to the equation of the form

$$\log(t_R) = A + B\ (T)$$

where "t_R" is the rupture time in hours, "T" is the test temperature in ^{o}F, and "A" and "B" are the regression constants. The data fit was then used to determine the rupture life at different test temperature for the augmented stress. Both linear and nonlinear (quadratic) regression analyses on the data were performed using commercially available statistical and graph plotting softwares for IBM PC's.

3.3 TENSILE TESTING

Room temperature and elevated temperature tensile tests of samples extracted from the submerged arc weldment with the longitudinal specimen axis parallel to the welding direction as well as transverse to the welding direction (to contain weld metal, HAZ and base metal in the gage length) was carried out for A&T, N&T and PWHT(C1.2). Only the all-weld-metal specimens extracted parallel to the welding direction were tested in the temper parameter study. Standard 0.25 inch gage diameter specimens were employed as per the ASTM E8. Values determined from the tensile test include 0.2 percent yield strength, ultimate tensile strength, percent elongation and percent reduction in area.

3.4 METALLOGRAPHIC PREPARATION

Microstructural analysis of the weld metal, heat affected zone and base metal was performed using the SEM and STEM. Because of the exceptionally fine microstructure of the material optical microscopy was of minimal value. SEM examinations upto 20,000X were employed to characterize the morphology of the major microconstituents. The alloy carbides in the microstructure proved to be too small to analyze using the SEM. As an alternative the carbides were extracted from the surface of polished and etched specimens using carbon film replication techniques. With the aid of a STEM, the resulting extraction replicas were examined at magnifications upto 100,000X with selected carbides identified by their morphology, X-ray spectra and chemical composition.

Samples to be examined microstructurally in the SEM were cut, mounted and ground on successively fine emery papers starting with 120 grit and ending with 600 grit. Coarse polishing was accomplished using 6 micron diamond paste. Fine polishing was done with an 0.05 micron alumina powder suspended in distilled water. A three step polish-etch technique was used to prevent a disturbed metal layer on the surface. The samples were etched in a 2 percent nital solution in most cases.

In preparation for viewing in the SEM, the epoxy on the metallographic mount was coated with carbon paint to provide a conductive path for the electrons from the sample to the microscope stage. To improve resolution at high magnifications, the surface of the specimen was sputtered with gold to produce a surface layer approximately 200 angstroms thick.

An AMR 900 Scanning Electron Microscope was used to examine the microstructures. Experience revealed that the best micrographs were obtained when the polished surface of the metallographic specimen was given a relatively heavy etch and viewed with the specimen tilted about 30 degrees towards the detector.

For the preparation of carbon extraction replicas the specimens mounted in epoxy were mechanically polished to metallographic quality as described earlier. The specimens were then electroetched in 10% HCl-90% methanol solution using a current density of 0.20 to 0.25 amp/cm^2 for 30-40 seconds. Carbon was deposited on the specimen (100-200A) using standard vapor deposition techniques. The specimens which appeared golden yellow to light blue after carbon deposition

gave the best results because of optimum carbon film thickness. The specimens which turned black after carbon vapor deposition were polished and coated again. After carbon deposition the specimen surface, except for the area of interest, was painted with enamel. After the enamel paint dried the replica was electroetched again in 10% HCl-90% methanol solution using the same conditions and the replica was floated in distilled water. The replicas were collected on the dull side of 200/50 SPI copper grids and preserved carefully in covered pyrex dishes on filter paper for drying and future TEM/STEM study.

The STEM/TEM study was accomplished on a Hitachi H-800 microscope (with a Gatan Model 607 for STEM image) equipped with an energy dispersive X-ray spectrometer (Kevex Quantum detector) which is interfaced with Delta 4 Processor for data acquisition. A beam spot diameter of about 10nm was used for all analysis work with an accelerating voltage of 100KeV, resulting in an overall resolution of approximately 30nm. The spectrum acquired was analyzed by the dedicated processor for calculation of the composition of the carbide particles using thin film approximation and correction for background.

CHAPTER 4

RESULTS AND DISCUSSION

The goal of this program was to investigate the effects of heat treatment on the stress rupture properties of 2 1/4Cr-1Mo weldments. 2 1/4Cr-1Mo steel has been extensively used for pressure vessel applications. Submerged arc welding has been the most popular process for fabrication of pipes and pressure vessels because of the high productivity of the process. This process is most suitable where high deposition rates are required for optimum economy. Some of the recent failures of hot reheat pipes in the industry fabricated by submerged arc process, while in service within its design lifetime has encouraged this research to be undertaken. Postweld heat treatment (either A&T or N&T or PWHT (C1.2)) is normally used subsequent to welding. Thus, as one phase in this program a submerged arc weldment was fabricated to study the effects of the A&T, N&T and PWHT (C1.2) heat treatment on the stress rupture strength.

The most popular postweld heat treatment in current industry practice is subcritical (below Ac1) as required by the ASME/B31.1 codes. The temperature and time of the subcritical heat treatment affects the initial creep strength of the weld metal. The creep strength of 2 1/4Cr-1Mo steel or weld metal is based on the carbide type, size and distribution. PWHT is associated with carbide coarsening process and thus the severity of PWHT determines the

"status" of carbides in the weld metal, thus dictating its creep strength. Elevated temperature service (or creep testing) is also associated with a carbide coarsening process which is governed by similar laws of diffusion which controls carbide coarsening process during PWHT. Thus, it is felt that it is possible to predict life of welded components in service from a knowledge of its prior PWHT plus service history. Therefore, to examine the loss of stress rupture strength after PWHT at various temperatures, a state-of-the-art SMA weldment was fabricated. The time and temperature of PWHT was combined together to form a parameter which is termed as "temper parameter" throughout this study.

The macrographs of SA Weldment and SMA weldments are shown in figures 16 and 17, respectively. The preparation of the weldments are described in detail in chapter 3. The macrographs clearly show the sequence of bead placement. No discontinuities were found in either of the weldments by radiography or during subsequent metallographic examination.

4.1 CARBON MIGRATED "SOFT" ZONE IN SA WELDMENT

The chemical composition of base metal and weld metal of the submerged arc weldment is shown in Table 2. It can be seen that there is a difference in the chromium content of the base metal and weld metal. The base metal contains 2.07% Cr and the weld metal contains 2.69% Cr. Upon subsequent heat treatment of the weldment a ferritic band appeared adjacent to the fusion line in the HAZ. This ferrite band is due to carbon migration from the low chromium side

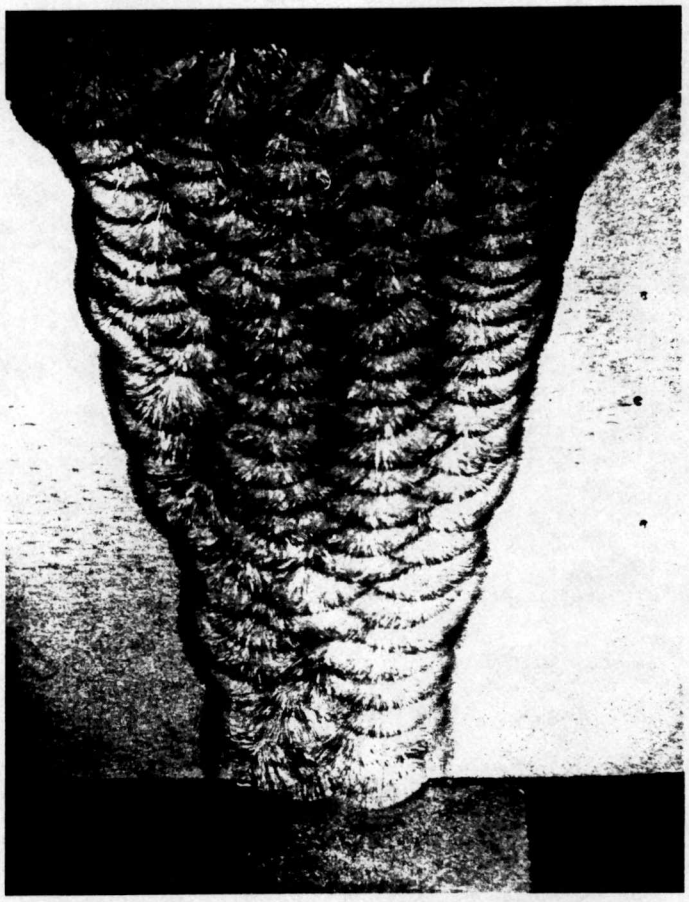

Figure 16. Macrograph of the submerged arc weld in as-welded condition, 1.4X, Hrubec's etch.

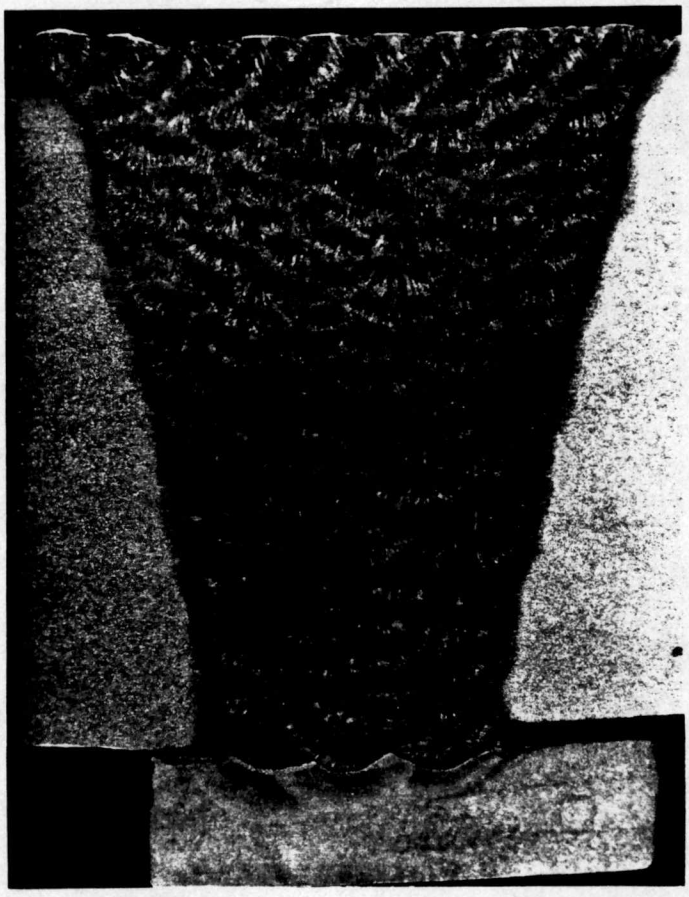

Figure 17. Macrograph of the shielded metal arc weld in PWHT (1050°F-25 hrs.) condition, 1.4X, $3HCl\text{-}2H_2O\text{-}1H_2O_2$ etch.

(high activity of C) to the high Cr side (low activity of C). The properties of such a carbon denuded zone occurring in welds of matching composition has not been previously investigated with respect to its effect on long term behavior in service.

The occurrence of such a carbon denuded "soft" zone caused by migration of carbon from the lower alloying element side to the higher alloying element side has been reported in literature[105-112]. However, all investigators have discussed the occurrence of such a soft zone between dissimilar metal welds such as austenitic to ferritic steel and high alloy ferritic steel to low alloy ferritic steel.

In the literature[105], failures due to a weakened "soft" ferritic zone dates back to 1935 when carbon steel boiler drums were welded with austenitic electrodes in order to avoid subsequent PWHT. Research on joining of such low alloy ferritic steel to austenitic steel using austenitic steel electrodes has shown the presence of large ferrite grains in the low alloy steel HAZ along the fusion line. Emerson and Hutchinson[105] have indicated that stabilizing the carbides of the low alloy steel by use of alloying elements such as vanadium and titanium has a beneficial effect in retarding the formation and growth of such exaggerated soft ferrite grains. Further studies showed that carbon migration is not a serious problem during operation at temperatures as high as 1050°F since the diffusion rate of carbon in ferrite is relatively slow at 1050°F. The major reason for development of such a zone in welded steam piping is due mainly to the higher temperatures of postweld heat

treatment and thus the zone is present when the component begins service. A review of published and unpublished literature on dissimilar metal welding conducted by Thielsch[106] showed that many service failures have taken place due to presence of such a soft carbon denuded zone along the fusion line. A hardness survey on 4.9%Cr-0.7%Mo-0.16%C steel welded with 25Cr-19Ni electrode removed from service after 10,000 hours at 1290°F showed a hardness difference of about 160DPH between the soft zone and the adjacent carbon enriched weld metal[107]. Christoffel and Curran[108] conducted tests on about 12 combinations of low alloy ferritic and high alloy ferritic and austenitic steel weldments and concluded that carbon migration had a profound effect on physical properties and the decision of use of such combinations at temperatures at which carbon migration may occur should be carefully made. In other published research[109] laboratory tests conducted on a full size austenitic-ferritic transition joint showed satisfactory behavior at 3500psi and 1100°F under cyclic temperature testing with super-critical steam pressure. A recent review of available literatures conducted by Lundin[112] considered various problems in dissimilar metal welds in which carbon migration and subsequent development of a soft zone has been given the prime importance. Thus, the literature reported incidents of failures and successful operation of transition joints is confusing. Under what conditions a transition joint will fail or successfully operate is not clearly evident.

However, the occurrence of such a "soft" zone in 2 1/4Cr-1Mo steel weldment, because of differences in Cr concentrations between

the base metal and weld metal, have not been reported in the literature. The carbon denuded zone is primarily due to chromium differences although, Mn and Si differences are also believed to play a role in the development of such a ferrite band.

The long term effect on behavior of a "soft" region in a "matched" chemistry weldment is unknown. Several recent failures in utility steam piping which were reported to occur along the fusion line encouraged this study to be undertaken to determine the significance of such a zone on long time service of weldments.

The "soft" carbon denuded ferritic zone was seen to be the most prominent and widest in A&T heat treatment of the submerged arc weldment. In the N&T condition this soft zone was found to be a few grains wide and for a subcritical post weld heat treatment this zone was nonexistent in most areas. Figure 18 shows the extent of "soft" zones in the A&T and N&T condition. Thus, it can be concluded that carbon migration from the low Cr region to the high Cr region occurs during both the austenitization heat treatment and during cooling from the austenitization temperature. During annealing and normalizing the austenitization temperature ($1700^{o}F$) and hold time (1 hour) was the same. So it is reasonable to believe that the carbon migration from the base metal side of the fusion line to the weld metal, controlled by diffusion laws, will be to the same extent in both cases during the austenitization heat treatment. The differences in the extent of "soft" zone in annealed and normalized structure is hence due to the slow cooling during annealing and faster cooling during normalizing.

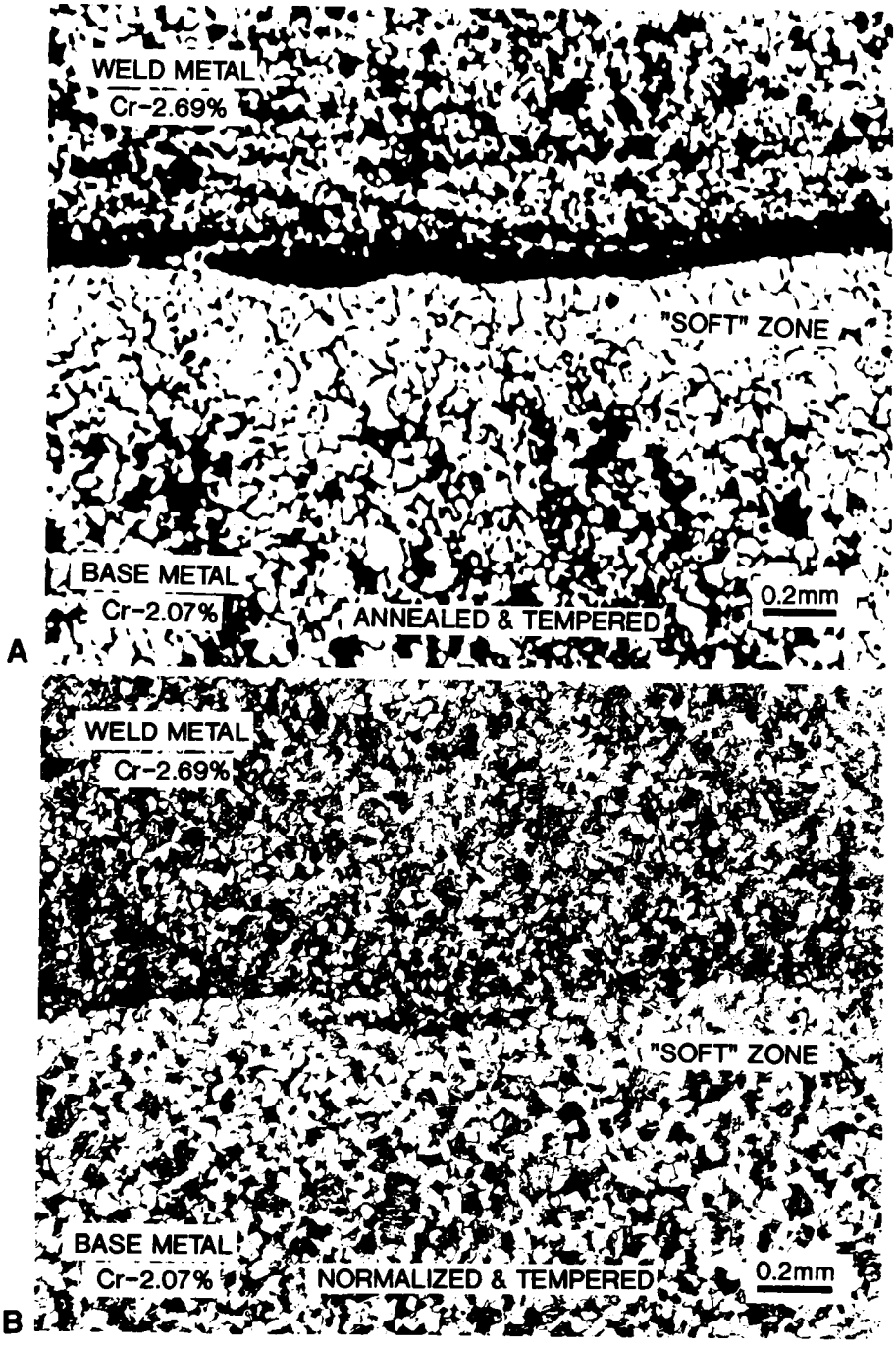

Figure 18. "Soft" zone in SA weldment in (a) A&T condition, (b) N&T condition, 50X, 2% nital etch, OLM.

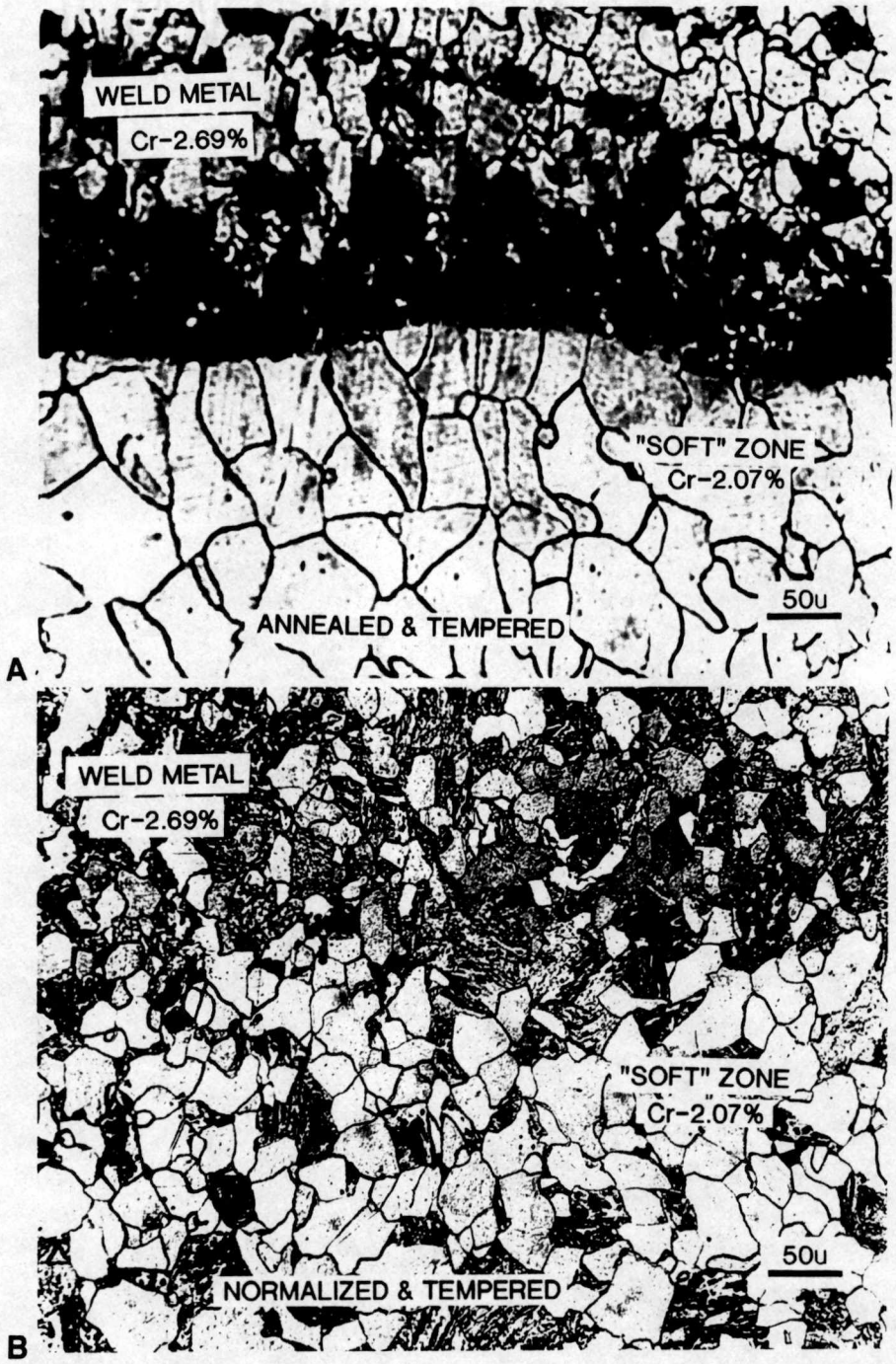

Figure 18. Continued
(c) A&T condition, (d) N&T condition, 200X, 2% nital etch, OLM.

The diffusion rate of carbon in ferrite and austenite depends on the temperature, the driving force for diffusion being the difference in activity of carbon. The equation for calculating the diffusion coefficient is given as

$$D = D_o \, e^{-(Q/RT)}$$

where, D_o is a constant, Q is the activation energy and R and T have their usual meaning. The value of D_o and Q is different for carbon diffusion in ferrite and austenite and is given as

in ferrite D_o=0.006 cm^2/sec Q=80,000 J/mole

in austenite D_o=0.2 cm^2/sec Q=135,000 J/mole.

From the above expression the diffusion coefficients of carbon in austenite and ferrite can be calculated for different temperatures. At 1700°F, D for carbon in austenite is $2.647X10^{-7}$ cm^2/sec, and at 1300°F, D for carbon in ferrite is $3.183X10^{-7}$ cm^2/sec. So, it is clear that carbon moves faster in ferrite even at a lower temperature. This is because of the fact that ferrite is body centered cubic and is less densely packed compared to face centered cubic austenite. Hence, the diffusivity of carbon in ferrite is higher than in austenite and in the intercritical region this difference is still substantial. For example, at 1400°F, D in austenite is $2.981X10^{-8}$ cm^2/sec, and D in ferrite is $5.404X10^{-7}$ cm^2/sec which is more than an order of magnitude higher. So, it is reasonable to believe that the difference in the extent of soft zones in N&T and A&T conditions is due to faster cooling in N&T and slower cooling in A&T.

The subsequent tempering at 1300°F for two hours is not significant in the development or extension of this soft zone, since the weld subcritically PWHT to Class 2 specification, which constitutes a hold of 25 hours at 1300°F failed to develop a "soft" zone beyond one grain width. However, prolonged exposure at elevated temperatures during service can cause such ferritic zones to develop and grow. Unpublished work at the University of Tennessee[113] has shown several such incidences in utility pipings (the pipe was installed in service after a subcritical PWHT and hence it is reasonable to believe that the soft zone was almost nonexistent after PWHT) where ferritic zones have appeared during service exposure both within passes in weld metal and along the fusion line. Examples of such soft zones are shown in figures 19a and b. The soft zones illustrated in figure 19 not only show a ferritic band along the fusion line and along weld passes but also excessive growth of the ferritic grains in these regions. This sample was extracted from a 2 1/4Cr-1Mo base metal-2 1/4Cr-1Mo weld metal submerged arc weldment installed in service after subcritical PWHT and had approximately 20 years of service at 1050°F.

In the current work the "soft" zone in the A&T heat treated condition was the widest for the heat treatments conducted and thus hardness measurements were performed to determine the extent of softening in this region compared to the adjacent carbon enriched region and the base metal and weld metal remote from the interface. Hardness measurements on A&T specimens revealed a hardness approximately 35 DPH lower in the soft zone compared to the adjacent

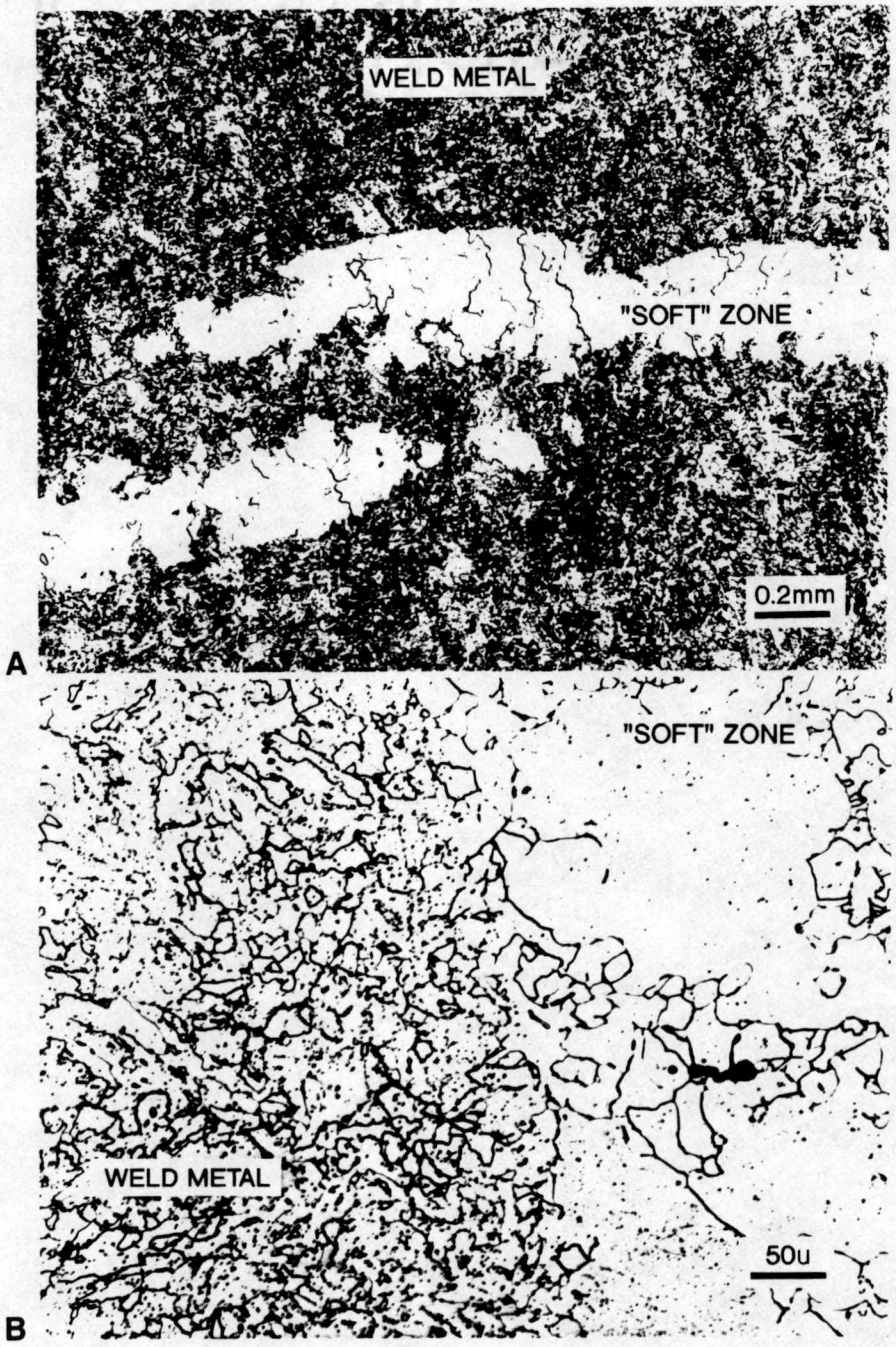

Figure 19. "Soft" zones in 2 1/4Cr-1Mo base metal, 2 1/4Cr-1Mo weld metal service exposed weldment (184,000hrs.-1050°F-4.5KSI) subcritically PWHT prior to service, (a) between weld passes, 50X, (b) along fusion line, 200X, 2% nital etch, OLM.

enriched zone. The soft zone was found to be 15 DPH softer than base metal and 10 DPH softer than the weld metal remote from the fusion line. Knoop indentations in the soft zone and the adjacent carbon enriched zone are shown in figure 20. A hardness difference of 35 DPH indicates a difference in tensile strength of about 17.5 Ksi at room temperature and 13.6 Ksi at 950°F which is significant when considering elevated temperature applications.

4.2 TENSILE TEST RESULTS AND DATA ANALYSIS

Tensile specimens of base metal and weld metal extracted parallel to the welding direction, and tensile specimens extracted transverse to the welding direction (to contain base metal, HAZ (including the above mentioned "soft" zone) and weld metal in the gage length) from the submerged arc weldment were tested at room temperature, 950°F and 1050°F in the A&T, N&T and PWHT (C1.2) conditions. The offset 0.2% yield strength, ultimate tensile strength, % elongation and % reduction in areas are shown in Table 5. One important behavior noticed from the tensile testing was that none of the transverse specimens ruptured in the "soft" zone. All the transverse specimens regardless of the condition of heat treatment ruptured in the weld metal away from the fusion line. This may be due to the fact that the ferritic zone is more ductile than the adjacent harder regions and so work hardens faster and to a greater extent due to plastic flow than the adjacent regions. Such behavior has been reported in the literature[107,108] in that tensile specimens from transition joints between dissimilar metals did not rupture in

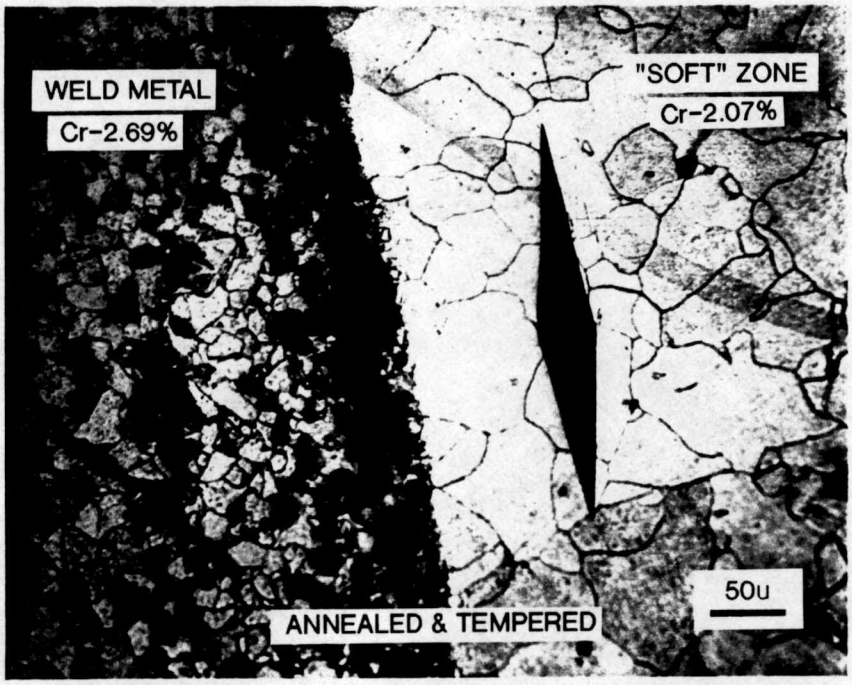

Figure 20. Knoop indentations in A&T SA weld revealing that the hardness of the "soft" zone is about 35 DPH lower than the adjacent carbon enriched zone, 200X, 2% nital etch, OLM.

Table 5. Tensile test results of A&T, N&T and PWHT(Cl.2) submerged arc weldment.

Specimen	Test Temp. (°F)	0.2% Offset Yield Str. (Ksi)	Ultimate Str. (Ksi)	Elong. %	RA %
BM-PWHT	RT	46.4	72.3	34.0	77.3
WM-PWHT	RT	57.7	77.1	28.7	71.0
TT-PWHT	RT	48.4	73.3	27.8	76.7
BM-A&T	RT	42.5	68.5	41.0	73.3
WM-A&T	RT	40.1	64.5	43.7	77.6
TT-A&T	RT	40.2	66.4	32.7	74.1
BM-N&T	RT	51.1	76.4	34.6	74.9
WM-N&T	RT	50.1	78.7	33.6	74.9
TT-N&T	RT	51.9	75.1	35.0	71.5
BM-PWHT	950	32.5	56.1	30.6	77.1
WM-PWHT	950	43.5	56.3	32.9	79.3
TT-PWHT	950	39.4	57.1	26.9	77.2
BM-A&T	950	28.2	59.6	33.0	70.7
WM-A&T	950	26.2	54.6	36.0	69.4
TT-A&T	950	25.0	55.9	31.0	69.4
BM-N&T	950	40.5	60.1	34.0	68.5
WM-N&T	950	40.6	57.8	27.0	73.7
TT-N&T	950	37.2	58.1	25.0	69.4
BM-PWHT	1050	30.6	45.5	33.7	80.3
WM-PWHT	1050	41.4	53.6	36.0	82.7
TT-PWHT	1050	35.9	47.0	23.8	79.8
BM-A&T	1050	26.2	49.1	34.5	78.4
WM-A&T	1050	24.4	45.8	47.0	78.7
TT-A&T	1050	22.9	47.4	33.2	76.1
TT-A&T-A	1050	21.5	50.1	28.9	74.9
BM-N&T	1050	36.7	50.6	45.3	82.9
WM-N&T	1050	30.7	48.9	42.8	81.9
TT-N&T	1050	37.4	49.2	31.5	80.6
TT-N&T-A	1050	27.5	48.2	31.0	78.7

BM-Base Metal
WM-Weld Metal
TT-Transverse Tensile
PWHT-Cl.2 (1300°F-25 hrs.)
A&T-Annealed and Tempered } Austenitized 1700°F
N&T-Normalized and Tempered } Tempered 1300°F-2 hrs.
A&T-A } Additional Treatment 1300°F-5.5 hrs.
N&T-A

the soft zone. In such cases the rupture was seen to occur in the low alloy ferritic material. This behavior may also be due to a constraint effect exerted by the adjacent regions, stronger than the soft zone, thereby resulting in rupture in the weld metal as opposed to rupturing in this ferritic zone. Research conducted at the University of Tennessee under 1987 WRC grant-in-aid[114] to determine the structure and properties of "soft" zones developed between 2 1/4Cr-1Mo base metal welded with 9Cr-1Mo weld metal showed that the rupture of tensile specimens occurred in the 2 1/4Cr-1Mo base metal as opposed to the "soft" ferrite region developed as a result of PWHT. However, a strain distribution study by Moire interferometry techniques on flat tensile specimens extracted from 2 1/4Cr-1Mo base metal-9Cr-1Mo weld metal weldment subcritically PWHT to obtain a wide soft zone showed that at first plastic flow occurred in the soft zone and subsequently the flow pattern changed and final rupture of the specimen occurred in the base metal. However, this study was performed at room temperature. Stress rupture tests of the same material at elevated temperature showed that the specimens ruptured in the decarburized ferrite region because the work hardening effect was not significant at high temperatures due to rapid recrystallization and enhanced dislocation movement.

The data obtained from tensile tests on the base metal, weld metal and transverse specimens at different temperatures are shown in vertical bar graphs in figures 21 through 24. Figure 21 shows the tensile strength and figure 22 shows the yield strength of longitudinal weld metal, base metal and transverse specimens in A&T,

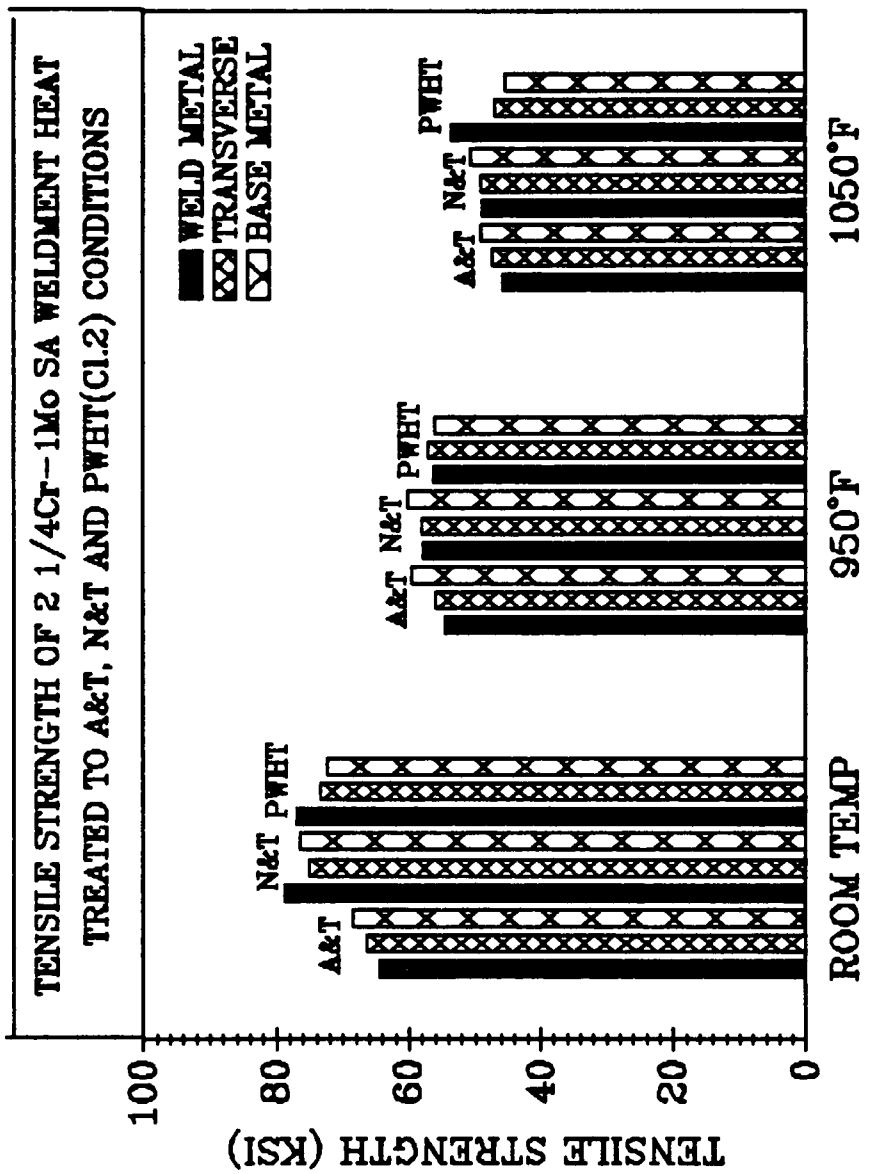

Figure 21. Tensile strength of 2 1/4Cr-1Mo SA weldment heat treated to A&T, N&T and PWHT(C1.2) conditions.

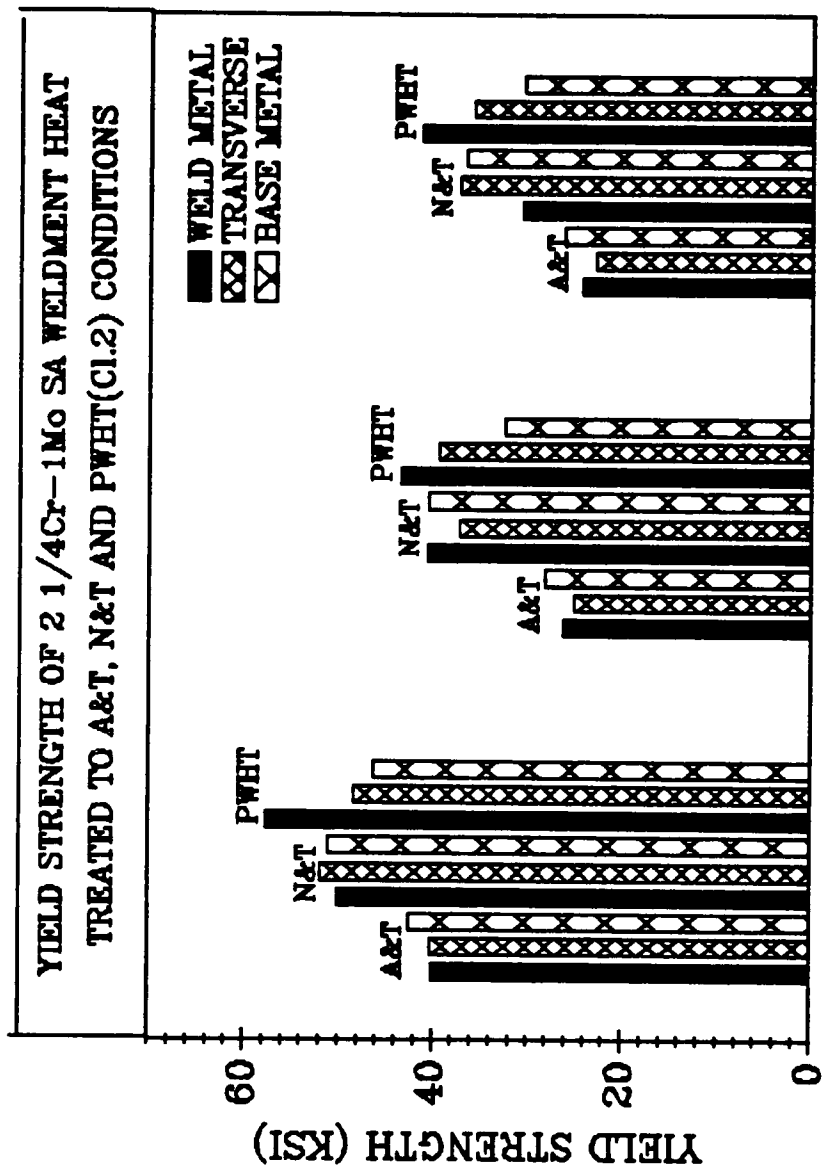

Figure 22. Yield strength of 2 1/4Cr-1Mo SA weldment heat treated to A&T, N&T and PWHT(Cl.2) conditions.

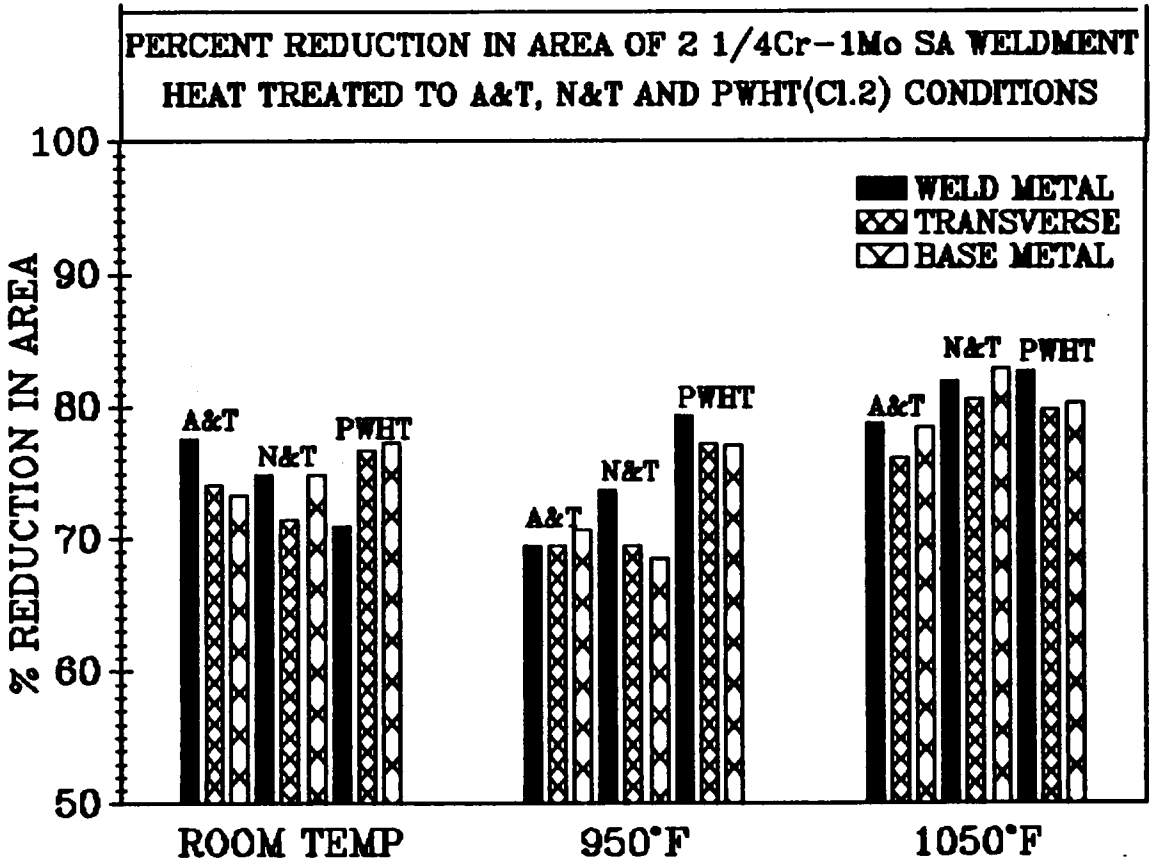

Figure 23. Percent reduction in area of 2 1/4Cr-1Mo SA weldment heat treated to A&T, N&T and PWHT(Cl.2) conditions.

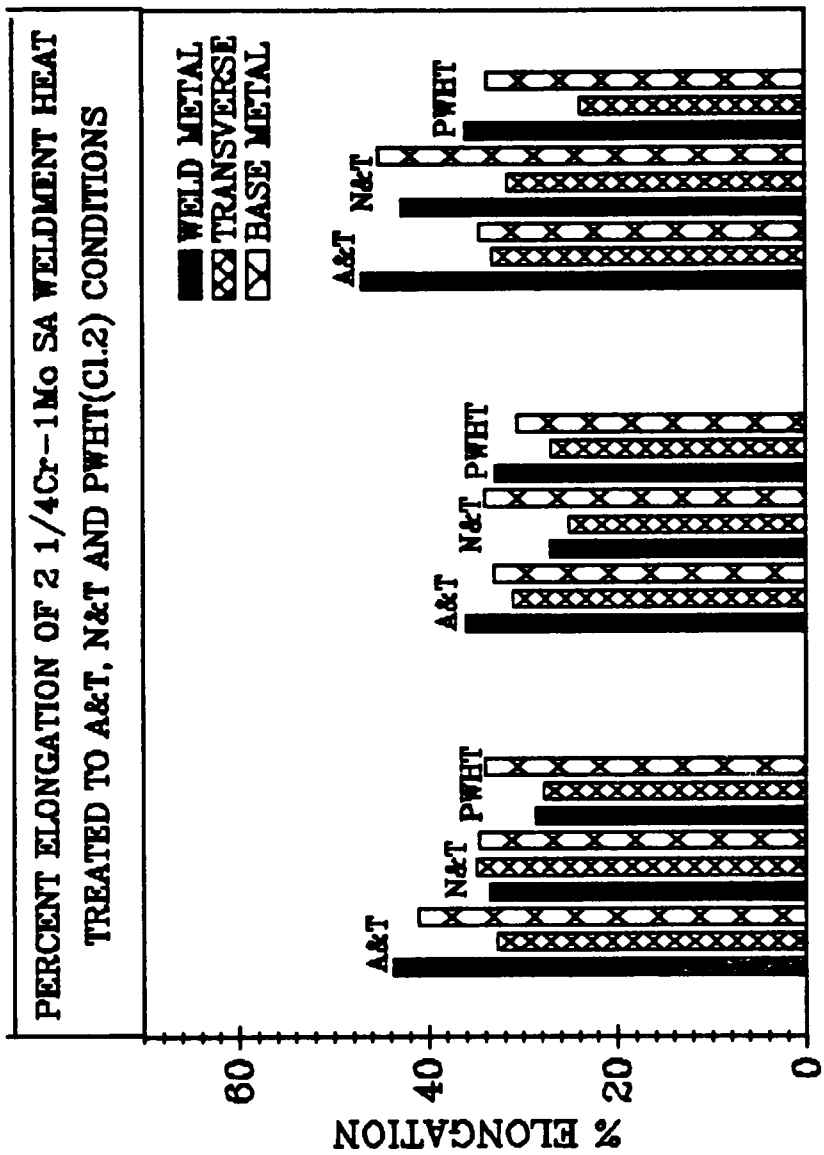

Figure 24. Percent elongation of 2 1/4Cr-1Mo SA weldment heat treated to A&T, N&T and PWHT(C1.2) conditions.

N&T and PWHT (C1.2) conditions tested at room temperature, 950°F and 1050°F. Since the transverse specimens ruptured in the weld metal the tensile strength and % reduction in area (figure 23) are, in general, the properties of weld metal perpendicular to the welding direction. In the A&T condition the base metal is strongest followed by transverse and longitudinally oriented weld metal (at all three test temperatures), respectively. The transverse tensile strength of weld metal in the A&T condition is higher than that in the longitudinal orientation but the yield strength of transverse specimens is lower. This points to the fact that the soft zone plastically deforms (yields) first, and then work hardens before the other regions of the specimen begin to yield which results in the decrease of the stress to cause 0.2% offset yield in the transverse tensile specimens. Also from Figure 23 and 24 it can be seen that weld metal oriented in longitudinal direction in the A&T condition of heat treatment exhibits a higher percent elongation and reduction in area at all the test temperatures compared to the weld metal tested in transverse direction.

In case of specimens extracted from the N&T condition the "soft" zone is not as wide as in the A&T condition. The tensile strength of weld metal in longitudinal and transverse orientation are about the same at 950 and 1050°F but at room temperature the former is slightly higher. However, the percent reduction in area and percent elongation in N&T condition are always (except percent elongation at room temperature) higher in the longitudinal orientation than in transverse orientation. In the PWHT (C1.2)

condition the tensile and yield strength of the weld metal in longitudinal orientation is higher than base metal and weld metal in transverse orientation. The base metal was in normalized and tempered condition before welding. The additional tempering for 25 hours at 1300°F during PWHT is responsible for the reduction in tensile strength and yield strength of the base metal which still exhibits class 2 properties outlined under ASTM specifications for SA 387 Grade 22 steel.

Tensile tests of weld metal oriented parallel to the welding direction from the SMA weldment (post weld heat treated to different temper parameters) were conducted at room temperature and 950°F. Table 6 shows the properties obtained from tensile testing. It can be seen that tensile strength of weld metal with a temper parameter of 32.3 (TP-A) and 33.4 (TP-B) exceeds the strength limits specified by PWHT (Cl.3) condition (which specifies the tensile strength to be between 90 and 110 KSI). Temper parameters of 32.3 and 33.4 were achieved by tempering for 25 hours at 1050 and 1100°F, respectively. Weld metal postweld heat treated to a temper parameter of 34.4 (TP-C) achieved by tempering at 1150°F for 25 hours is within class 3 tensile requirements. Tensile strengths for PWHT with temper parameters of 35.3 (TP-D) and 36.6 (TP-E) conforms to both class 3 and class 2 requirements. It is to be noted that the temper parameter of 35.3 was a result of tempering at 1100°F for 25 hours followed by aging at 1193°F for 21.5 hours to simulate service exposure of 100,000 hours at 950°F. The higher temper parameters of 37.7 (TP-F) and 38.7 (TP-G) meet class 2 requirements. However, the

Table 6. Results obtained from tensile testing of SMA weld metal postweld heat treated to different temper parameters.

Code	Temper Parameter*	Test Temperature (°F)	UTS (KSI)	0.2% offset YS (KSI)	%Elongation	%Reduction in Area
TP-A	32.3	RT**	129.6	115.3	20.5	66.9
		950	100.7	87.2	16.1	59.3
TP-B	33.4	RT	115.1	102.3	20.1	70.3
		950	89.4	78.3	21.1	68.2
TP-C	34.4	RT	105.6	92.8	21.6	72.6
		950	76.9	68.7	23.6	73.5
TP-D	35.3	RT	98.3	82.1	22.1	75.0
		950	69.6	62.0	19.1	77.1
TP-E	36.6	RT	90.9	75.0	26.0	75.7
		950	65.3	57.0	26.7	77.7
TP-F	37.7	RT	83.0	65.6	30.4	77.1
		950	58.3	50.3	25.4	81.0
TP-G	38.7	RT	79.5	62.1	31.5	77.2
		950	60.0	45.8	29.3	78.8

* Temper Parameter = $(T + 460)(20 + \log T) \times 10^{-3}$
** RT - Room Temperature

percent elongation and reduction in area meet requirements for both class 2 and class 3 for all the temper parameters used in this study which means that even tempering to a temper parameter of 32.3 (TP-A) is sufficient to impart sufficient ductility and toughness to the weld metal.

The tensile strength of weld metals at both room temperature and 950°F decreases with increase in the temper parameter (see figure 25). The decrease in tensile strength at both temperatures is initially rapid as the temper parameter increases and then decreases more slowly with further increase in the temper parameter. The tensile strength of weld metal at 950°F was found to be 22 percent lower than that at room temperature. The hardness of weld metal was determined and exhibits the same trend as that of the tensile strength with increase in temper parameter as shown in figure 26. Baker and Nutting[18] have investigated the effect of tempering time and temperature on the hardness of quenched and tempered and normalized and tempered 2 1/4Cr-1Mo steel and their observations also show a rapid decrease in hardness during the initial stages of tempering (also they observed a secondary hardening phenomena before the hardness began to decrease which was not evident in the present study). Further increase in the temper parameter decreased the hardness but at slower rate. Similar results have been reported by Pilling and Ridley[36] for tempering of quenched 2 1/4Cr-1Mo steel with varying carbon contents. The drop in hardness was found to be faster for lower carbon steels. Figure 27 shows the 0.2% offset yield strength at room temperature and 950°F as a function of the temper

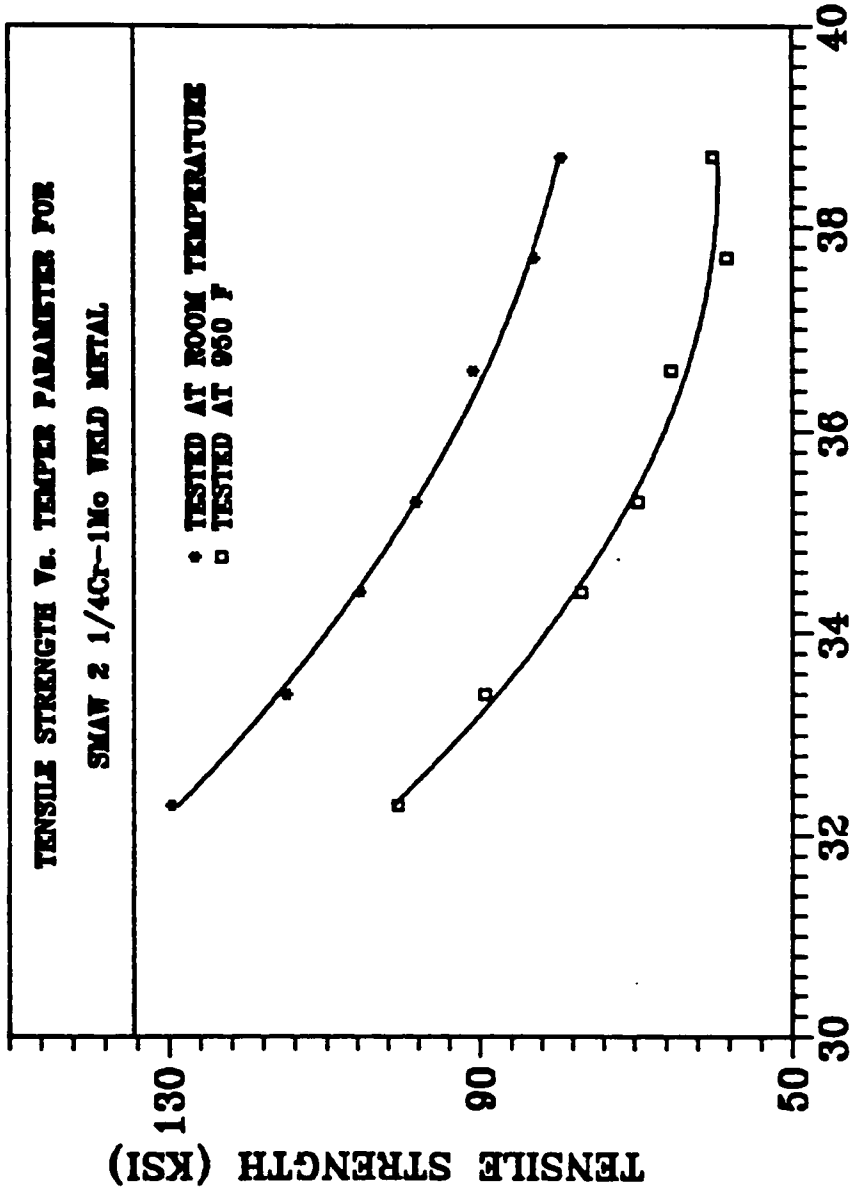

Figure 25. Tensile strength versus temper parameter for SMAW 2 1/4Cr-1Mo weld metal.

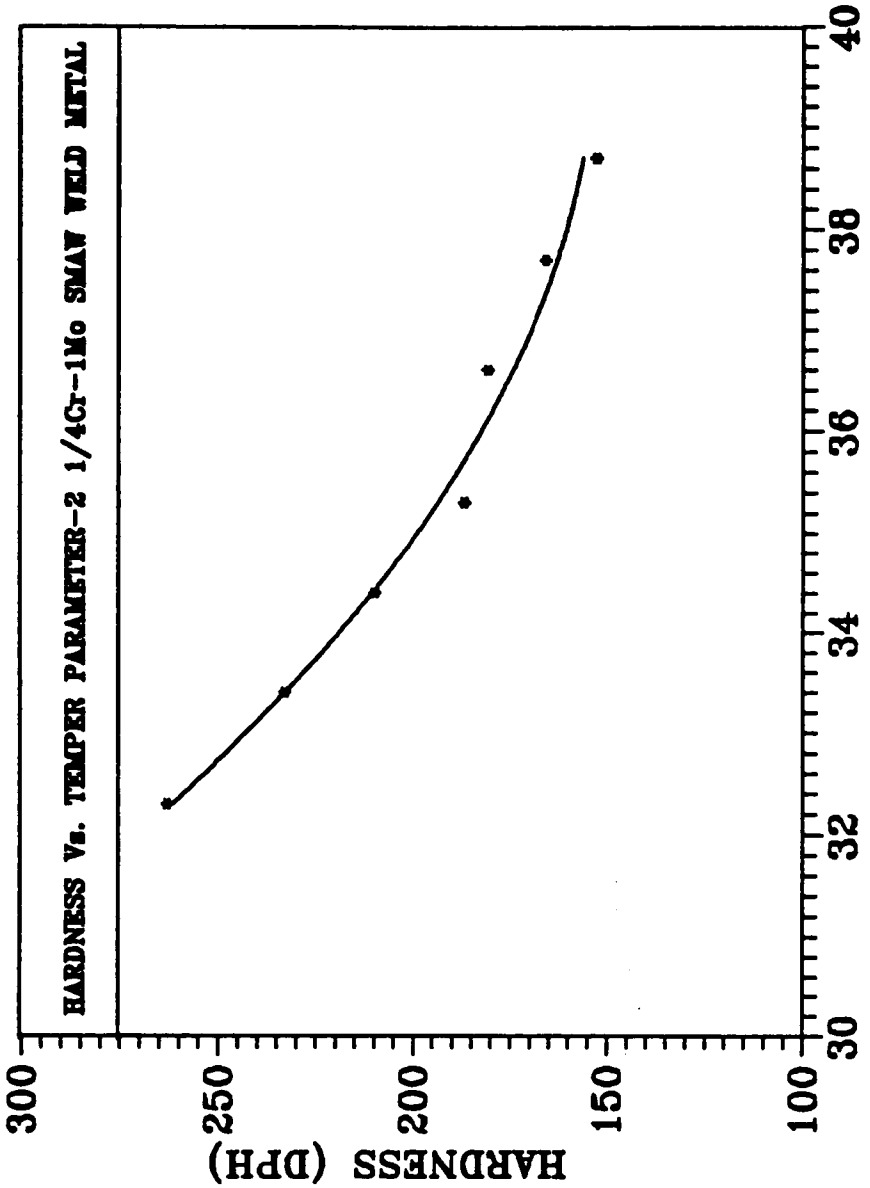

Figure 26. Hardness versus temper parameter for SMAW 2 1/4Cr-1Mo weld metal.

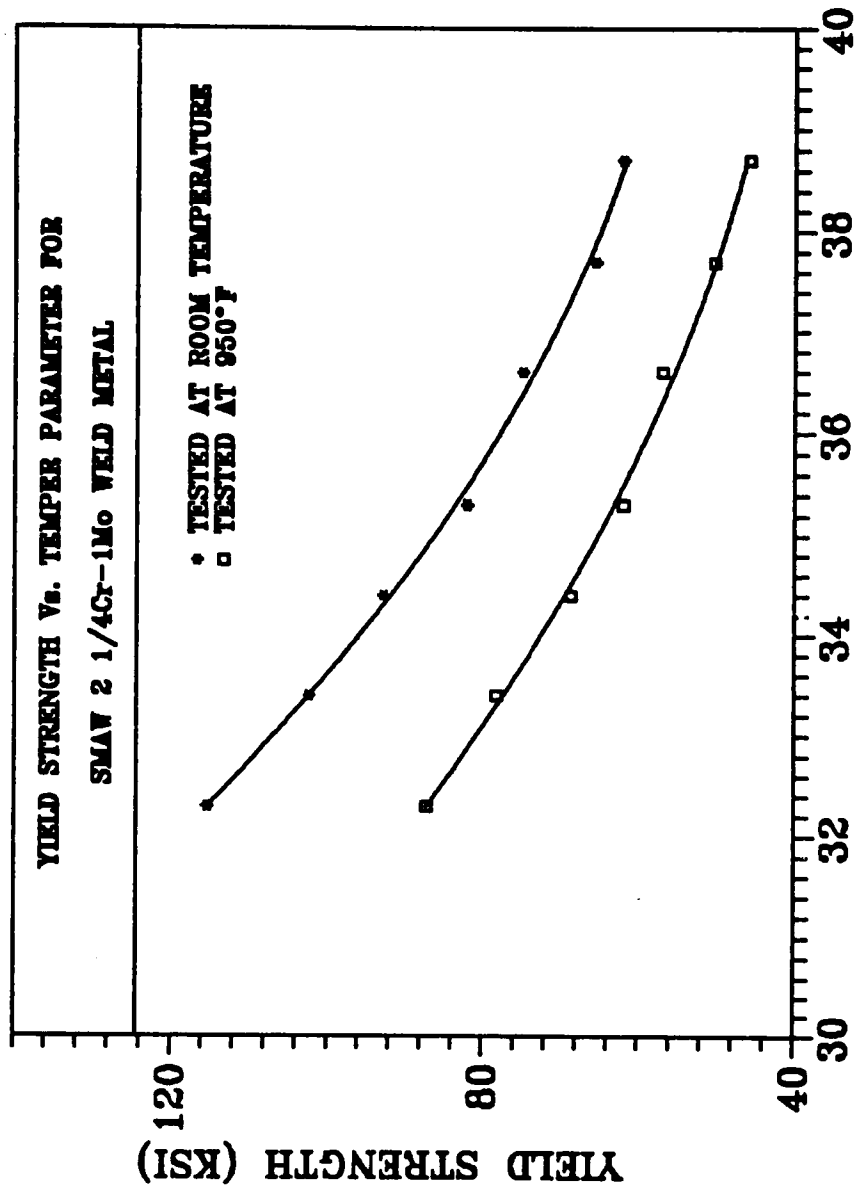

Figure 27. Yield strength versus temper parameter for SMAW 2 1/4Cr-1Mo weld metal.

parameter. At both the test temperatures the behavior is similar although the yield strength at 950°F is about 25% lower than the yield strength measured at room temperature. The characteristics of the curves obtained from tensile testing and hardness measurements as a function of the temper parameter follow the same pattern. Such decrease in hardness, tensile and yield strength with an increase in the severity of tempering is associated with the coarsening of carbide particles resulting in an increase of the interparticle spacing. Such behavior has been reported by Lundin et al.[4] during a similar study involving class 2 and class 3 post weld heat treatment of 2 1/4Cr-1Mo SMA weld metal.

Figure 28 shows the percent elongation and reduction in area of the specimens from the SMA weld metal heat treated to different temper parameters tested at room temperature and 950°F. The percent reduction in area at lower temper parameters is less at 950°F than at room temperature. However, at higher temper parameters the weld metal exhibited higher percent reduction in area at 950°F than at room temperature. In general, the percent reduction in area increases with increase in the temper parameter with the magnitude of increments greater at 950°F than at room temperature. The percent elongation also shows similar trend as the percent reduction in area except at a temper parameter of 35.3 (TP-D) in which there is a drop in the percent elongation compared to a temper parameter of 34.4 (TP-C). The temper parameter of 35.3 was achieved by PWHT at 1100°F for 25 hours followed by aging at 1193°F for 21.5 hours to simulate service exposure of 100,000 hours at 950°F. This abnormality may be

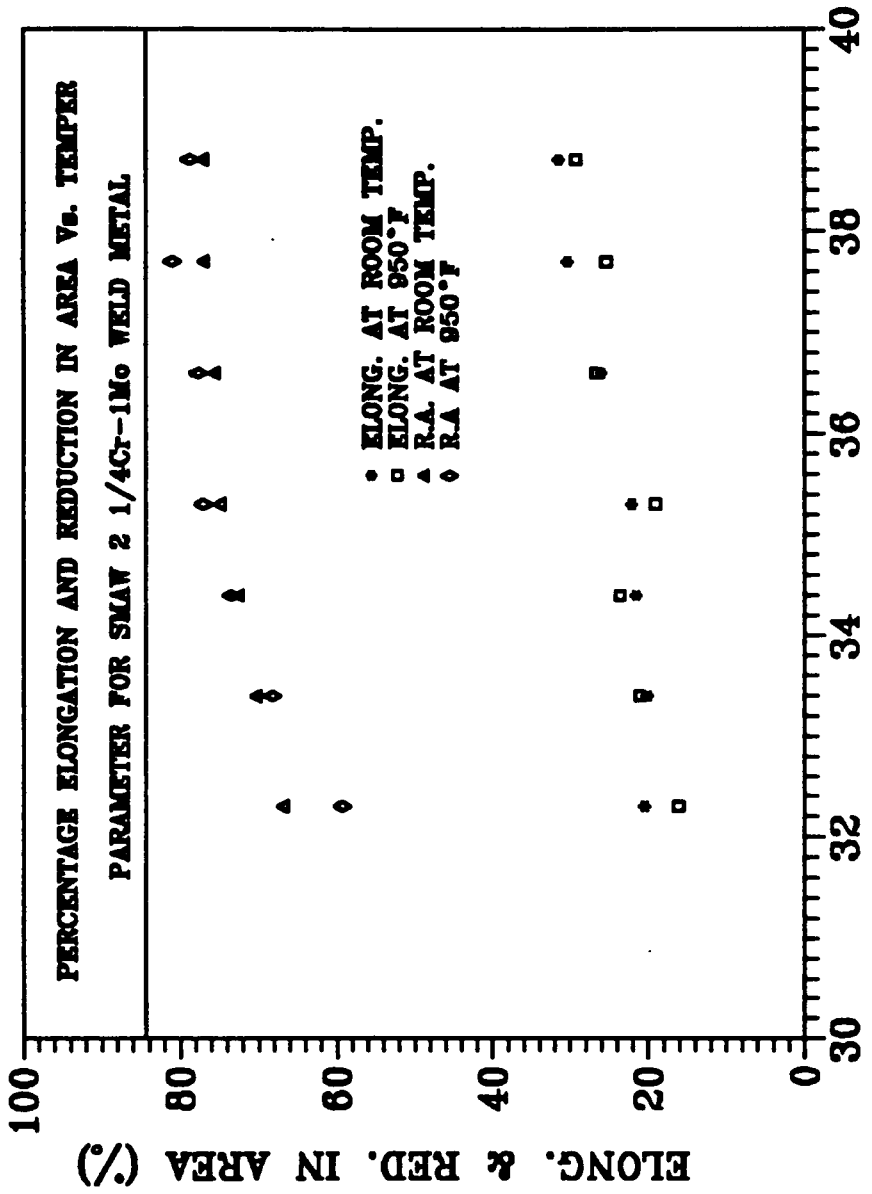

Figure 28. Percentage elongation and reduction in area versus temper parameter for SMAW 2 1/4Cr-1Mo weld metal.

due to temper embrittlement which is known to occur in 2 1/4Cr-1Mo steels near 1100°F.

Hardness is defined as the resistance of a material to indentation or plastic deformation. Hardness usually correlates well with the tensile and yield strength of steels and so for 2 1/4Cr-1Mo SMA weld metal postweld heat treated to different temper parameters (and hence hardness) a correlation may be expected. Bland[8] had found excellent correlation between hardness and room temperature tensile strength of 2 1/4Cr-1Mo weld metal. Room temperature and 950°F tensile strength and yield strength was seen to correlate well with the hardness values in this study resulting in a straight line regression fit as shown in figures 29 and 30. Such a master curve can be very useful for determination of tensile strength and yield strength of 2 1/4Cr-1Mo SMA weld metal (this relation may be valid for weld metals deposited by other fusion processes as well) by a simple measurement of hardness where material, time or economy does not permit direct tensile testing. The equations derived from the straight line fit between hardness and tensile strength and yield strength are as follows:

$$UTS_{RT} = 0.46\ HV + 8.82$$

$$UTS_{950^{\circ}F} = 0.40\ HV - 5.67$$

$$YS_{RT} = 0.50\ HV - 14.44$$

$$YS_{950^{\circ}F} = 0.38\ HV - 11.97$$

where, UTS and YS have their usual meaning in KSI and HV is the diamond pyramid hardness measured using a 10Kg load.

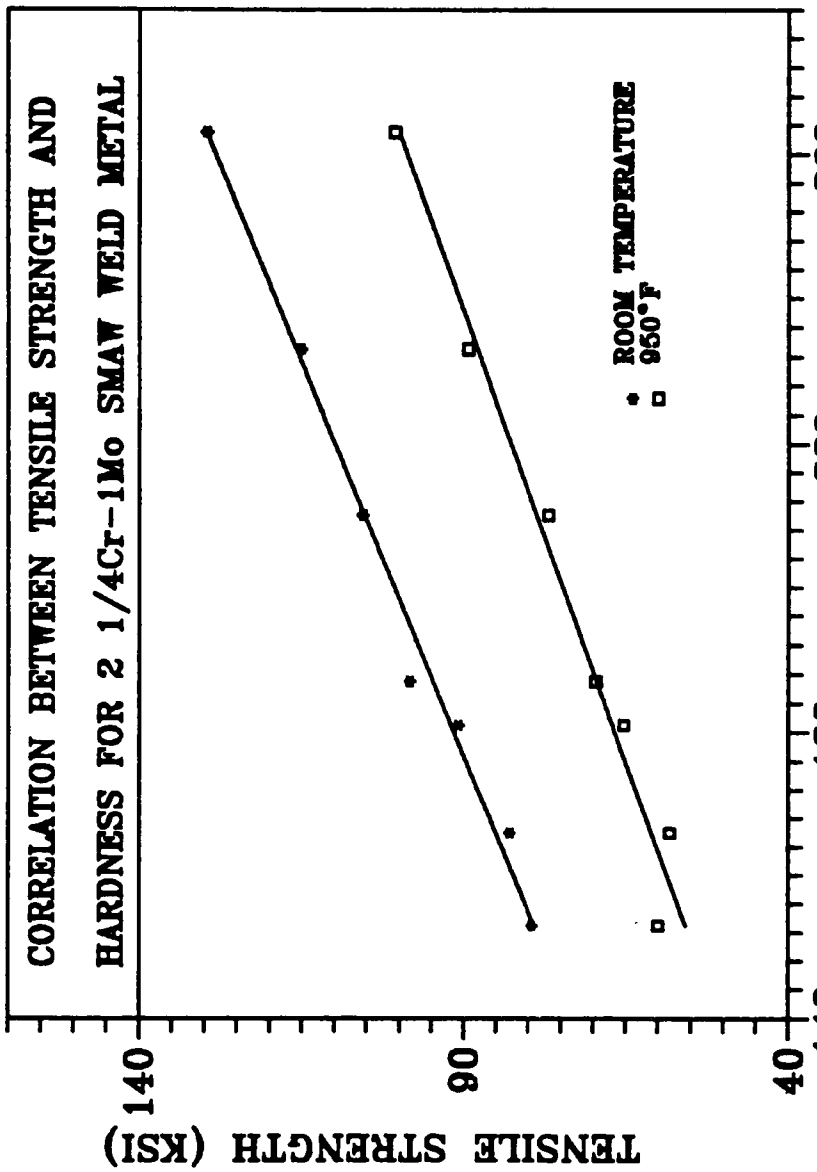

Figure 29. Correlation between tensile strength and hardness for 2 1/4Cr-1Mo SMAW weld metal.

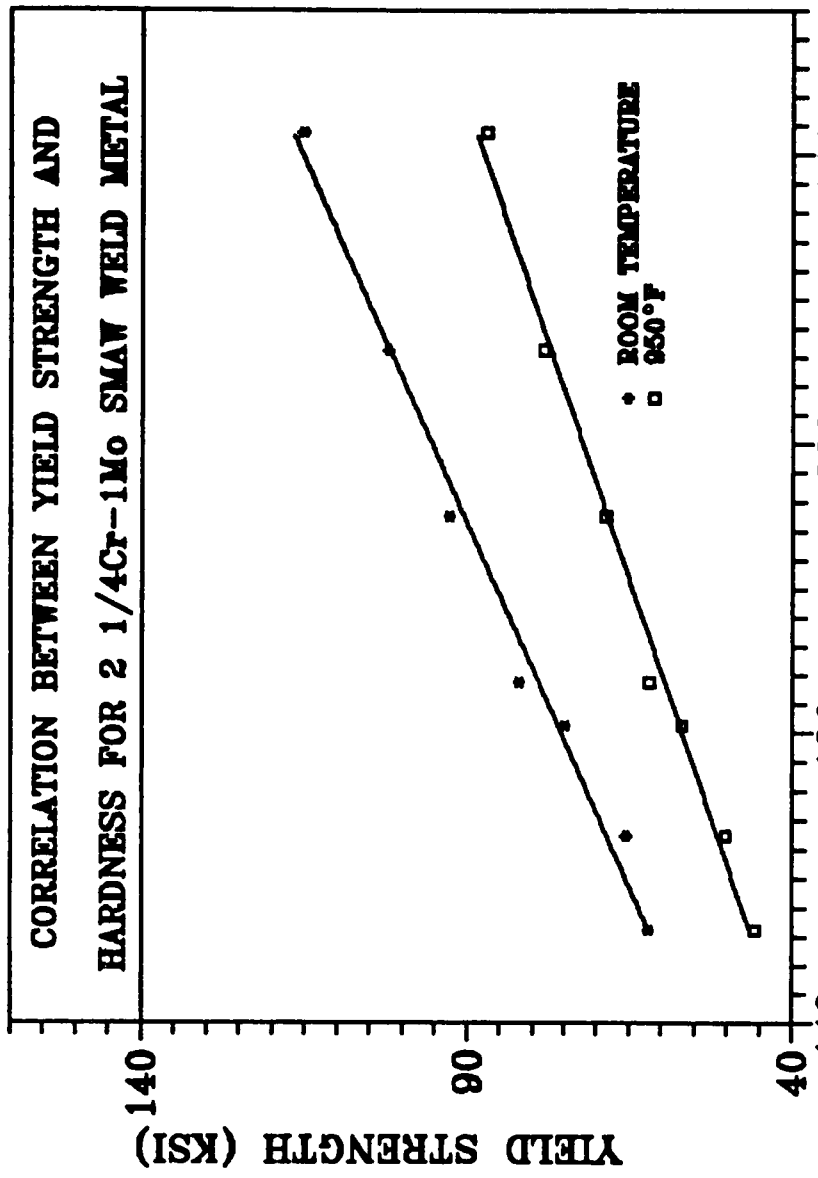

Figure 30. Correlation between yield strength and hardness for 2 1/4Cr-1Mo SMAW weld metal.

4.3 STRESS RUPTURE TEST RESULTS AND DATA ANALYSIS

Over 100 stress rupture specimens have been tested as a part of this study. The cumulative test time is over 150,000 hours. Weld metal creep specimens were extracted parallel to the welding direction and composite cross weld specimens were extracted transverse to the welding direction with the HAZ at the center of the specimen gage length from the submerged arc weldment heat treated to A&T, N&T and PWHT(Cl.2) conditions. Stress rupture testing was conducted at 950°F and 1050°F. Additional isostress rupture testing was carried out on specimens extracted transverse to the welding direction from the submerged arc weldment heat treated to A&T condition, at 11 KSI at four temperatures between 1150 and 1225°F at 25F° interval. All-weld-metal creep test specimens were extracted parallel to the welding direction from the SMA weldment postweld heat treated to seven different temper parameters. Four specimens with the same temper parameter were tested at 950°F with the time to rupture spanning the range of hundred hours to several thousand hours. Four weld metal specimens from each of the temper parameters of 32.3, 34.4, 36.6 and 37.7 were isostress rupture tested at 16.5 KSI.

Results obtained from stress rupture testing were analyzed using extrapolation techniques which enable determination of 100,000 hour rupture stress as described in chapter 3. The Larson-Miller parameter technique was easier to use because it allows plotting of all of the rupture data on a single curve. The stress for 100,000 hour rupture life at a temperature of interest was obtained by

inserting the Larson-Miller parameter which described the time/temperature combination into the log stress versus Larson-Miller parameter equation determined by regression and then solving for stress. Staying within the parameter range described by the data, the 100,000 hour stress thus obtained was an interpolated value and hence did not exhibit the degree of uncertainty characteristics of values which necessarily are determined by curve extrapolations using the log stress/log rupture time analysis method. Another benefit of this interpolation technique is that 100,000 hour rupture stresses may be obtained for temperatures at which no data are available, ie., as long as the Larson-Miller parameter value characteristic of 100,000 hour at that temperature falls within the parameter range described by the data. Thus, extrapolation beyond the parameters encompassed by the data was not attempted.

In contrast to the Larson-Miller technique, the log stress/log rupture time method required a curve to be determined at each test temperature. As a result the data had to be partitioned by test temperature, thereby greatly reducing the number of data points available for derivation of each curve. Hence, in some cases a sufficient number of data points to "average out" the scatter characteristics of rupture data were not available. In such cases the curves obtained by regression analysis became descriptive of the few data available rather than that of the material in general. As a result, the 100,000 hour stress derived from extrapolation of the curves are affected as well. Thus, efforts to observe the influence

of factors such as postweld heat treatment on 100,000 hour stress are significantly hampered.

Isostress testing at various temperatures and then extrapolating to the service temperature to determine the rupture time at the stress level is gaining wide popularity because of the fact that this type of testing is the only method available to date, to quantify the remaining life of service exposed components. Other methods of determining remaining life of exposed components are qualitative in nature and fail to accurately predict the remanent lifetime. Isostress rupture testing suffers from the disadvantage that the available data on a material has to be partitioned on the basis of stress level and so relatively few data are available for this type of analysis. Also the tests are conducted at temperatures much higher than the operating temperature which results in evaluation of the material at temperatures other than service temperature. This method also suffers from the disadvantage that the rupture stress for 100,000 hour can not be determined and so comparison with available data in the literature is not possible. However, in this technique the data fits a straight line regression equation while exhibiting little scatter and so relatively few data points are required to obtain the straight line relation between the log rupture time and the test temperature. Also, it is not possible to predict behavior of the material at stresses other than at the tested stress level. In addition, a slight change in the slope of the line described by the data may result in large shift in the extrapolated rupture life (by as much as factor of 2).

4.4 RESULTS AND DATA ANALYSIS OF A&T, N&T AND PWHT(Cl.2) SA WELDMENT STRESS RUPTURE TESTS

Results of stress rupture testing of longitudinal weld metal and transverse weldment specimens in A&T, N&T and PWHT(Cl.2) conditions from the SA weldment are shown in tables 7 and 8, respectively. The data obtained from isostress creep tests of transverse specimens in A&T condition are shown in table 9. Log stress/log rupture time plot of longitudinal all weld metal specimens at 950 and 1050°F are shown in figures 31 and 32, respectively. The stress rupture data at 950 and 1050°F have been combined into Larson-Miller parameter which is shown in figure 33. From figure 31 it can be seen that at 950°F the stress rupture properties of the SA weld metal in the N&T heat treated condition is superior to that of weld metal subcritically PWHT(Cl.2) or A&T. The rupture stresses for 100,000 hour life for A&T, N&T and PWHT(Cl.2) weld metal at 950°F and 1050°F determined by extrapolation of these curves are given in table 10. It can be seen that at 950°F the N&T weld metal has the highest stress for a 100,000 hour rupture life followed by PWHT(Cl.2) and A&T. At 1050°F the log stress/log rupture time curves from the SA weld metal heat treated to same three conditions are shown in figure 32. From this figure it can be seen that for low rupture times, the N&T and PWHT(Cl.2) have better creep properties than the A&T but extrapolation to longer rupture times (>40,000 hours) clearly reveals that A&T is superior to the N&T and PWHT(Cl.2). Also, it is evident that stress rupture strength of N&T and PWHT(Cl.2) material approaches the same value at about 100,000 hours. Similar behavior

Table 7. Creep rupture test results of all-weld metal A&T, N&T and PWHT(Cl.2) specimens from SA weldment.

Test Temp. (°F)	Condition	Stress (Ksi)	Rupture Time (Hours)
950	A&T	35.0	28.5
	A&T	26.0	760.2
	A&T	24.9	700.0
	A&T	23.1	1737.2
	N&T	35.0	167.0
	N&T	26.0	3998.0
	N&T	24.9	7830.2
	N&T	23.1	9512.2
	PWHT	44.0	63.6
	PWHT	35.0	114.4
	PWHT	32.0	181.0
	PWHT	30.0	229.3
	PWHT	28.0	527.1
	PWHT	25.0	1729.2
1050	A&T	23.0	46.9
	A&T	16.5	465.3
	A&T	15.0	1553.3
	A&T	14.4	2360.0
	N&T	23.0	361.4
	N&T	16.5	2967.0
	N&T	15.0	4417.4
	N&T	14.4	9107.4
	PWHT	27.0	12.0
	PWHT	25.0	41.3
	PWHT	22.0	149.4
	PWHT	20.0	222.1
	PWHT	18.0	533.9
	PWHT	17.0	622.1
	PWHT	15.0	3928.1
	PWHT	13.0	4011.6

A&T - annealed and tempered
N&T-normalized and tempered
} Austenitized 1700°F, tempered 1300°F - 2 hours

PWHT-Postweld Heat Treated (1300°F - 25 hrs.)

Table 8. Creep rupture test results of transverse composite A&T, N&T and PWHT(Cl.2) specimens from SA weldment.

Test Temp. (°F)	Condition	Stress (Ksi)	Rupture Time (Hours)
950	A&T	40.0	177.3**
	A&T	34.0	464.9**
	A&T	31.0	650.8**
	A&T	30.0	1751.6**
	N&T	40.0	60.1**
	N&T	34.0	310.8**
	N&T	30.0	1453.3**
	N&T	29.0	2422.4**
	PWHT	34.0	125.3*
	PWHT	30.0	359.6*
	PWHT	28.0	489.5*
	PWHT	24.0	1031.6*
1050	A&T	23.0	102.0*
	A&T	16.5	262.1*
	A&T	15.0	1104.9*
	A&T	14.4	5240.7*
	N&T	23.0	437.5**
	N&T	16.5	1466.1**
	N&T	15.0	3226.9**
	N&T	14.4	4492.4**
	PWHT	23.0	56.5*
	PWHT	16.5	850.0*
	PWHT	15.0	1636.3*
	PWHT	13.5	2939.1*

A&T--annealed and tempered } Austenitized 1700°F
N&T--normalized and tempered } Tempered 1300°F-2 hours
PWHT--Post Weld Heat Treated (1300°F - 25 hrs.)
*--rupture in base metal
**--rupture in weld metal

Table 9. Isostress creep rupture test results of transverse A&T specimens from SA weldment.

Test Temperature (°F)	Stress (KSI)	Rupture Time (Hours)
1225	11.0	54.8
1200	11.0	96.1
1175	11.0	263.1
1150	11.0	531.1
1150	10.0	786.0*

* 0.505 inch gage diameter specimen
All specimens ruptured in the weld metal

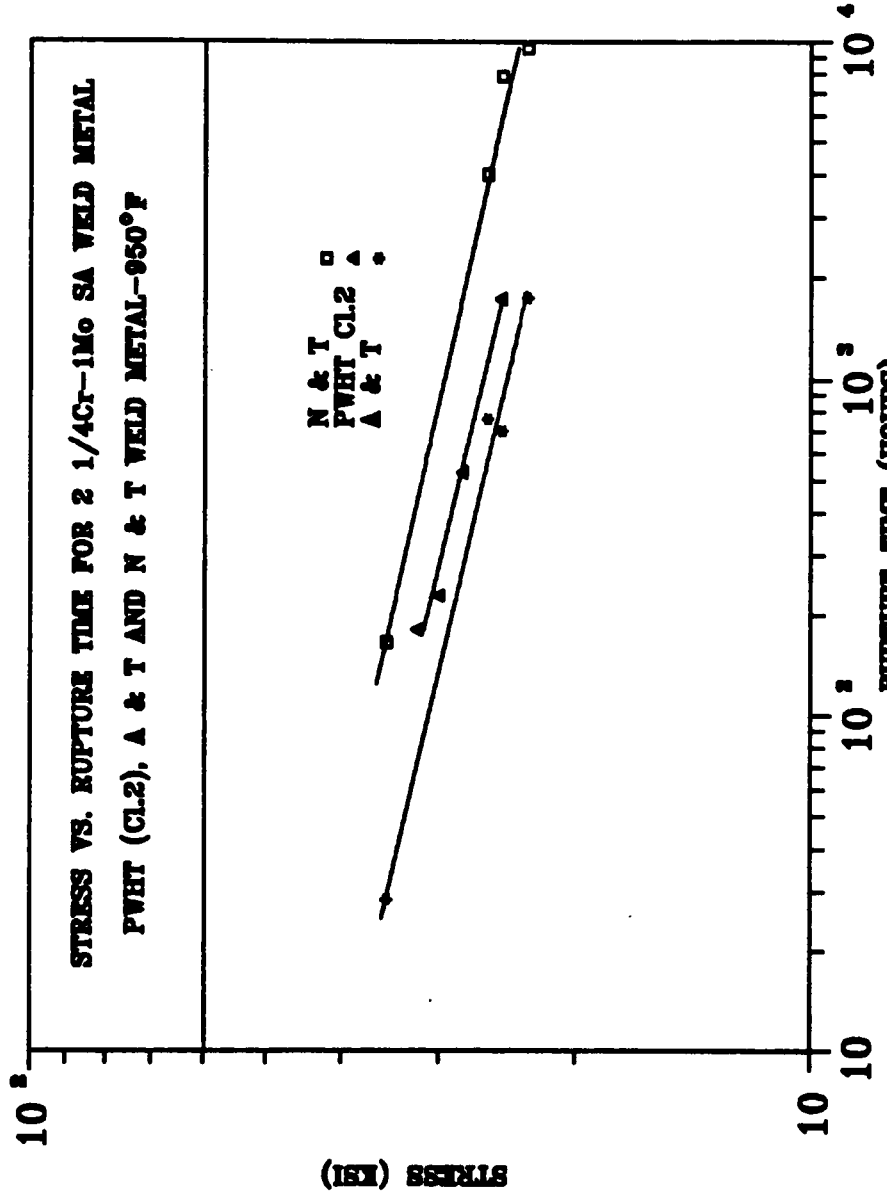

Figure 31. Stress versus rupture time plot for 2 1/4Cr-1Mo SA weld metal in A&T, N&T and PWHT(C1.2) conditions tested at 950°F.

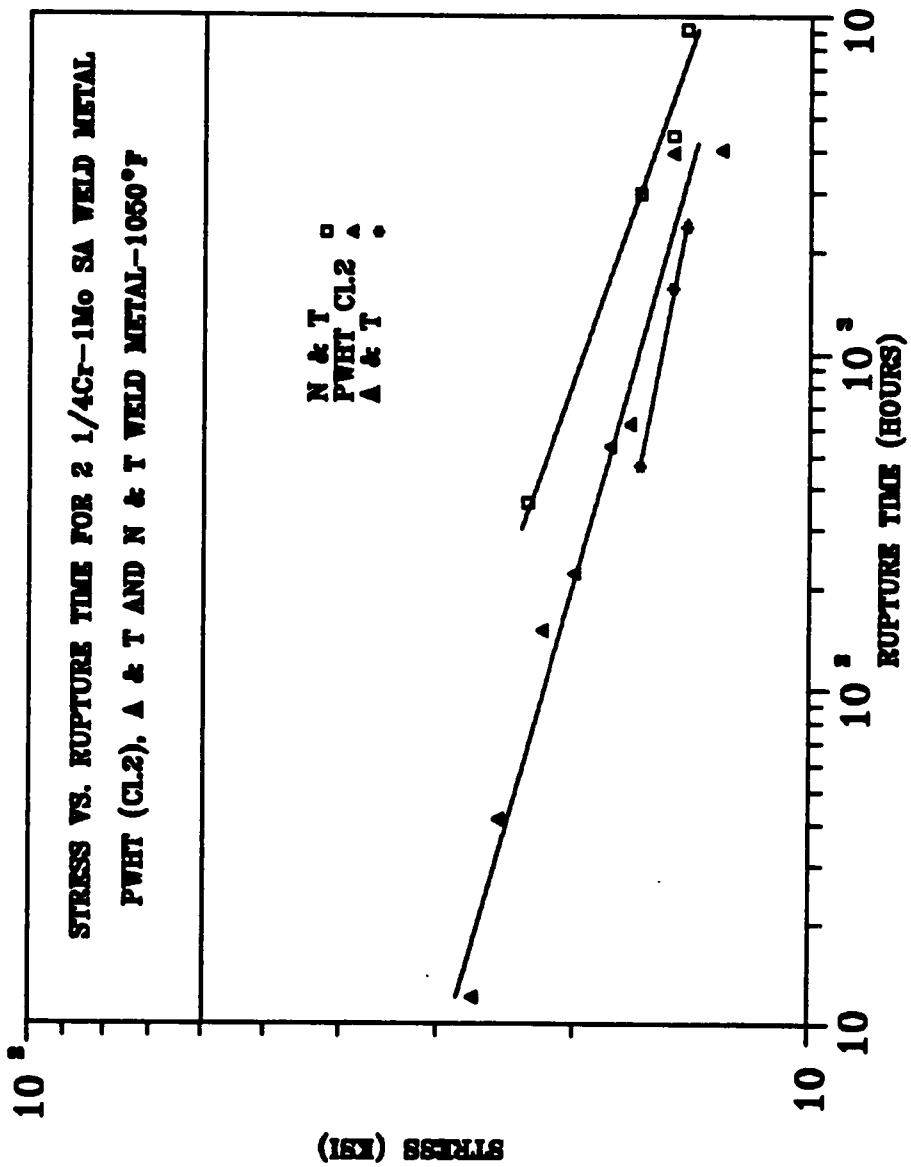

Figure 32. Stress versus rupture time plot for 2 1/4Cr-1Mo SA weld metal in A&T, N&T and PWHT(Cl.2) conditions tested at 1050°F.

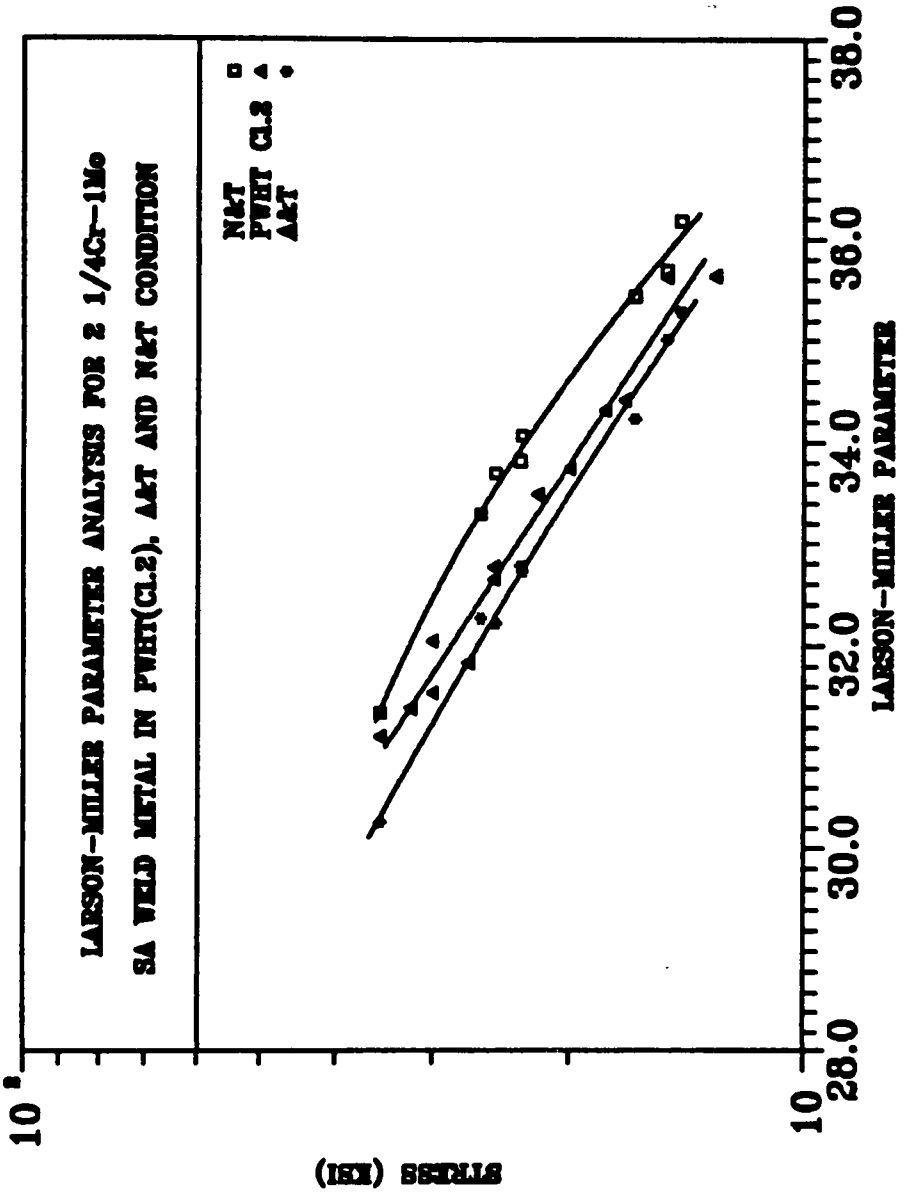

Figure 33. Larson-Miller parameter plot for 2 1/4Cr-1Mo SA weld metal in A&T, N&T and PWHT(Cl.2) conditions.

Table 10. Extrapolated 100,000 hour rupture stress for SA weldment heat treated to A&T, N&T and PWHT(Cl.2) conditions.

Heat Treatment	Temperature (°F)	Weld Metal		Cross Weld	
		Log s/log t_R	LMP	Log s/log t_R	LMP
A&T	950 1050	15.5 10.6	14.2 -	18.0 12.5	14.9 -
N&T	950 1050	19.0 9.7	17.4 -	20.8 9.9	16.3 -
PWHT (Cl.2)	950 1050	16.4 9.5	15.0 -	11.6 8.7	14.2 -

for 2 1/4Cr-1Mo steels has been found by Klueh[1] and Emmanuel et al.[11]. Emmanuel et al.[11] have indicated that heat treatment by N&T does not enhance the long time elevated temperature properties of 2 1/4Cr-1Mo steel when the service temperature exceeds 1000°F. He found that the kinetics of loss of strength of 2 1/4Cr-1Mo steel depends on prior heat treatment and test temperature. At low temperatures (<500°C or 932°C), the normalized and tempered steel containing 100% bainite is slightly stronger. Only for low rupture times, at temperatures 500 and 600°C (932 and 1112°C) normalized and tempered steel is stronger than annealed steel. Above 600°C (1112°C), normalized and tempered steel is weaker than annealed steel. This behavior of steels, differently heat treated, has been attributed to carbide coarsening, and the change of chemistry and type of carbides in different microconstituents (bainite/ferrite). The changes in carbides are directly linked to molybdenum remaining in solid solution (in ferrite) and the combination of the two ie. the "status" of carbides and the molybdenum remaining in solid solution in ferrite dictates the loss in strength upon exposure to elevated temperature under stress. The reason for the difference in stress rupture properties being related to the difference in carbide coarsening in A&T and N&T material will be further described in more detail in a later section devoted to microstructural analysis.

The superiority of A&T material at 1050°F for a rupture life of 100,000 hours is not evident from the Larson-Miller plot (see figure 33). This is due to the fact that the highest Larson-Miller parameter for the N&T condition is 36.2 whereas 100,000 hours at

1050°F results in a Larson-Miller parameter of 37.75. However, from figure 33 it is clear that A&T and N&T materials (by extrapolation) show a crossover behavior at a Larson-Miller parameter of about 38.8 which, transformed to time at 1050°F, results in 500,000 hours. This discrepancy in extrapolated values for the two analyses is a result of insufficient data points used in the Larson-Miller analysis not encompassing the range required for valid prediction and on the principles on which the two techniques are based. This drawback can only be eliminated by conducting more creep rupture tests (for longer rupture times) which will eliminate the uncertainty of predictions by mitigating the scatter in the stress rupture data. From the technique standpoint, log stress/log rupture time technique assumes that the microstructure is relatively stable so that a straight line relation can be established and the Larson-Miller Parameter technique is based on an Arrhenius relation implying creep rupture to be a thermally activated process. During creep rupture testing the microstructure is not stable and undergoes changes with respect to carbide size, morphology and distribution. Also, creep is not only a thermally activated process but also associated with mechanical deformation and strain sensitive processes. Hence, the assumptions on which these techniques are based are not very rigorous and exhibit slight discrepancy in obtained extrapolated values.

The basis for conducting stress rupture tests of composite specimens extracted transverse to the welding direction was to evaluate the significance of the carbon denuded "soft" zone brought about by migration of carbon from the lower chromium base metal side

to the higher chromium weld metal side along the entire fusion line of the weldment. However, none of the creep specimens ruptured in this zone. The metallurgical reason for such behavior is explained in a later section devoted to microstructural analysis.

The data obtained from testing of composite specimens are given in table 8. Log stress/log rupture time plot of the data obtained from tests conducted at 950°F and 1050°F are shown in figures 34 and 35, respectively. These two figures reveal that at 950°F, the N&T heat treated material shows superior stress rupture properties followed by the A&T and PWHT(Cl.2). At short rupture times, specimens subjected to the A&T condition showed higher rupture life than the N&T specimens. The reason for such behavior is not clear. At 1050°F the strength of the weldment in the transverse direction was found to be higher for the A&T condition (for longer rupture times) than the N&T or PWHT(Cl.2). It is to be noted however, that the rupture location in the A&T specimens shifted from weld metal (when tested at 950°F) to base metal (when tested at 1050°F). The N&T specimens ruptured in weld metal and the PWHT(Cl.2) specimens ruptured in base metal at both test temperatures. Some additional isostress testing was conducted on A&T specimens and these ruptured in the weld metal at temperatures between 1125 and 1250°F.

The strength of weld metal in longitudinal direction and strength of weldment in transverse direction reveals that the ranking of heat treatments at the two test temperatures remain the same except for the PWHT(Cl.2) condition. At 950°F the N&T is superior and at 1050°F the A&T material has better creep rupture properties.

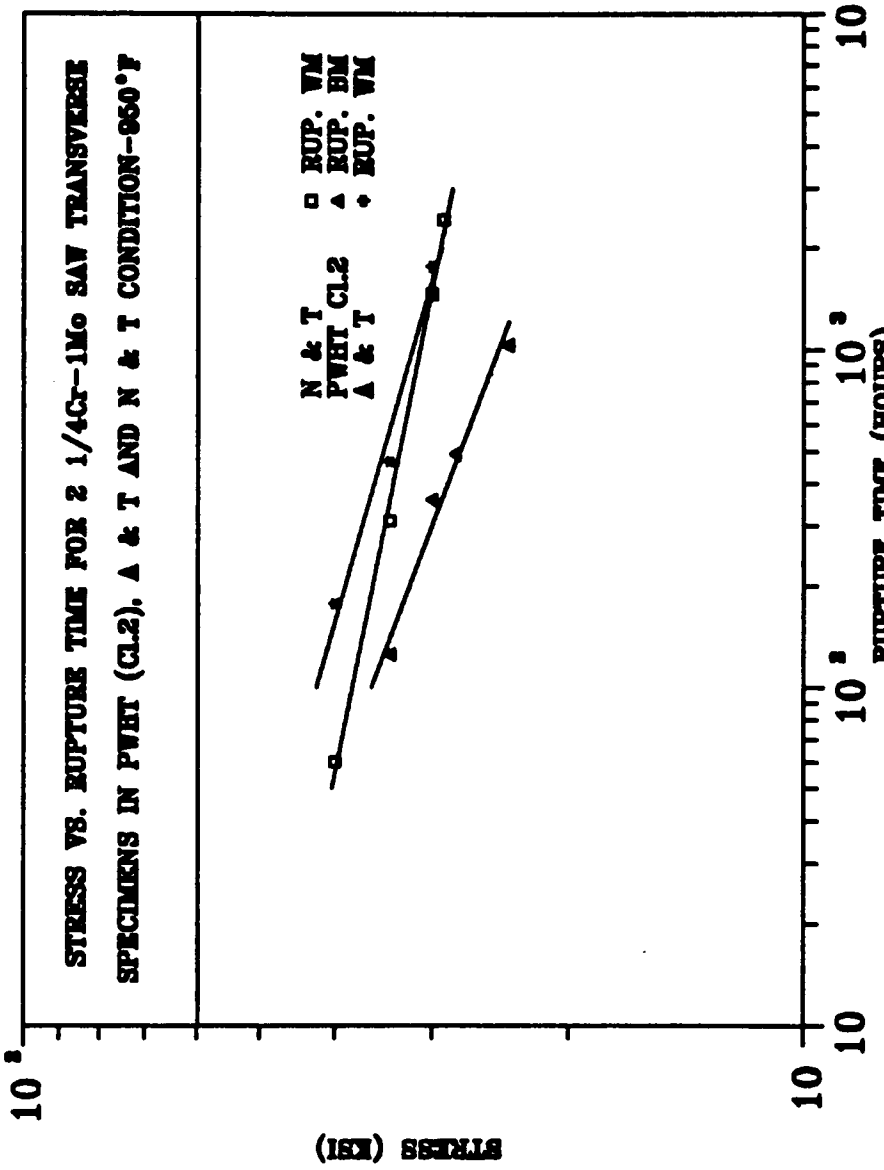

Figure 34. Stress versus rupture time plot for 2 1/4Cr-1Mo SA transverse weldment in A&T, N&T and PWHT(Cl.2) conditions tested at 950°F.

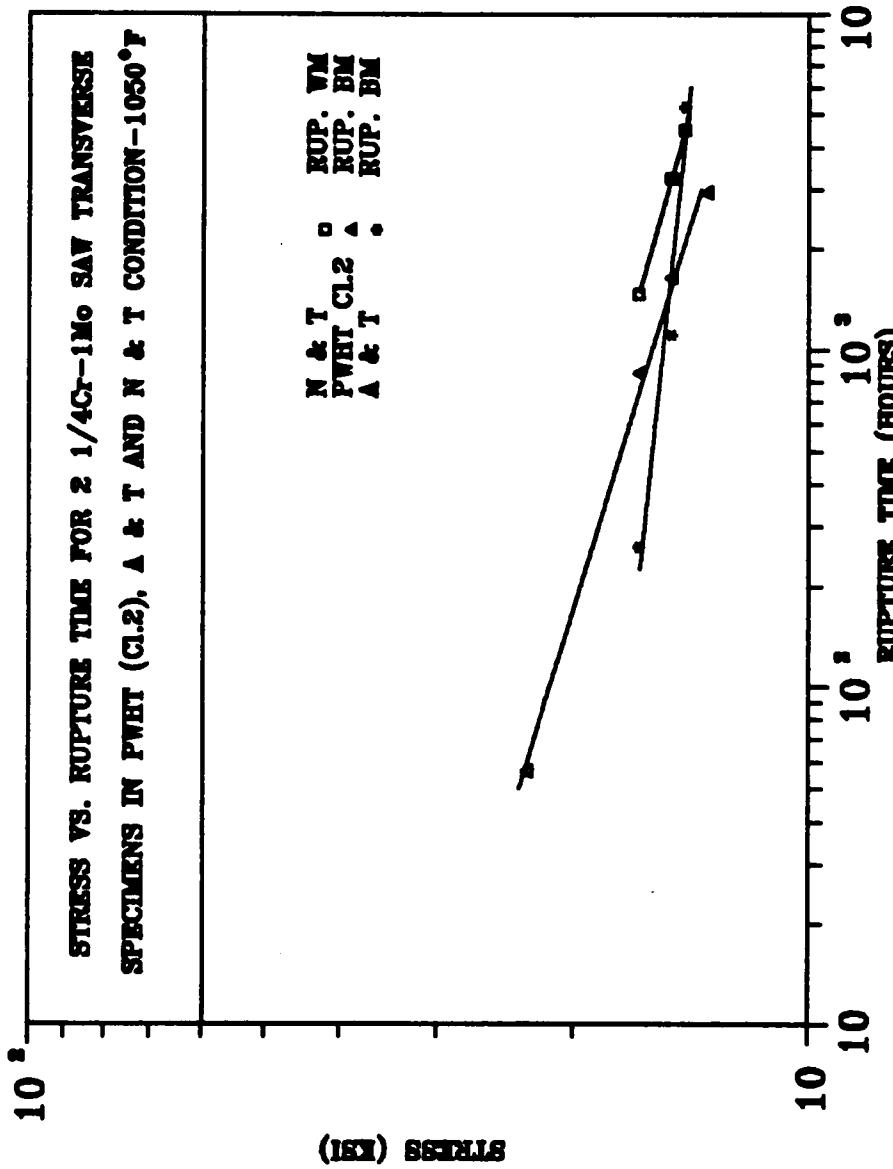

Figure 35. Stress versus rupture time plot for 2 1/4Cr-1Mo SA transverse weldment in A&T, N&T and PWHT(Cl.2) conditions tested at 1050°F.

For all-weld-metal tests the creep rupture properties in the PWHT(C1.2) condition falls between N&T and A&T at 950°F and PWHT(C1.2) and N&T are equally as strong at 1050°F (100,000 hour life). However, for tests conducted on composite specimens extracted perpendicular to the welding direction a lower strength of PWHT(C1.2) at both test temperatures is revealed. As mentioned above, the reason for such behavior is due to rupture of the composite specimens in the base metal. The base metal was originally in the normalized and tempered condition and along with the subsequent PWHT it has undergone severe tempering, thus becoming weaker than the weld metal. This is also evident in the tensile test results in which the base metal has a much lower tensile strength than the weld metal.

A Larson-Miller plot for the data obtained from testing of composite specimens at 950 and 1050°F is shown in figure 36. From the extrapolation of this plot the ranking of stress rupture strength of different heat treatments remain the same at 950 and 1050°F. The weldment in the N&T condition has superior strength followed by A&T and PWHT(C1.2) at 950°F. Due to the shift in the rupture location for the A&T specimens at different test temperatures significant scatter of the data is evident in the Larson-Miller plot. Whether the Larson-Miller master curve for the A&T condition is representative of the material is questionable due to this scatter. Extrapolated 100,000 hour rupture stresses for the different heat treatment conditions are shown in table 10. Isostress rupture testing at 11 KSI was conducted to further determine whether the rupture location of the transverse composite specimens would shift

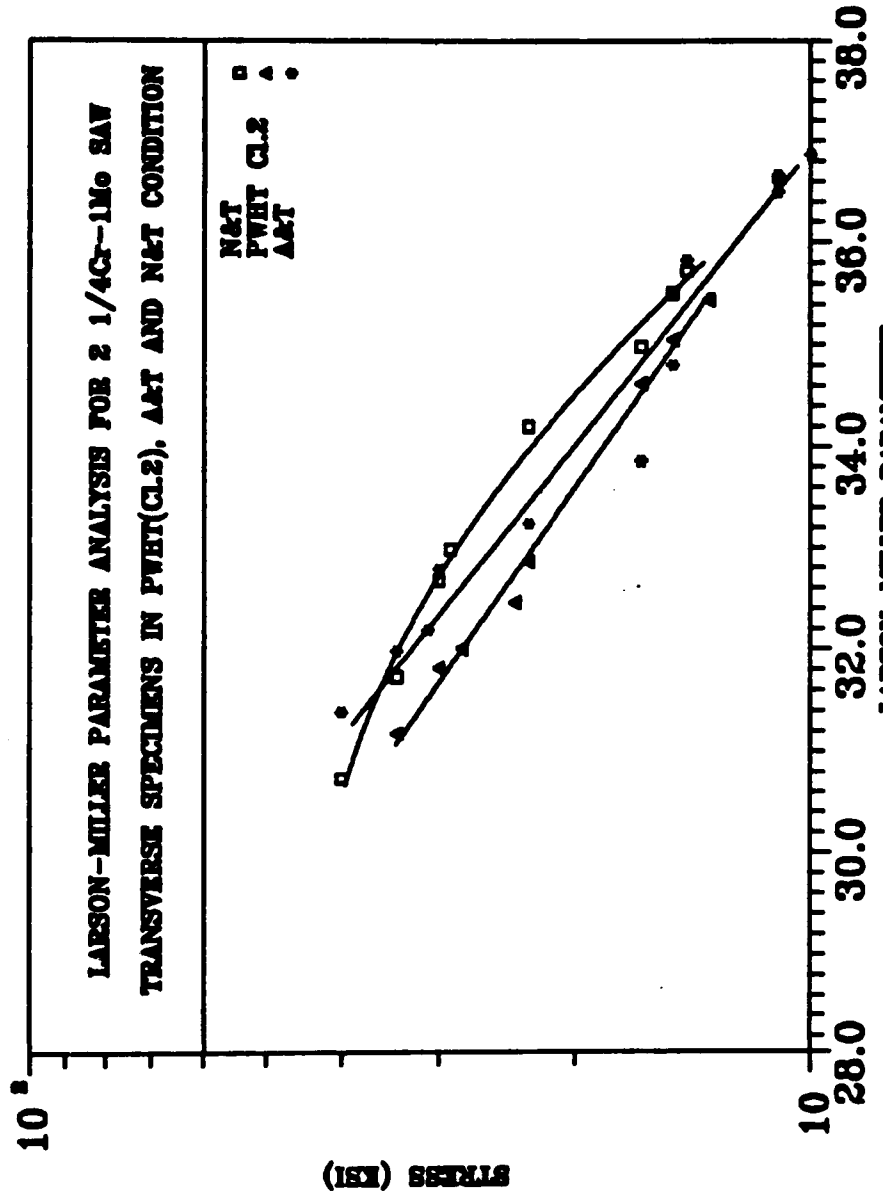

Figure 36. Larson-Miller parameter plot for 2 1/4Cr-1Mo SA transverse weldment in A&T, N&T and PWHT(Cl.2) conditions.

into the "soft" zone observed. These tests were conducted on the A&T weldment because this condition produced the widest soft zone. Also in order to determine if a restraint effect of the adjacent (stronger) regions were acting to affect rupture of the soft zone, a 0.505 inch gage diameter specimen was creep tested at 1150°F. The results of the isostress tests and 0.505 inch diameter specimens are presented in table 9. However, none of the test specimens ruptured in the "soft" zone (rupture occurred in the weld metal). The isostress curve for the A&T condition is shown in figure 37. The data points fall in a straight line (regression fit) and can be extrapolated to determine time to rupture at 950 and 1050°F at the stress level of 11 KSI. Extrapolation shows that the rupture life will be 300,000 hours at 950°F and 12,750 hours at 1050°F at a stress of 11 KSI. The 100,000 hour rupture life will be at 985°F corresponding to a rupture stress of 11 KSI. These results are in excellent agreement with those obtained from Larson-Miller parameter technique but the log stress/log rupture time extrapolation shows a significantly higher stress rupture strength.

4.5 STRESS RUPTURE RESULTS AND DATA ANALYSIS OF THE SMAW WELD METAL SUBCRITICALLY PWHT TO VARIOUS TEMPER PARAMETERS

Most postweld heat treatments being utilized by the fabricators of elevated temperature pressure components are of the subcritical type. It is a well known fact that as the time and/or temperature of such postweld heat treatments is increased there is a decrease in the stress rupture strength. Data available in the literature has been

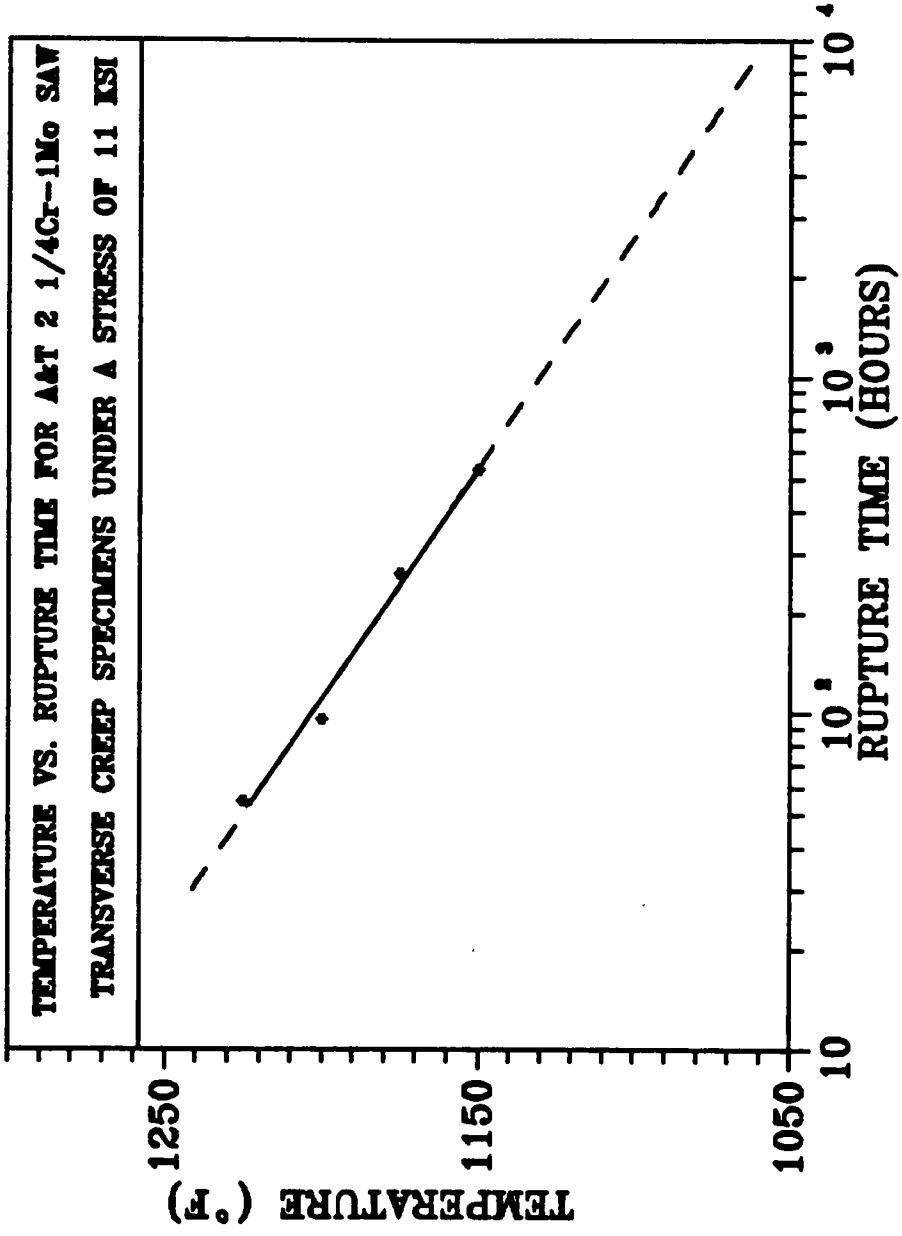

Figure 37. Temperature versus rupture time plot for 2 1/4Cr-1Mo SA transverse weldment in A&T condition isostress rupture tested at 11 KSI.

analyzed by Lundin et al.[4] by partitioning all the available data falling within different temper parameter ranges. This analysis revealed that as the severity of tempering increases there is a decrease in the 100,000 hour rupture strength of subcritically postweld heat treated 2 1/4Cr-1Mo weld metal. Thus, it was felt that if a relation could be found between the temper parameter and extrapolated stress rupture strength for 100,000 hour rupture life, it will be possible to predict life of the pressure vessels and components based upon the prior PWHT and service exposure. Therefore, all weld metal specimens extracted with the axis parallel to the welding direction from the SMA weldment postweld heat treated to a range of temper parameters were creep tested at 950°F. The data obtained are presented in table 11. Further, for selected temper parameters, isostress testing was conducted at 16.5 KSI in the temperature range of 1075°F at 25F° interval to 1200°F resulting in rupture lives between 100 to several 1000 hours. The data obtained are shown in table 12. Log stress/log rupture time curves, Larson-Miller parameter plot and isostress curves resulting from the analysis of the data obtained are shown in figures 38, 39 and 40, respectively. From these figures it is evident that the rupture stress for 100,000 hour rupture life decreases with an increase in the temper parameter. Stress for 100,000 hour rupture life obtained from extrapolation of the data by log stress/log rupture time and Larson-Miller parameter techniques are presented in table 13. The decrease in the rupture stress with increase in the temper parameter appears to be of a quadratic form as depicted in figure 41. Figure

Table 11. Results of stress rupture tests conducted on PWHT SMA 2 1/4Cr-1Mo weld metal.

Code	Temper Parameter	Test Temperature (°F)	Stress (KSI)	Rupture Time (Hrs.)
TP-A	32.3	950	80.0 70.0 60.0 50.0	276.2 465.4 1646.8 2194.1
TP-B	33.4	950	70.0 60.0 50.0 42.0	190.2 758.9 1099.9 2718.8
TP-C	34.4	950	53.0 48.0 45.5 43.0	138.1 348.5 911.0 1429.9
TP-D	35.3	950	52.0 45.0 40.0 35.0	11.7 78.6 342.2 2362.9
TP-E	36.6	950	52.0 47.0 40.0 35.0 32.5 30.0	9.0 34.1 98.5 537.9 773.1 2216.4
TP-F	37.7	950	45.0 40.0 35.0 33.0 30.0 26.0	7.9 123.7 180.8 308.8 434.1 2179.4
TP-G	38.7	950	40.0 35.0 30.0 26.0	78.4 251.7 445.1 1411.9

Table 12. Results of isostress rupture tests conducted on PWHT SMA 2 1/4Cr-1Mo weld metal.

Code	Temper Parameter	Test Temperature (°F)	Stress (KSI)	Rupture Time (Hrs)
TP-A	32.3	1200	16.5	51.0
		1150	16.5	227.1
		1125	16.5	629.6
		1100	16.5	1014.2
TP-C	34.4	1175	16.5	134.8
		1150	16.5	241.6
		1125	16.5	411.6
		1100	16.5	1132.4
TP-E	36.6	1150	16.5	144.1
		1125	16.5	345.4
		1100	16.5	524.7
		1075	16.5	1349.8
TP-F	37.7	1150	16.5	69.4
		1125	16.5	182.2
		1100	16.5	318.3
		1075	16.5	815.4

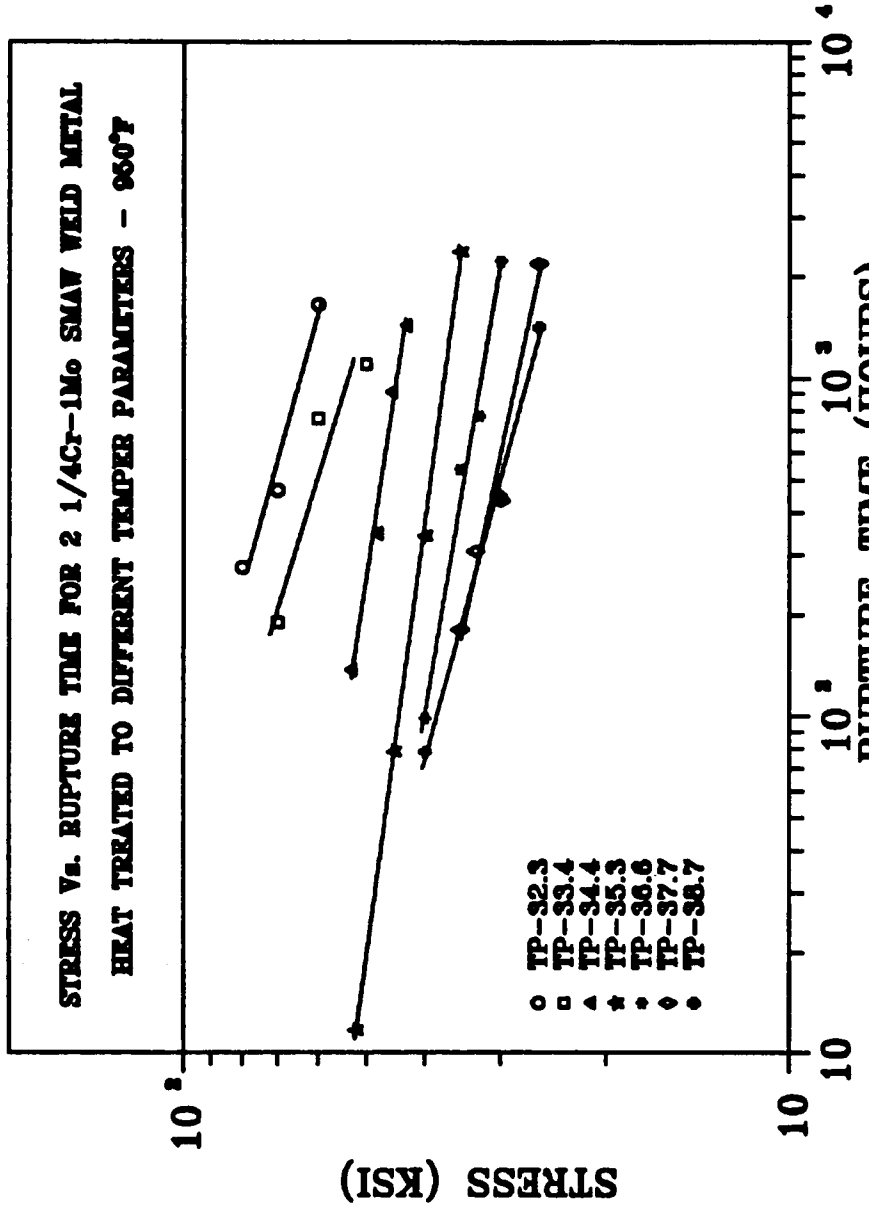

Figure 38. Stress versus rupture time plot for 2 1/4Cr-1Mo SMA weld metal postweld heat treated to different temper parameters and tested at 950°F.

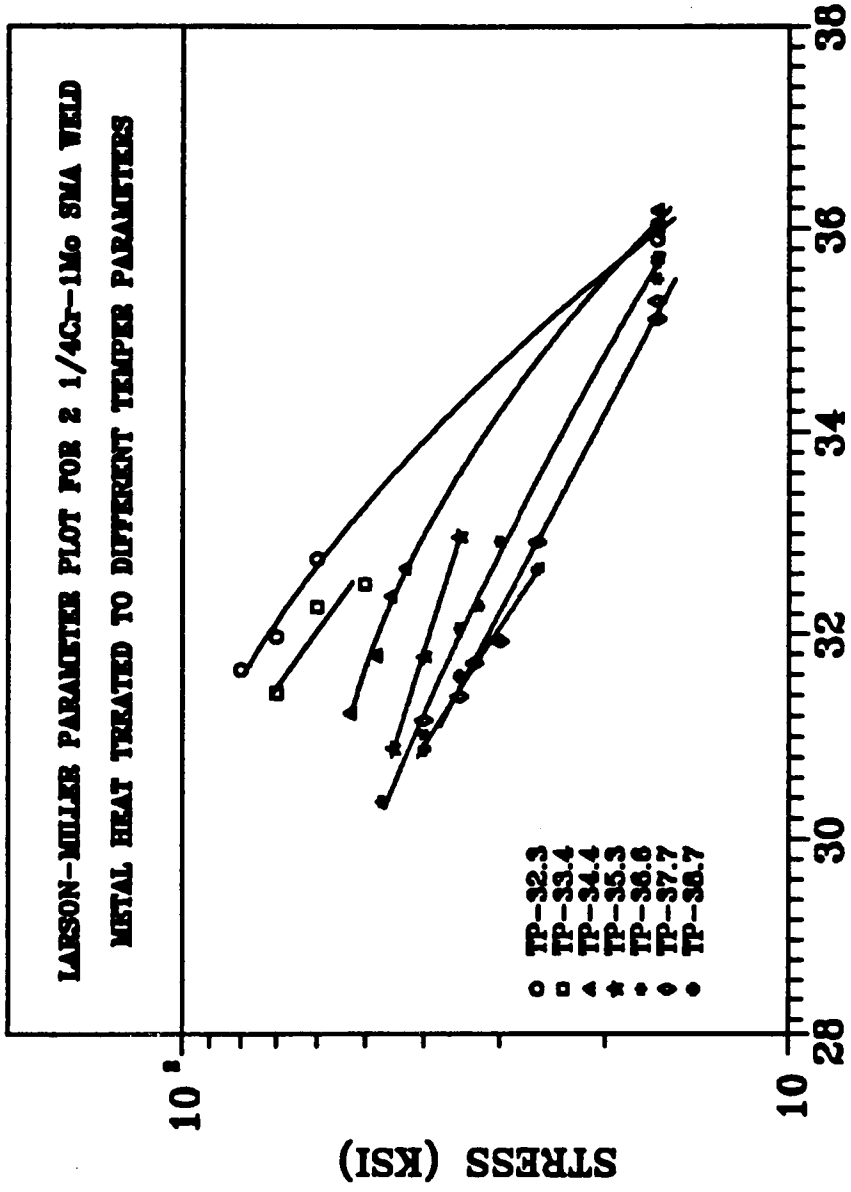

Figure 39. Larson-Miller parameter plot for 2 1/4Cr-1Mo SMA weld metal postweld heat treated to different temper parameters.

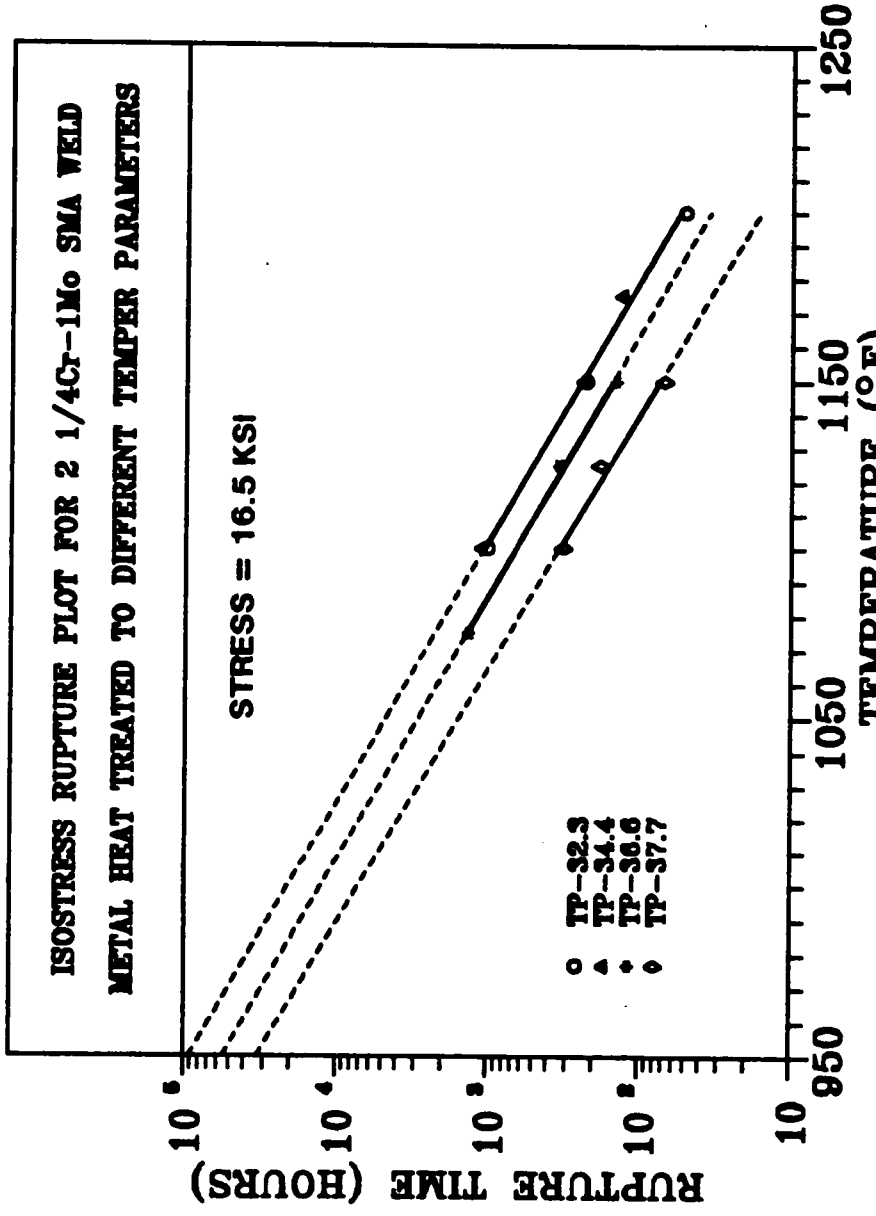

Figure 40. Isostress rupture plot for 2 1/4Cr-1Mo SMA weld metal postweld heat treated to different temper parameters.

Table 13. Extrapolated 100,000 hour rupture stress of PWHT SMA 2 1/4Cr-1Mo weld metal at different temper parameters.

Code	Temper Parameter	100,000 hour Rupture Stress (KSI)	
		Log s/ Log t_R	LMP
TP-A	32.3	31.6	24.1
TP-B	33.4	30.5	-
TP-C	34.4	30.2	22.8
TP-D	35.3	26.3	-
TP-E	36.6	21.0	19.2
TP-F	37.7	16.4	16.2
TP-G	38.7	13.6	-

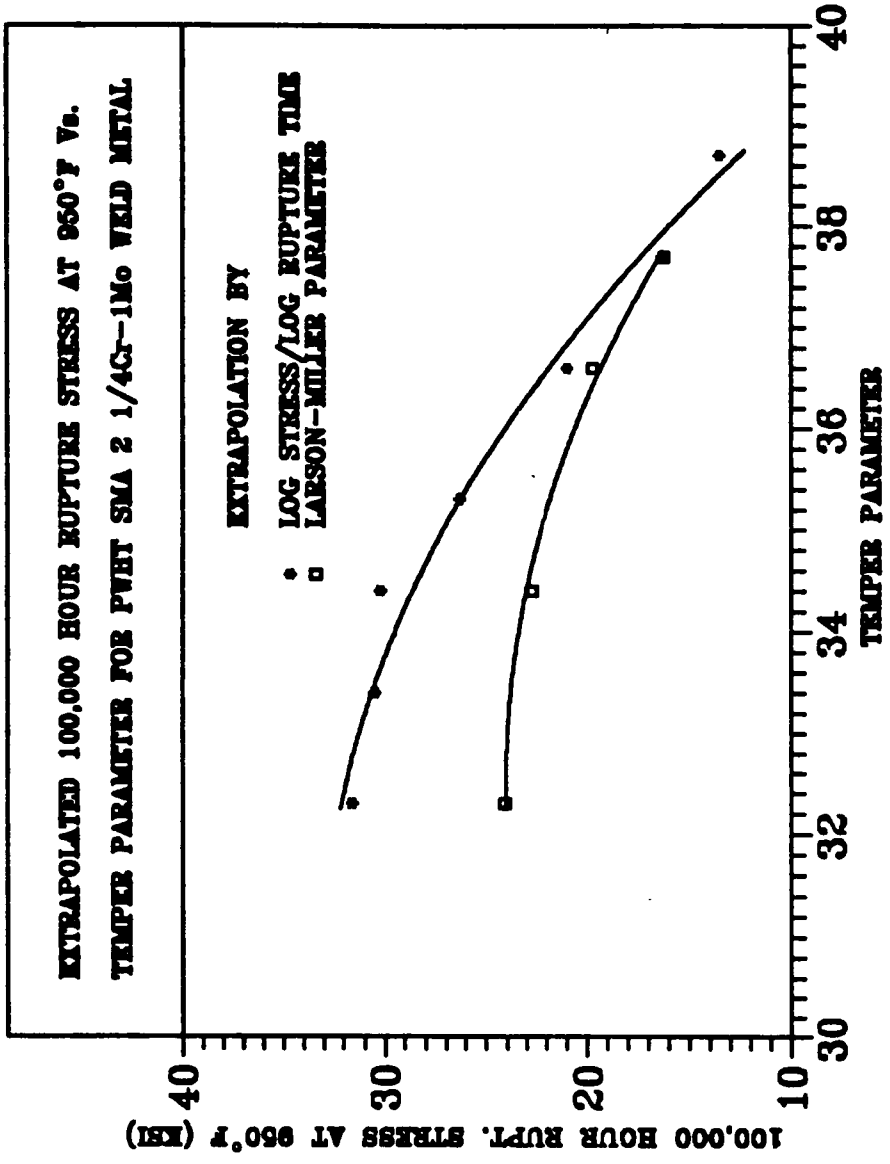

Figure 41. Plot of extrapolated 100,000 hour rupture stress at 950°F versus temper parameter for PWHT SMA 2 1/4Cr-1Mo weld metal.

41 also reveals the difference between the 100,000 hour rupture stress determined by the two methods of analysis. The log stress/log rupture time technique appears to predict a higher 100,000 hour stress than by Larson-Miller technique; the difference between the two being greater at the lower temper parameters. This can be explained by the assumptions inherent in the two techniques. Log stress/log rupture time technique assumes that the microstructure is stable at the test temperature which is not true in these cases, especially at lower temper parameters. At higher temper parameters (PWHT temperatures much higher than the test temperature) the carbides have already coarsened and are "semi" stable and further exposure at test temperatures much lower than the PWHT temperature (eg. 950^{o}F test temperature as compared to 1300^{o}F PWHT temperature) does not appreciably change the carbide size and distribution. Larson-Miller parameter type of analysis is based on an Arrhenius type of equation which assumes creep to be a thermally activated process controlled by laws of diffusion. This assumption is completely void since creep is also associated with mechanical deformation or strain sensitive processes. For example, the rate of growth of a creep cavity by vacancy condensation is enhanced by creep deformation of the surrounding material.[80] In addition, the choice of 20 as the value of constant in the Larson-Miller parameter is not theoretically rigorous. In this investigation it was found that for isostress tests at 16.5KSI different Larson-Miller parameters are evident (see figure 39). From the few test data at 16.5 KSI for the different temper parameters it was found that the constant C varied

from 12.4 to 20.18. The value of the constant C was determined by plotting 1/(T+460) versus log time and determining the slope and Y-axis intercept at log time equal to zero. Hence, the shorter time tests at higher temperatures can not accurately predict the long time behavior at lower temperatures since the mechanisms operating at higher temperatures do not necessarily operate at lower temperatures and vice versa.

Isostress rupture test data at various temperatures (shown in table 12) have been plotted and are presented in figure 40 to illustrate that the data fits a straight line regression equation as is also indicated by many other researchers[98,99,102]. The data obtained from testing specimens with temper parameters 32.3(TP-A) and 34.4(TP-C) were found to fall very close to each other and thus the regression fit was determined using the data from tests for both the temper parameters. Extrapolation of the isostress curves can be done to generate two types of information. First, it can be used to obtain the rupture life at the operating temperature and secondly, it can be used to determine the operating temperature at which rupture will occur after a specified interval of time (eg. 100,000 hours). Both sets of data from extrapolation of isostress rupture curves are given in table 14.

Surprisingly, the values determined from extrapolation of isostress tests were found to be very conservative - even lower than that determined by the Larson-Miller parameter technique (this is true for all temper parameters). For example, for a temper parameter of 32.3(TP-A) at 16.5 KSI rupture stress the rupture life at 950^{o}F

Table 14. Results obtained from extrapolation of 16.5 KSI isostress rupture curves for PWHT SMA 2 1/4Cr-1Mo weld metal.

Code	Temper Parameter	Temperature for 100,000 Hour Rupture Life (°F)	Rupture Life at 950°F (Hrs)
TP-A	32.3	947	92,000
TP-C	34.4	947	92,000
TP-E	36.6	930	55,000
TP-F	37.7	913	33,000

determined by Larson-Miller parameter technique by a quadratic regression fit was found to be 371,000 hours whereas, by isostress curve extrapolation, it was found that at 16.5 KSI the rupture life at 950°F is 92,000 hours. This further illustrates the difference between the extrapolation techniques used and therefore the difference between the resulting extrapolated values. It is evident that the log stress/log rupture time technique resulted in the highest extrapolated rupture strength followed by Larson-Miller parameter technique and isostress rupture testing technique. So, the choice of a suitable technique for determination of long term behavior must be selected with caution along with prior experience and understanding of the material under investigation.

This study to determine the effect of severity of postweld heat treatment on the long term properties indicate that the creep properties deteriorate with the increase in the PWHT time and temperature. However, at low temper parameters 32.3 (TP-A) to 34.4 (TP-C) the 100,000 hour rupture stress appears to be almost equal. At higher temper parameters the 100,000 hour rupture stress decreases rapidly with an increase in the severity of tempering. Some long time tests (10,000 hours) are underway and the results from these tests will be helpful in arriving at a concrete conclusion.

Earlier research conducted by Roger, Phelps and Murphy[118] have indicated an inferiority of creep strength for weld metals deposited by automatic high heat input-high deposition rate processes. In this study almost identical weld metal compositions were obtained by SAW and the SMAW processes. The main differences in the chemistry of the

SA weld metal and the SMA weld metal is that the SA weld metal contains 2.69% Cr and 0.19%Ni whereas the SMA weld metal contains 2.15% Cr and 0.04% Ni. This difference in chemistry should however, result in superior stress rupture properties of the SA weld metal. SA weld metal was heat treated at 1300°F for 25 hours (C1.2) and SMA weld metal was heat treated at 1300°F for 25 hours followed by additional aging at 1193°F for 21.5 hours to simulate 100,000 hours service exposure at 950°F. From a comparison of the stress rupture data obtained from the tests at 950°F (shown in figure 42) it is clearly evident that 2 1/4Cr-1Mo weld metal deposited by shielded metal arc welding has superior creep properties than that deposited by submerged arc welding. This may be true for other high temperature steels as well. In this study the SMA weld had received additional tempering at 1193°F for 21.5 hours compared to that of SA weld metal although the temper parameters are not significantly different. SA weld metal in PWHT (C1.2) condition has a temper parameter of 37.66 and the SMA weld metal was tempered to a temper parameter of 37.69. Such a difference in the stress rupture strength of weld metal deposited by the two different techniques maybe due to the difference in chemical compositions and impurity element concentrations and/or the difference between the inclusion size, number and distribution. The former two reasons may be considered to be minor reasons for such behavior although the latter is suspected to be the main reason. Research being conducted at Combustion Engineering in Chattanooga and also some investigations underway at the University of Tennessee have shown that the stress rupture

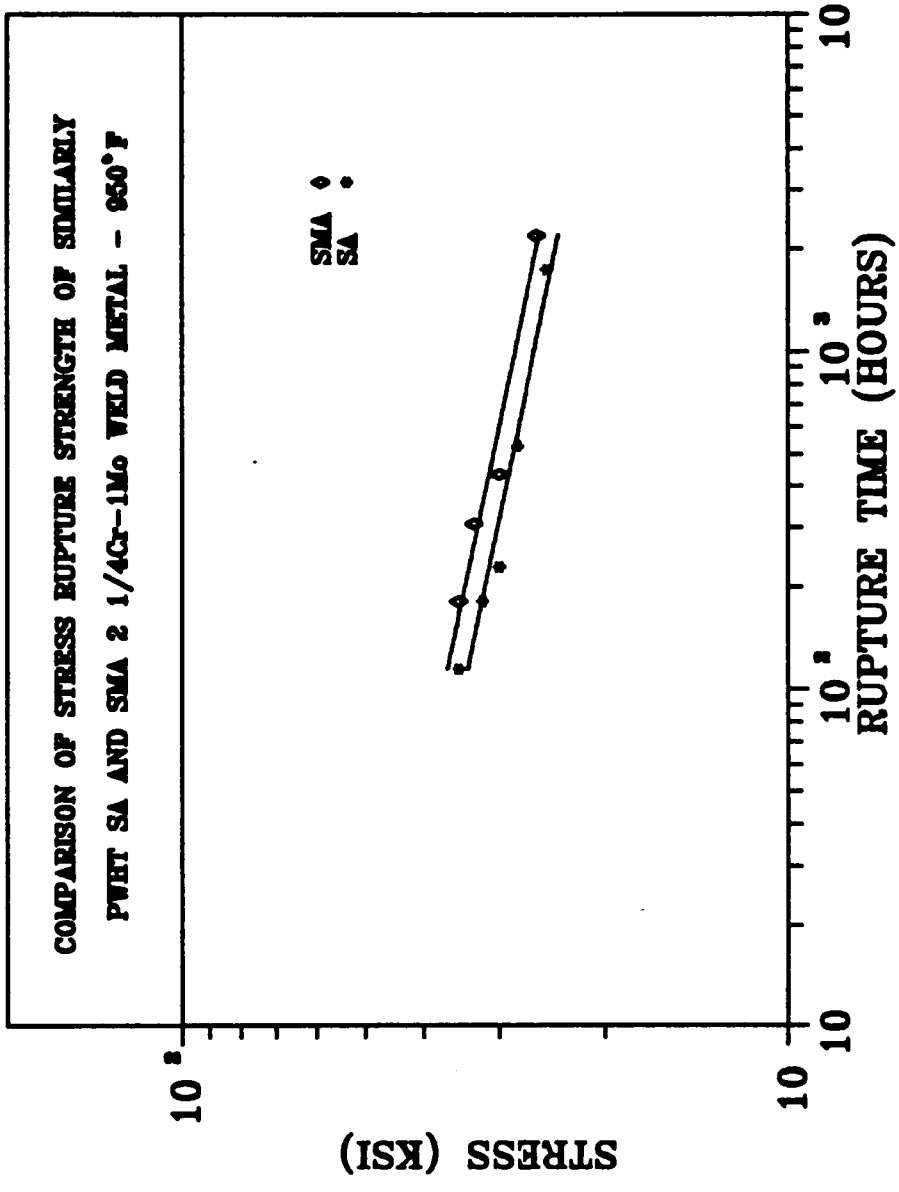

Figure 42. Comparison of stress rupture strength of similarly postweld heat treated SA and SMA 2 1/4Cr-1Mo weld metal at 950°F.

strength of 2 1/4Cr-1Mo weld metal depends on the inclusion size, distribution, composition, and volume fraction.

4.6 MICROSTRUCTURAL ANALYSIS OF SA WELDMENT HEAT TREATED TO THE A&T, N&T AND PWHT(C1.2) CONDITION

Microstructural analysis studies of 2 1/4Cr-1Mo steel in the A&T and N&T condition have been accomplished by researchers working on Cr-Mo steels.[1-7,9,11,18,20,32,38,42,46] The carbide coarsening kinetics in different microconstituents (eg. polygonal ferrite, bainite etc.) occurring in 2 1/4Cr-1Mo steel has been studied quite extensively.[1,18] The main aim of this portion of the study was to characterize the microstructure of the weld metal and HAZ as a function of the heat treatments employed, especially the "soft" ferrite band along the fusion line in the HAZ.

2 1/4Cr-1Mo weld metal in the as welded condition has been known to contain variations of upper bainite (massive, granular, lath) and some retained austenite-martensite aggregates or lower bainite. Polygonal ferrite in weld metal in the as welded condition is observed only if the carbon content is low (<0.04%). However, heating the weld metal above the A_3 temperature would result in complete alteration of the solidification substructure and subsequent cooling to room temperature will result in a mixture of proeutectoid ferrite and bainite, the relative proportion of which will depend on alloying elements and the cooling rate. In the PWHT(C1.2) condition the as welded structure is generally retained with an accompanying precipitation and coarsening of carbides. Figure 43 shows the

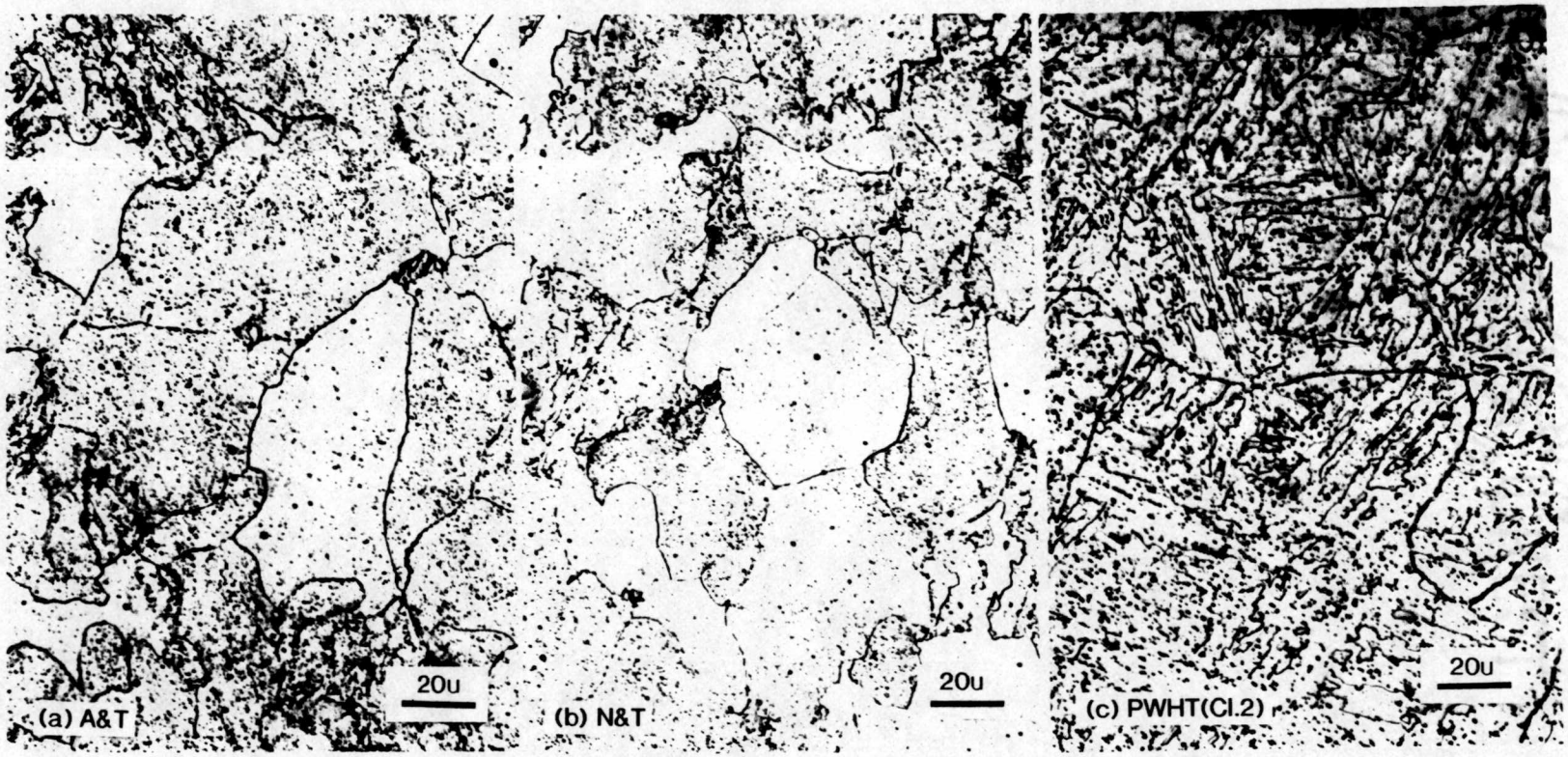

Figure 43. Microstructure of 2 1/4Cr-1Mo SA weld metal in A&T, N&T and PWHT(Cl.2) conditions, 500X, 2% nital etch, OLM.

optical microstructures of weld metal in the A&T, N&T and PWHT(C1.2) conditions. In the case of the A&T condition it is evident that the relative proportion of polygonal ferrite is much greater than in N&T condition. This is due obviously to the slow cooling from the austenitizing temperature which allows more time for the transformation to proeutectoid ferrite. The microstructure of the weld metal in the PWHT(C1.2) condition shows a 100% bainitic structure with readily visible bainite laths and clearly defined prior austenite grain boundaries. In the case of the A&T and N&T heat treatments the base metal and the weld metal experience similar cooling rates from the A_3 temperature and thus the base metal and weld metal exhibit similar microstructural features (see figure 44). The as-received base metal was in the normalized and tempered condition and additional subcritical PWHT has not changed the structure of the base metal. However, such PWHT results in coarsening of carbides but this can not be observed at the optical resolution.

Carbide distribution and morphology in 2 1/4Cr-1Mo steels are not revealed by OLM due to fine carbide structure and insufficient resolution of the light microscope. Hence, analytical microscope techniques based on electron optics have been used to further characterize the microstructural features so that it is possible to establish a firm microstructure-property correlation. The kinetics of carbide coarsening as well as their change in composition and type as a result of exposure to elevated temperature have been studied by Baker and Nutting[18] for quenched and tempered and normalized and

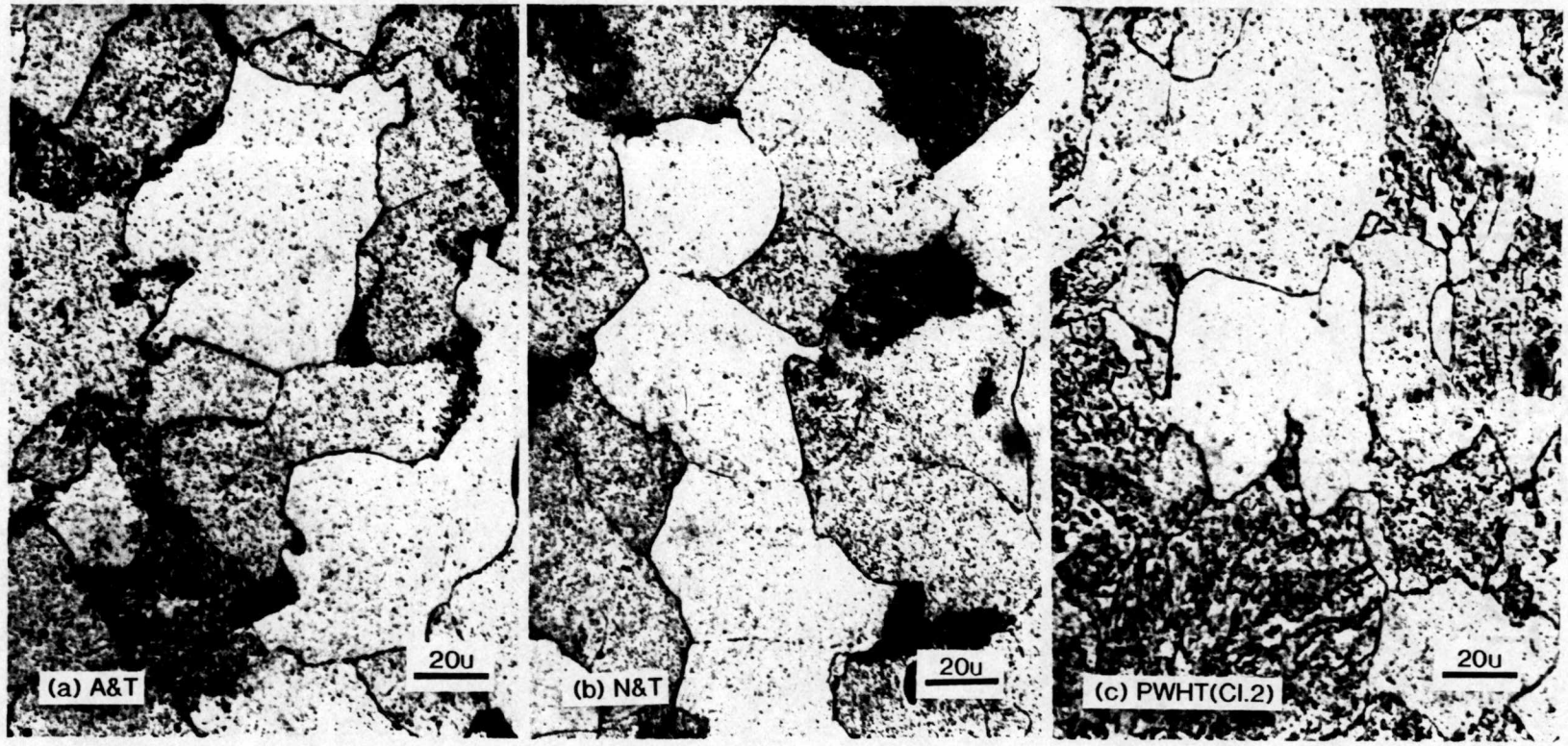

Figure 44. Microstructure of base metal of the 2 1/4Cr-1Mo SA weldment in A&T, N&T and PWHT(Cl.2) conditions, 500X, 2% nital etch, OLM.

tempered 2 1/4Cr-1Mo steel. This study revealed the difference between the stability of carbides in ferrite and bainite, the carbides in the former being more stable than in the latter. It is this stability of carbides which dictate the elevated temperature properties of the steel. However, the elevated temperature creep strength also depends on the tensile strength which is higher for the N&T than the A&T. Thus, for the selection of suitable heat treatments the service temperature will be the deciding factor. In other words, 2 1/4Cr-1Mo steel has been found to have the highest tensile strength in the N&T condition followed by the A&T condition but the creep strength is reduced more rapidly upon exposure at high temperature for N&T material followed by the A&T material. The loss in strength will depend on the temperature which determines the rate of diffusion of solute elements.

SEM micrographs of weld metal in the three heat treated conditions are shown in figures 45 and 46. The carbide distribution can clearly be seen. In the A&T and N&T condition the proeutectoid ferrite has finer carbide distribution than upper bainite. No other microconstituents were found in the A&T and N&T weld metals. In the PWHT(C1.2) condition the carbide structure is considerably coarser than in A&T and N&T condition. The microconstituents present in weld metal in PWHT (C1.2) were identified as lath and massive bainite.

The carbide distribution is usually clearly defined by SEM observation but the morphology, type, chemistry and size of precipitates are difficult to determine. This is because of the fact that carbides are embedded in the matrix and the resolution of SEM is

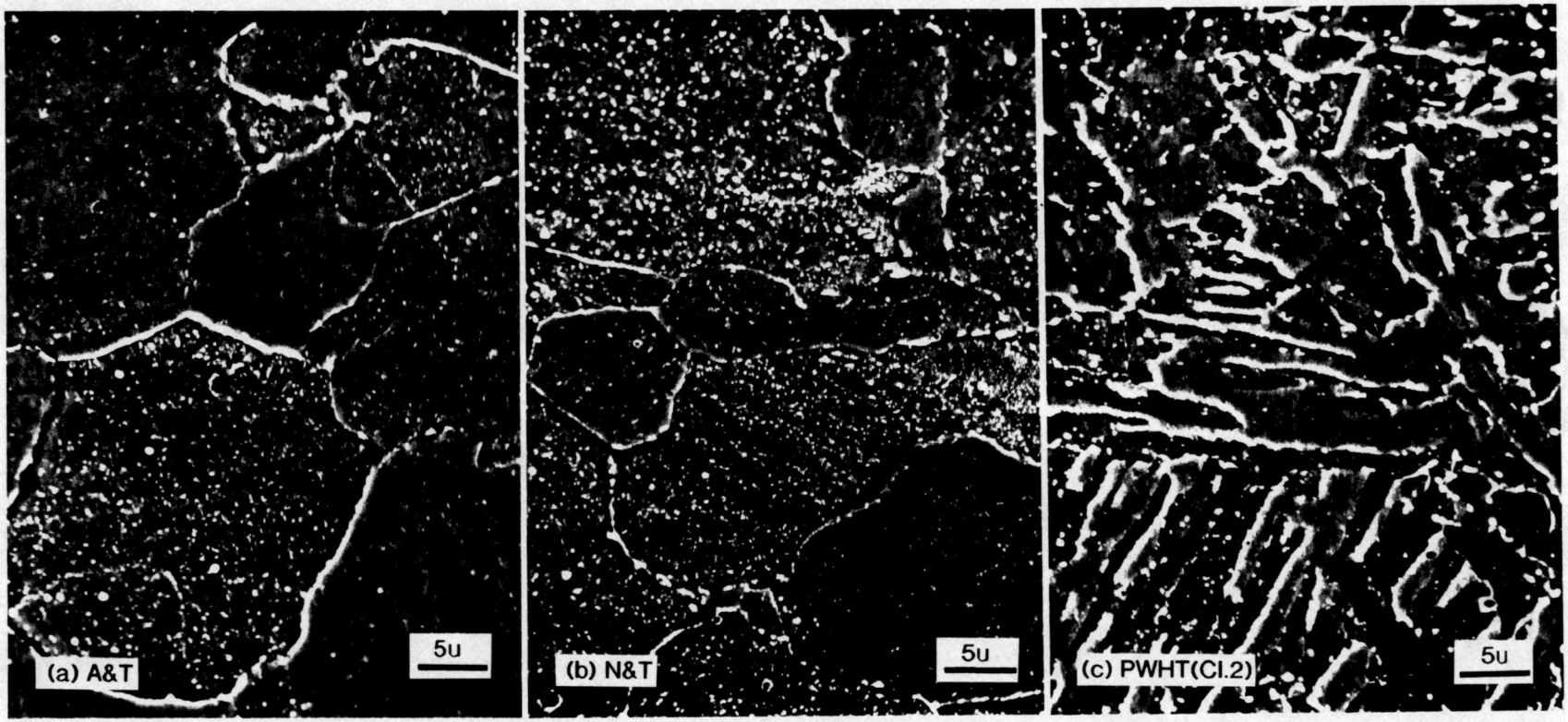

Figure 45. Microstructure of 2 1/4Cr-1Mo SA weld metal in A&T, N&T and PWHT(C1.2) conditions, 2000X, 2% nital etch, SEM.

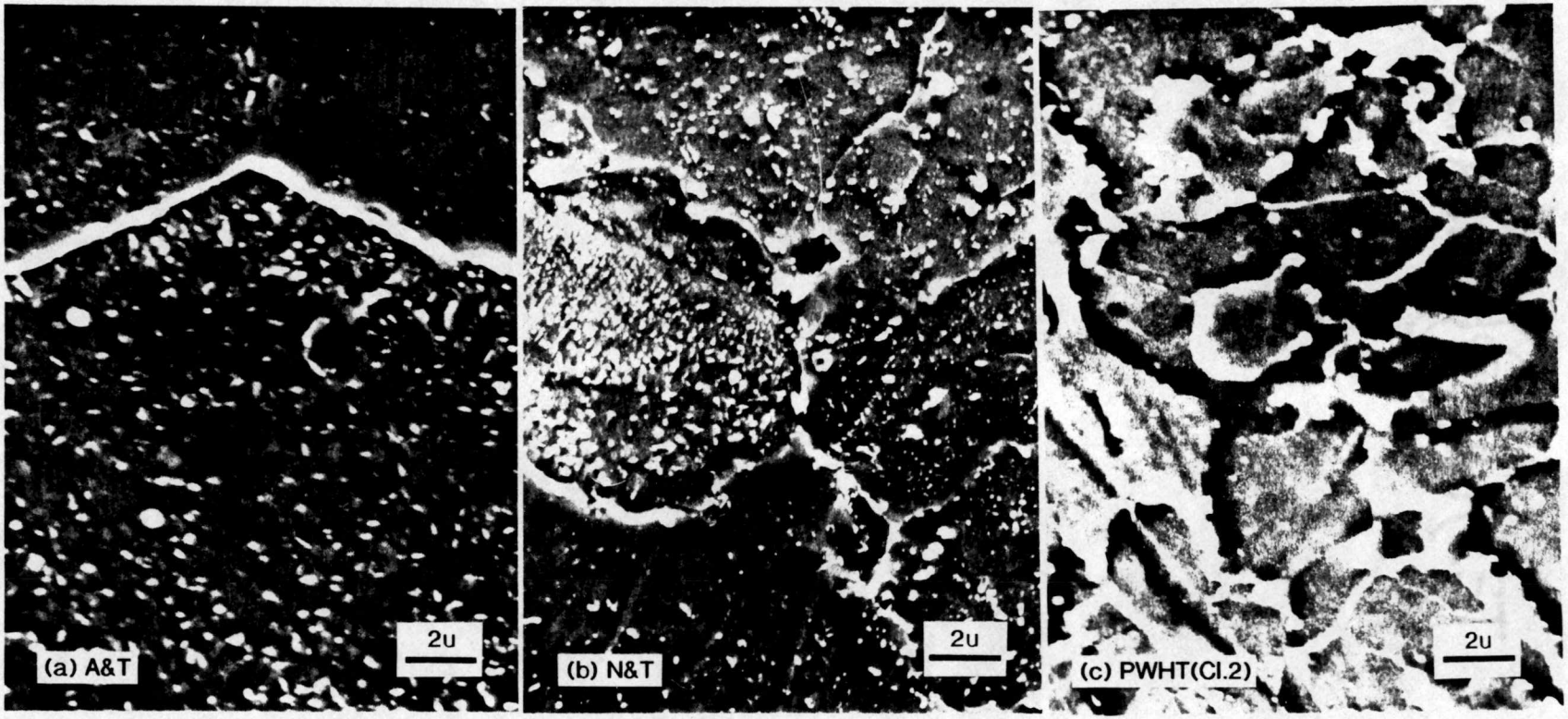

Figure 46. Microstructure of 2 1/4Cr-1Mo SA weld metal in A&T, N&T and PWHT(C1.2) conditions, 5000X, 2% nital etch, SEM.

not sufficient to conduct valid analysis. In addition, it is not possible to carry out microanalysis of the particles because of the possible interference with neighboring carbides and the background matrix which could result in misinterpretation. Thus SEM was only useful to determine the overall carbide distribution and identify the various transformation products.

To identify the precipitates, carbide extraction on a carbon film was found to be the best solution. Extraction replicas were observed and analyzed in the STEM mode and micrographs were obtained in the TEM mode for the best resolution and clarity. In the as-welded condition very fine carbide precipitates were observed. These are probably ϵ-carbides which are the first ones to form in the 2 1/4Cr-1Mo steel as pointed out by Baker and Nutting[18]. Selected area microanalysis conducted to determine the carbide type showed that the carbides contain chromium, iron and molybdenum. The microstructure of the SA weld metal in the as-welded condition as shown in figure 47, resembles those shown by Baker and Nutting[18] to contain ϵ-carbide and cementite. The few large particles seen in figure 47 were found to be inclusions containing Mn, Si and Al.

The carbides in heat treated SA weld metal (A&T, N&T and PWHT(C1.2) conditions) are shown in figures 48 and 49. Three different carbide morphologies were observed in the A&T condition. The short rod like precipitates were found to be $(Cr,Mo)_2(C,N)$ or M_2C type carbides. M_2C type carbides were also found to occur as long thin needles (figure 49a). The small dark particles, irregular in shape, were analyzed to be $M_{23}C_6$ type. $M_{23}C_6$ type carbides were

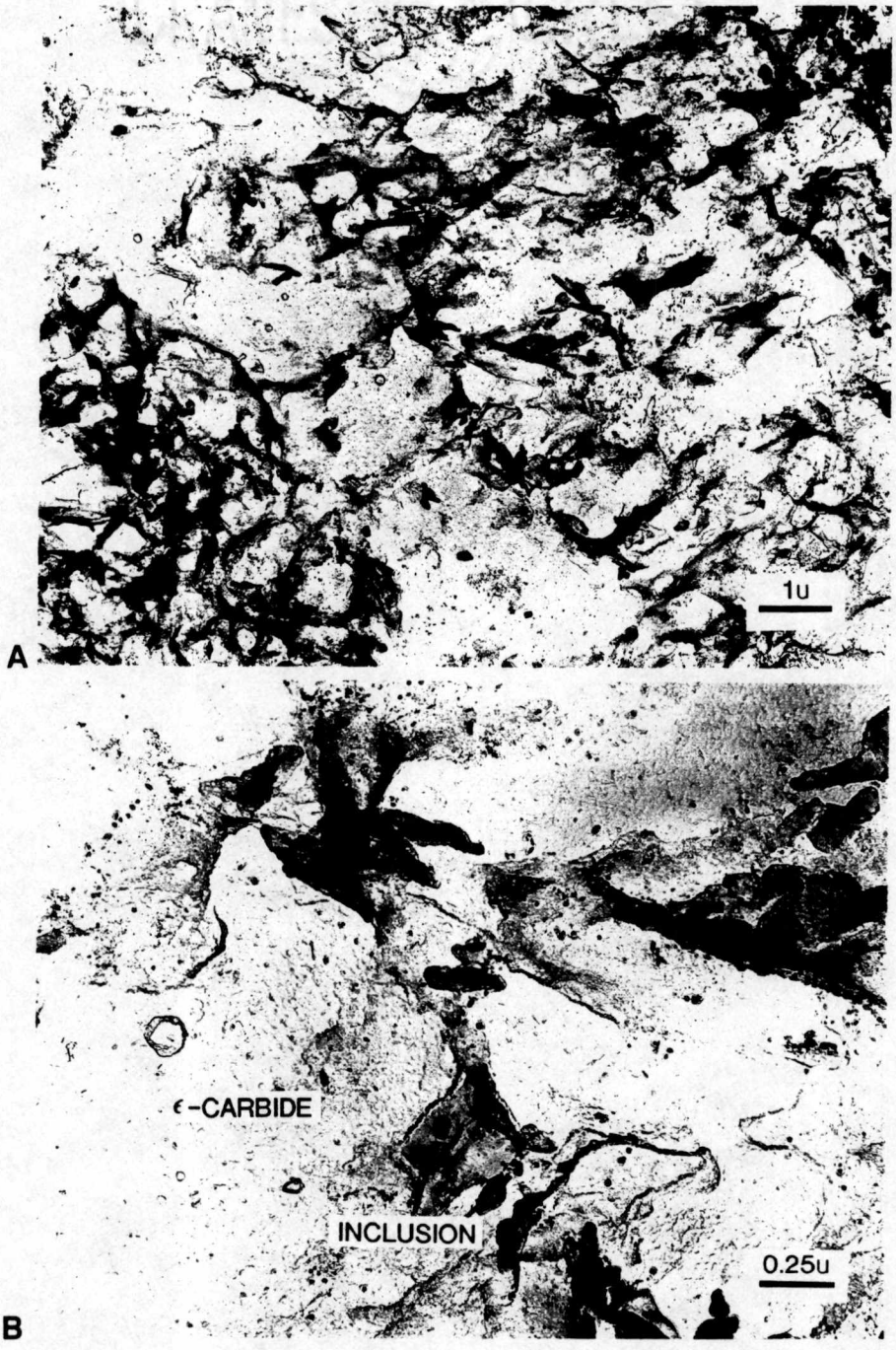

Figure 47. TEM photomicrographs of 2 1/4Cr-1Mo SA weld metal in the as-welded condition showing fine precipitates of ϵ-carbides and cementite, carbon extraction replica, (a) 10,000X, (b) 40,000X.

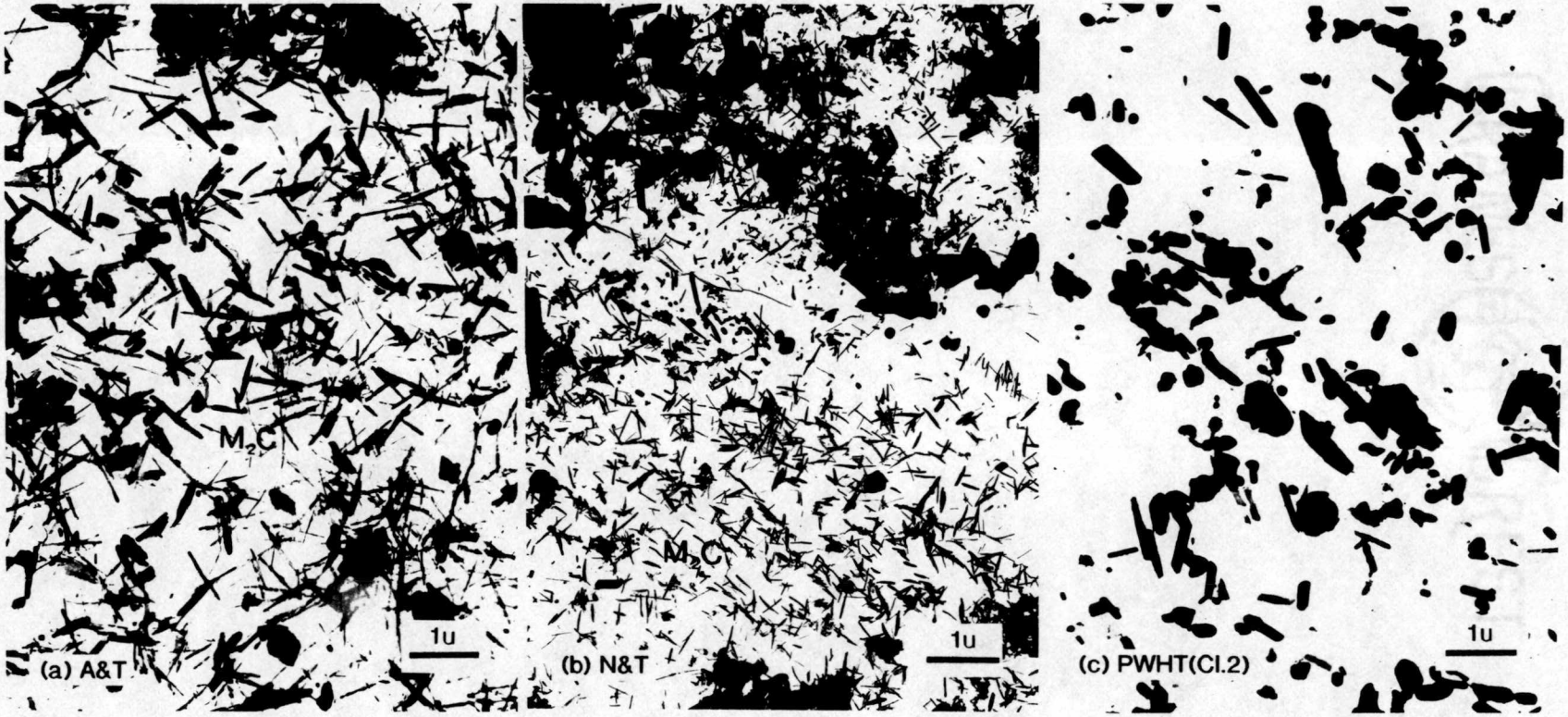

Figure 48. TEM photomicrographs of 2 1/4Cr-1Mo SA weld metal in A&T, N&T and PWHT(C1.2) conditions, carbon extraction replica, 10,000X.

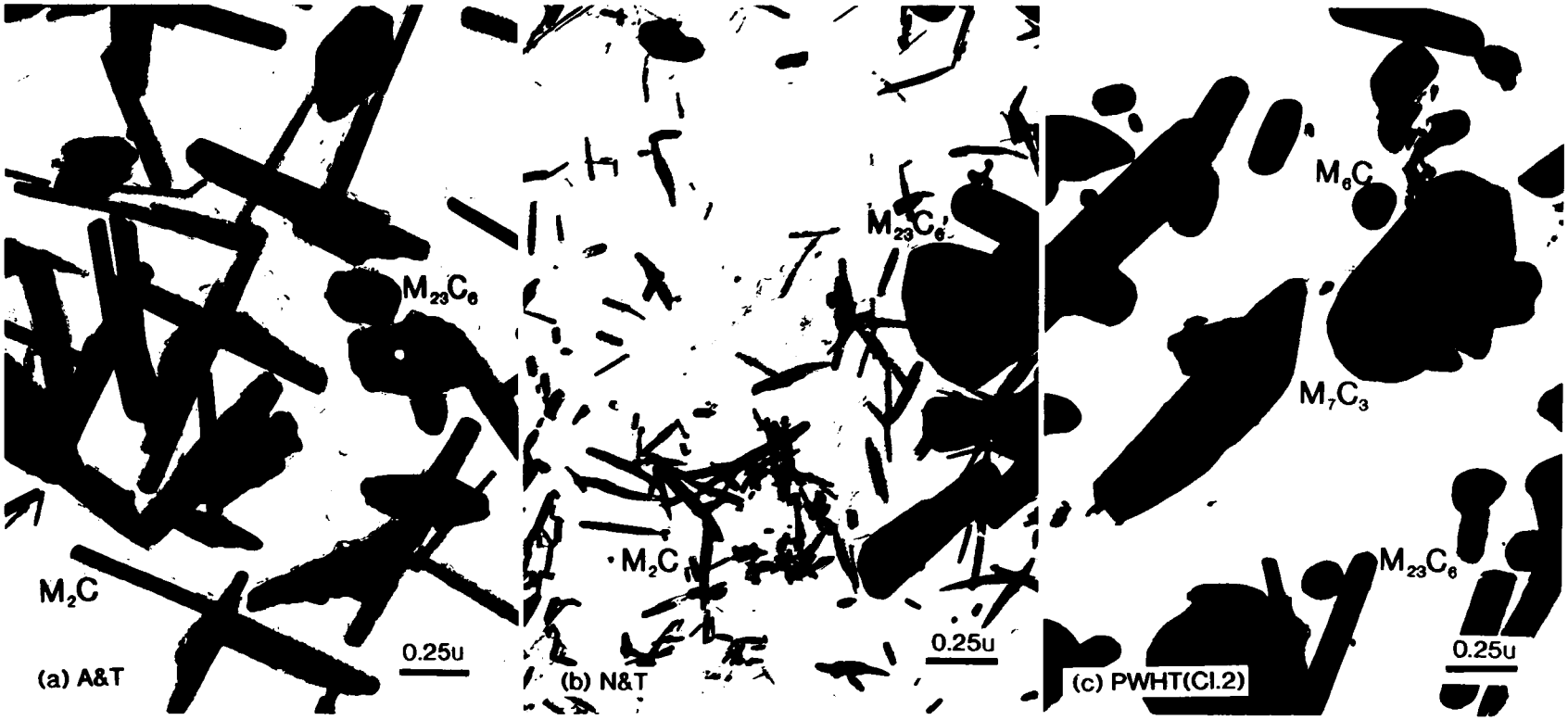

Figure 49. TEM photomicrographs of 2 1/4Cr-1Mo SA weld metal in A&T, N&T and PWHT(Cl.2) conditions, carbon extraction replica, 40,000X.

usually noted at the grain boundaries or the bainite lath boundaries. Within the ferrite grains the two types M_2C carbides were predominant. In general, the carbides in the A&T material were found to be coarser than those in the N&T material.

In the N&T condition irregular shaped $M_{23}C_6$ type carbides were found at the grain boundaries and at bainite lath boundaries and in the ferrite grains and bainite laths M_2C or M_2X type carbides were revealed. The occurrence of M_2X or $(Cr,Mo)_2(C,N)$ type carbo-nitrides have been reported to occur in 2 1/4Cr-1Mo steel base metal and weld metal by many researchers[34,37,38]. Unlike M_2C carbides, which are rich in molybdenum, $(Cr,Mo)_2(C,N)$ type carbo-nitrides are rich in chromium along with substantial amounts of molybdenum. Mo_2C type carbides have a face centered cubic crystal structure whereas, the $(Cr,Mo)_2(C,N)$ have been found to be hexagonal by Todd[35]. The difference between the two can be easily distinguished by their characteristic selected area X-ray diffraction spectra and electron diffraction patterns. M_2C type carbides were not found in the weld metal PWHT(Cl.2) except in very few areas. The carbides in the PWHT(Cl.2) weld metal in general were very coarse compared to the carbides in the A&T or N&T weld metal. Large particles of $M_{23}C_6$ were predominant in the microstructure followed by some small irregular shaped M_7C_3 type and M_6C type precipitates.

The base metal in the A&T and N&T conditions revealed similar structures as to the weld metal in the same heat treated conditions by SEM and TEM observation. SEM micrographs of base metal in the A&T, N&T and PWHT (Cl.2) conditions are shown in Figure 50. The base

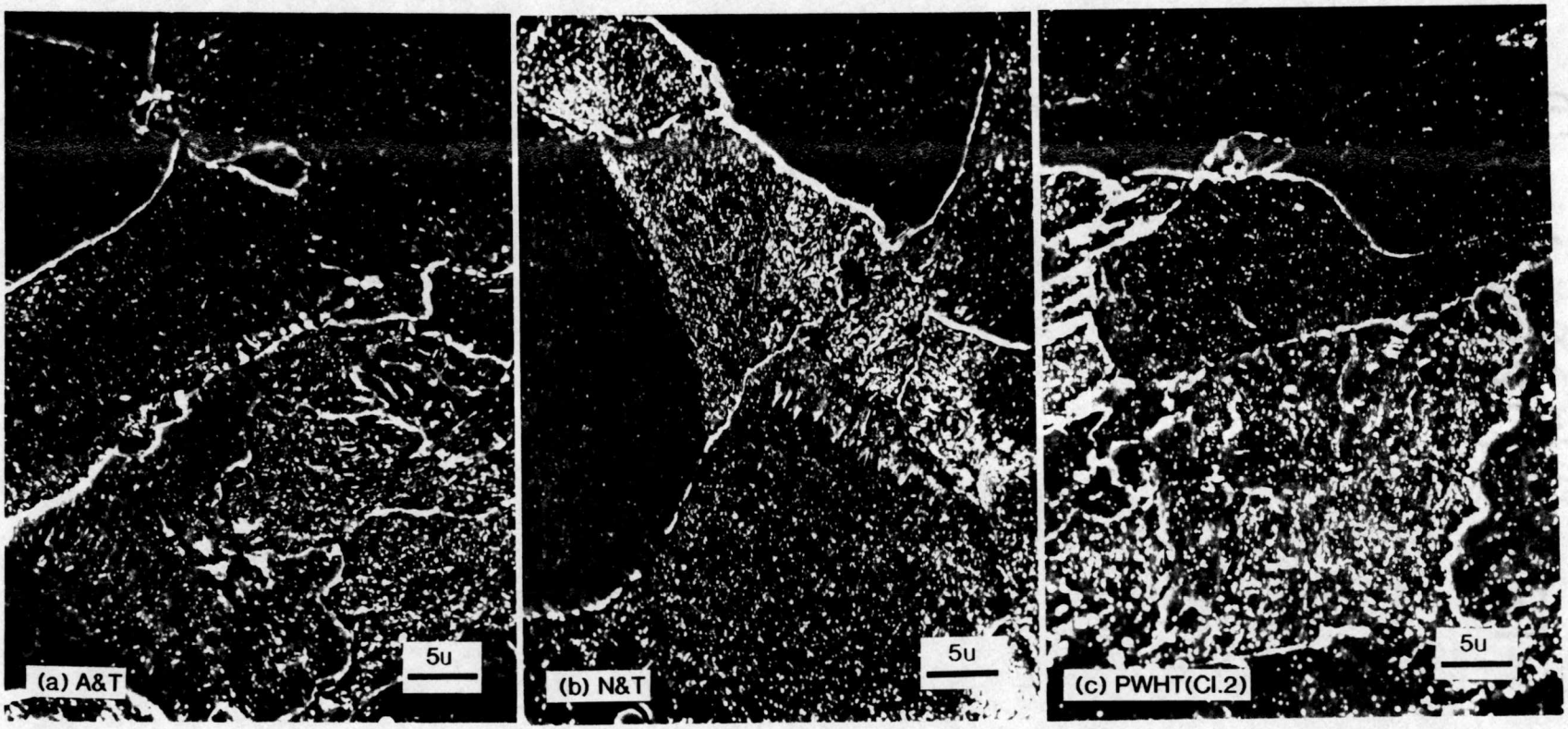

Figure 50. SEM photomicrographs of the base metal of 2 1/4Cr-1Mo SA weldment in A&T, N&T and PWHT(Cl.2) conditions, 2000X, 2% nital etch.

metal of the weldments in all the three conditions of heat treatment contained proeutectoid ferrite and bainite. The bainitic regions can be easily distinguished from the ferrite regions due to presence of coarser carbides. As indicated by Baker and Nutting[18] the carbides occurring in ferrite are more stable than the carbides in bainitic areas and they resist coarsening even during high temperature PWHT or elevated temperature service. In the PWHT (C1.2) condition it can be seen that the carbides are much coarser due to the additional tempering received by the base metal during PWHT. Figure 51 illustrates the carbide structure of the base metal in the three heat treatment conditions.

In the A&T condition the carbides in the base metal were again found to be coarser than in the N&T base metal. The base metal and weld metal of the A&T weldment has undergone the same heat treatment from the austenitization temperature followed by tempering. The base metal and weld metal of the N&T weldment has also undergone the same heat treatment from the austenitization. So it is reasonable to find similar carbide structures in the base metal and weld metal of the A&T material. In case of the N&T material also, the base metal and weld metal reveal similar carbide structure. Acicular carbides or carbonitrides (M_2X type) were found to be the predominant precipitate in the A&T and N&T base metal along with some rod shaped and irregular shaped $M_{23}C_6$ type carbides. The small irregular shaped particles found in the base metal were of the M_2X type. Two different morphologies of the same type of carbide in the same steel have been observed by many researchers and in particular, Woodhead

Figure 51. TEM photomicrographs of the base metal of 2 1/4Cr-1Mo SA weldment in A&T, N&T and PWHT(C1.2) conditions, carbon extraction replica, 20,000X.

and Quarrel[31] have shown several such examples. They have indicated that the identification of carbides should not be based upon its morphology since same type of carbide can occur in different shapes in the same steel. In the PWHT (C1.2) weldment the base metal had undergone tempering and this is reflected in the coarse carbide structure. However, few M_2C type carbides persist in the microstructure. The predominant morphologies were found to be large irregular shaped particles of the M_7C_3 and $M_{23}C_6$ types and thick cylindrical particles of the M_7C_3 type. Some small $M_{23}C_6$ type carbides and M_6C type carbides were also found.

As discussed in the earlier section, the "soft" carbon denuded zone was found to be more creep resistant than the adjacent fusion zone or the base metal. None of the stress rupture specimens ruptured in the "soft" zone although a hardness difference of about 35 DPH was found in this region compared to the adjacent carbon enriched region. SEM observations revealed that this zone was not devoid of carbides. Fine carbide in the ferrite grains of the "soft" zone can be seen in the SEM microstructure shown in figure 52. These carbides were identified as Mo_2C or $(Cr,Mo)_2CN$ (see figure 53). Thus, the "soft" zone has a fine dispersion of acicular carbides in a low carbon ferritic matrix from which the carbon in solid solution has migrated to the weld fusion zone during heat treatment driven by a difference in the level of chromium (activity of carbon). Molybdenum remaining in solid solution in the ferritic matrix acts as a solid solution strengthener. The "solute atmospheres" generated by the remaining molybdenum in solid solution along with fine carbide

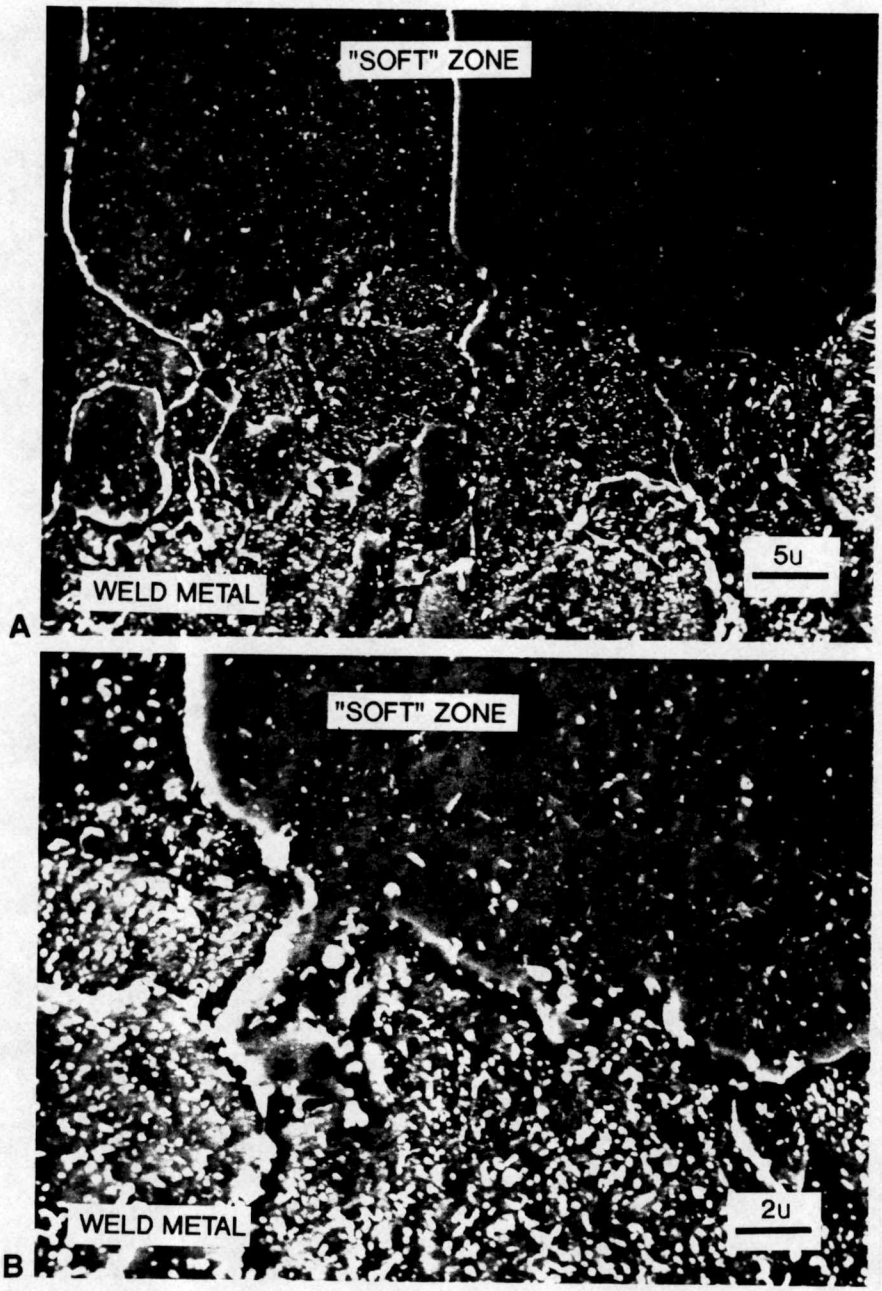

Figure 52. SEM photomicrographs of the "soft" zone in 2 1/4Cr-1Mo SA weldment in A&T condition. Note fine carbide precipitates in the ferrite grains, (a) 2000X, (b) 5000X, 2% nital etch.

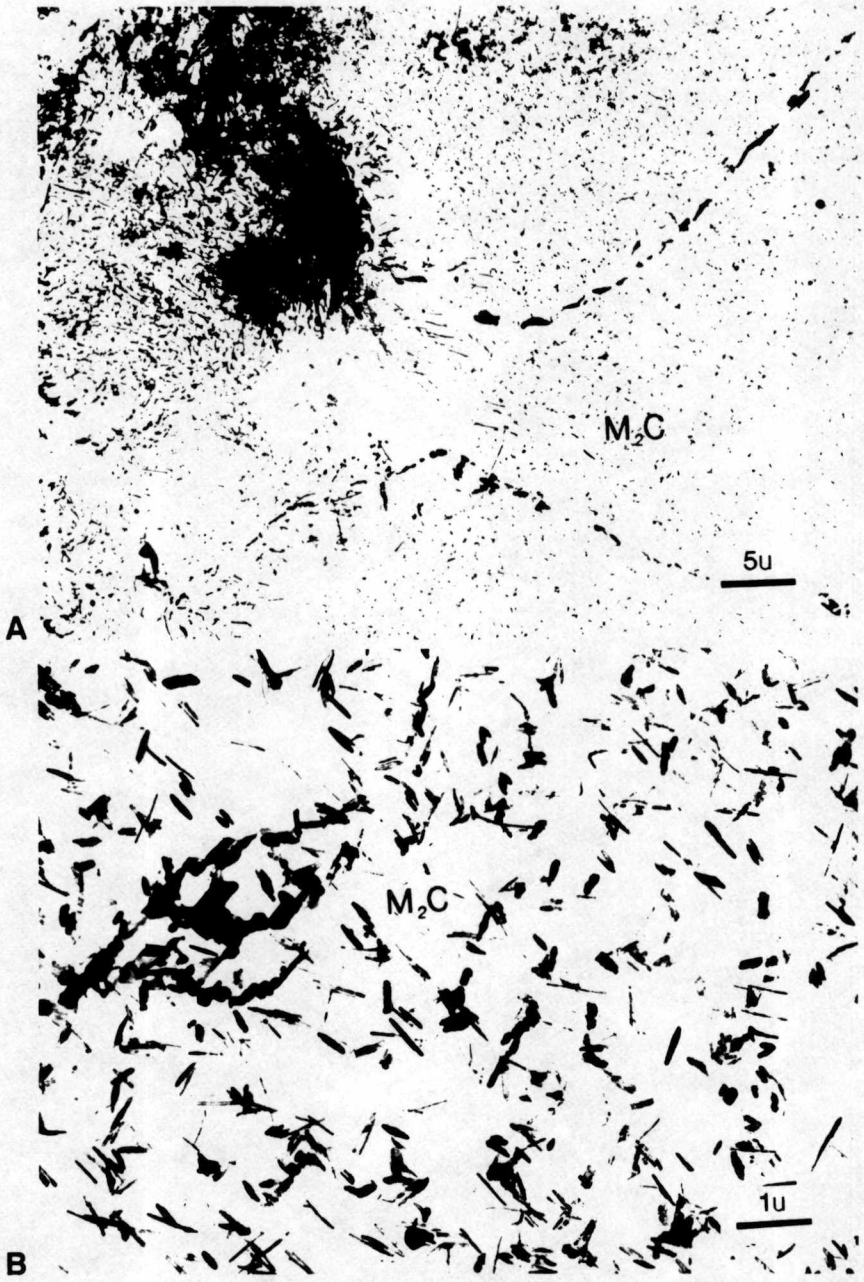

Figure 53. TEM photomicrographs of the "soft" zone in 2 1/4Cr-1Mo SA weldment in A&T condition. Note dense carbide precipitation in the weld metal side of fusion line and fine M_2C type carbides in the "soft" zone, carbon extraction replica, (a) 2000X, (b) 10,000X.

precipitates result in the ideal condition for creep resistance in this region of the alloy. Thus, the composite specimens do not rupture in this region.

From the above discussion, it is clear that the stress rupture strength of 2 1/4Cr-1Mo weld metal (or base metal) will depend on the microconstituents present and carbide size and distribution. A&T material has more polygonal ferrite in which the carbides are stable and hence has better creep properties at higher temperatures (>1050°F). The N&T material has less proeutectoid ferrite and more bainite than the A&T material and hence is superior at lower temperatures. The PWHT(Cl.2) material has almost a 100% bainitic structure with coarser carbides (than those in A&T and N&T conditions) due to tempering and hence its relative position in the stress rupture plots depends on the test temperature; superior to A&T at 950°F and inferior to N&T at 1050°F.

Comparing the base metal and weld metal microstructures, the cause for rupture in weld metal or base metal is clear except in the case of the A&T specimens in which the location of rupture changes from weld metal at 950°F to base metal at 1050°F and again to weld metal at 1125 to 1250°F. The reason for this was not clear from the microstructural analysis. There is very little difference in the microstructure of the base metal and weld metal and hence the shift in rupture location. Some subtle differences in the microstructure, responsible for this behavior, has not been revealed by the present study.

In the case of the N&T base metal it is clear that it is stronger than the weld metal. This is reflected in both the carbide size and type present in base metal and weld metal. The base metal contains mainly acicular M_2C type carbides whereas the carbides present in weld metal are M_2C type along with some comparatively coarser $M_{23}C_6$ type carbides at the prior austenite grain and lath boundaries. The reason for more rapid coarsening of carbides in weld metal compared to the base metal, probably lies in the solidification substructure segregation of solute elements which is characteristics of weld solidification. The diffusion distance required for the solute elements to join the carbides is greatly reduced due to such segregation and hence the carbides can coarsen more rapidly in the weld metal as compared to the base metal in which segregation is minimal due to the extensive prior thermal and mechanical treatments. In the PWHT(C1.2) condition the base metal which was originally in the normalized and tempered condition receives additional tempering along with the PWHT of the weld metal. This is the reason for the observed change in carbide type and size in the base metal compared to the weld metal and hence the transverse specimens in PWHT(C1.2) condition ruptured in the base metal.

4.7 MICROSTRUCTURAL ANALYSIS OF SMA WELD METAL POSTWELD HEAT TREATED TO DIFFERENT TEMPER PARAMETERS

In order to determine the microstructural features of 2 1/4Cr-1Mo SMA weld metal heat treated to various temper parameters, optical, SEM and STEM/TEM examination was performed. The main aim of

this investigation was to determine the changes of carbide size, type, distribution, morphology and chemistry upon heat treatment and establish a correlation between properties and microstructure.

Optical light microscopy conducted on the specimens heat treated to various temper parameters revealed that the microstructure of weld metal became more and more uniform with an increase in temper parameter. This can be seen in figure 54. From the micrographs it can be seen that the prior austenite grain boundaries etch darker for the low temper parameters (TP-A to TP-C). As the temper parameter increases this effect is lessened and for the higher temper parameters (TP-E to TP-G) the effect is absent. This etching phenomena is due to a large number of very fine carbide precipitates at the grain boundaries. This was confirmed by examination of the extracted carbides as shown in figure 55. The prior austenite in these regions may be the last to transform or there may be retained austenite in these regions which during subsequent tempering resulted in the dense carbide precipitated areas. The carbides in these regions were found to be of the M_2C type. The retained austenite or the austenite regions last to transform are usually rich in carbon, due to carbon diffusing away from the transformation product/austenite interface into austenite, hence resulting in subsequent dense carbide precipitation. At higher temper parameters these carbides coarsen rapidly and so the microstructure appears more uniform. A lath like bainitic structure is evident from the micrographs (figure 54) with the bainite lath thickness increasing with an increase in the severity of tempering. Krauss[30] has

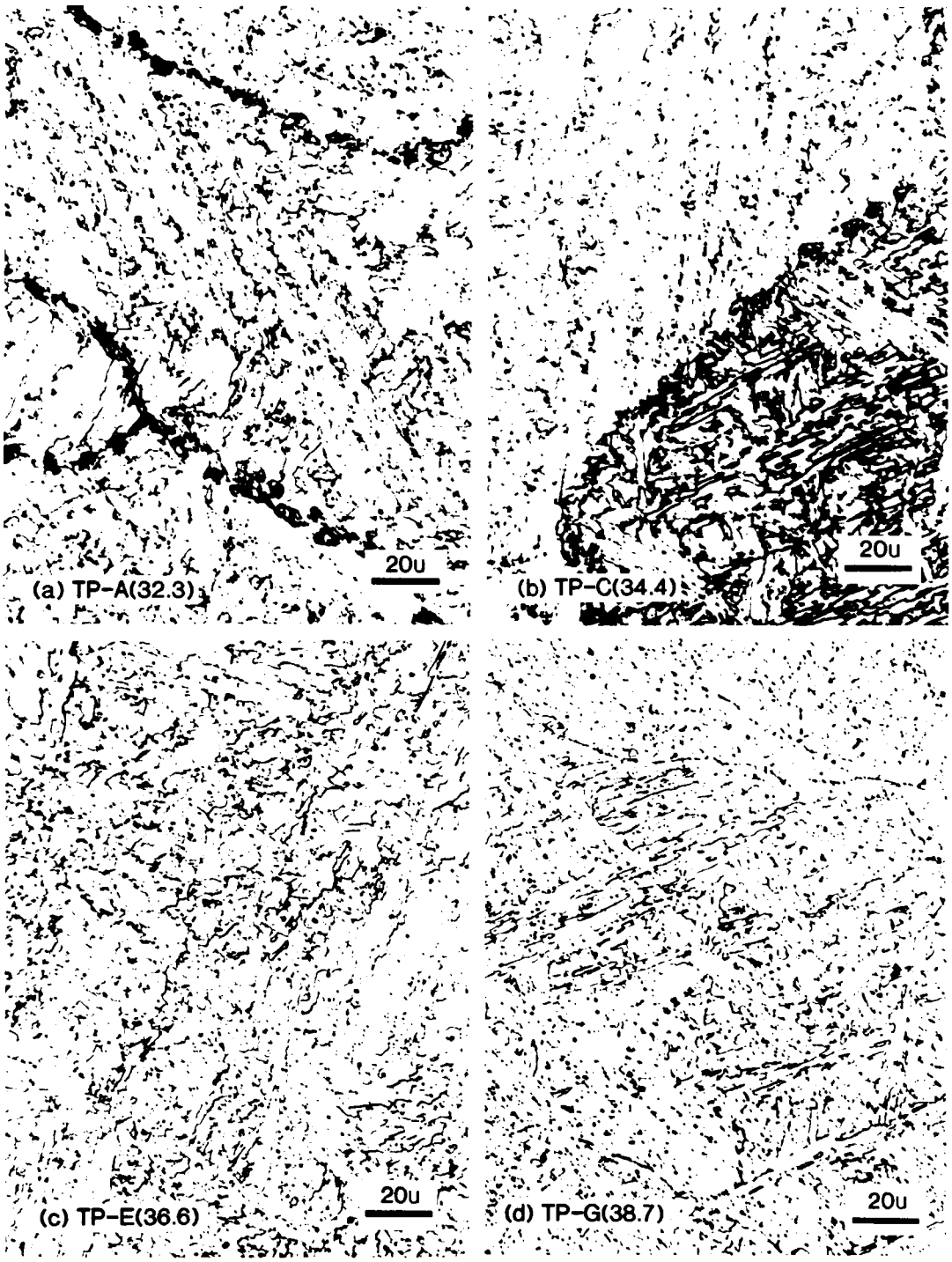

Figure 54. Optical micrographs of 2 1/4Cr-1Mo SMA weld metal postweld heat treated to different temper parameters, 500X, 2% nital etch.

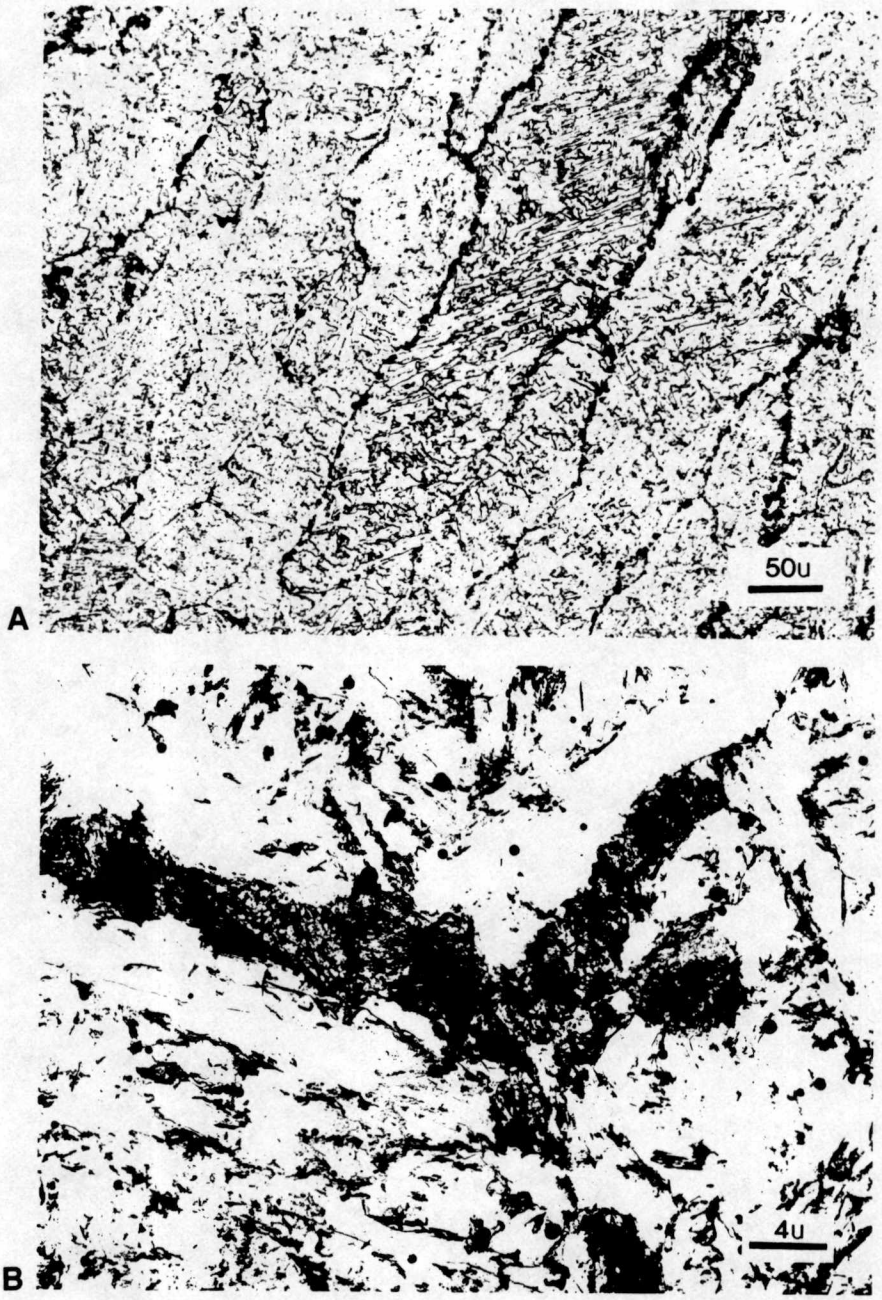

Figure 55. Dark etching regions at prior austenite grain boundaries in 2 1/4Cr-1Mo SMA weld metal heat treated to a temper parameter of 32.3(TP-A), (a) 200X, 2% nital etch, OLM, (b) 2500X, carbon extraction replica, TEM.

discussed the coarsening of lath like constituents upon tempering. The coarsening mechanism has been indicated to be based on the elimination of the low angle boundaries between laths having similar orientations. During PWHT the neighboring laths having an orientation difference of a few degrees merge together to produce wider elongated structures. According to Pickering[29] the orientation difference between neighboring bainite laths is often quite small, perhaps as small as 6 degrees. This coarsening of bainite laths was also clear during SEM and STEM/TEM examination of the PWHT weld metal.

SEM studies were conducted mainly to determine the distribution of carbides in the PWHT SMA weld metal and to determine the microconstituents present in the weld metal. Granular and massive bainite was found along with lath bainite in the microstructure. Figures 56 and 57 illustrate the different types of microconstituents in SMA weld metal. The granular microstructure consists of a bainitic-ferritic matrix in which small islands of irregular outline appear to show no evidence of internal structure at magnifications to 10,000X (see figure 56). The islands appear to be elevated above the surrounding ferrite matrix, indicating that they are etchant resistant. They also seem to be randomly distributed throughout the non-lath regions of the prior austenite grains. The carbides in granular bainite are comparatively finer than in the lath bainite.

Massive constituents, significantly larger than the islands in the granular bainite, have been observed in SMA weld metal to varying degrees (see figure 57). These constituents are also irregular in

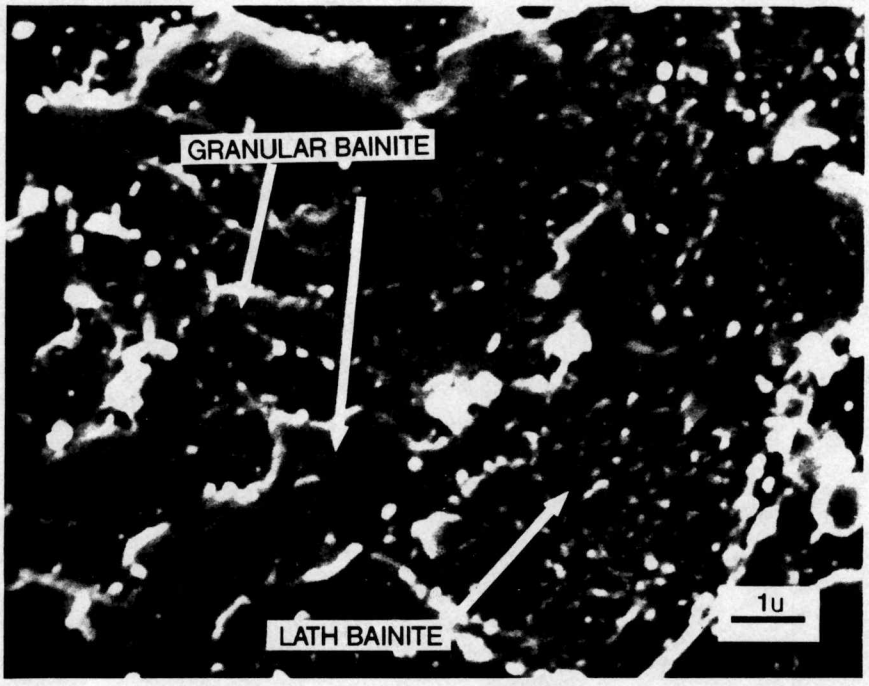

Figure 56. Granular bainite and lath bainite in 2 1/4Cr-1Mo SMA weld metal postweld heat treated to a temper parameter of 36.6(TP-E), 10,000X, 2% nital etch, SEM.

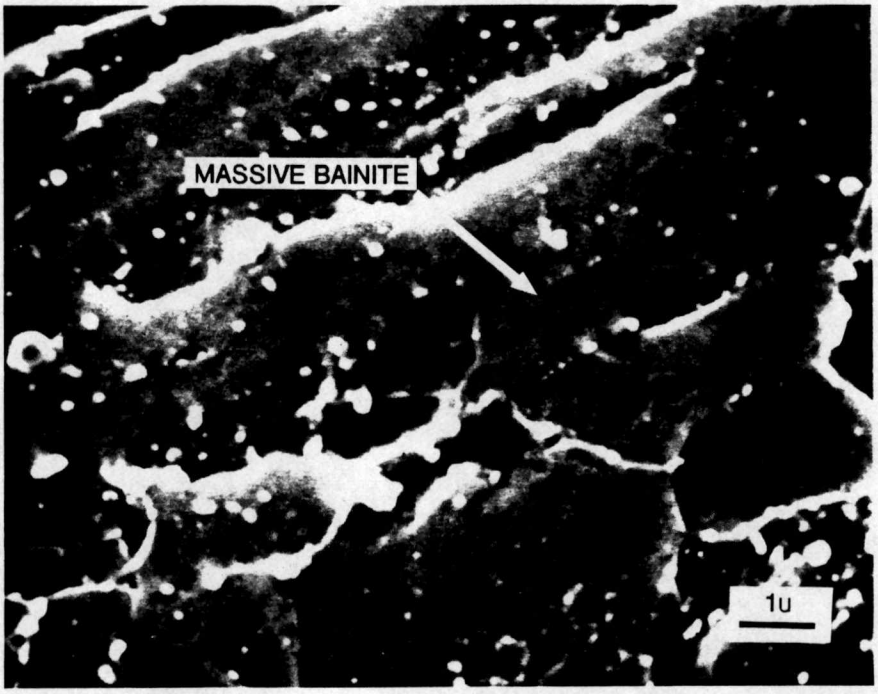

Figure 57. Massive bainite in 2 1/4Cr-1Mo SMA weld metal postweld heat treated to a temper parameter of 36.6(TP-E), 10,000X, 2% nital etch, SEM.

shape and are resistant to etching. Some of the massive bainite regions are elongated in one direction and are aligned with their longitudinal axis parallel to the surrounding lath bainite (figure 57). In some cases, particles may be discerned within the massive constituents.

Granular and massive bainites are known to be morphologies of upper bainite. Granular bainite, as observed in the weld metals in this study, has been described by Klueh[48] as islands of a second constituent dispersed in a bainitic-ferritic matrix. Oblak and Heheman[28] have indicated that it is easier for other forms of bainite to form when the transformation occurs during continuous cooling rather than isothermally.

The SEM study also showed coarsening of carbide precipitates, as the severity of the PWHT increased (figures 58 and 59). This was particularly true for the particles at the grain boundaries or lath boundaries. Carbides within the bainite laths were not very clear in the SEM, because of the inherent fineness of these carbides and their resistance to growth, because of their presence in a ferritic matrix.

TEM observations on carbon replicas, extracted from the surface of polished and etched SMA weld metal specimens, postweld heat treated to different temper parameters, further point to the fact that the carbides become coarser and coarser with increase in the severity of tempering. Figure 60a reveals general carbide structure in SMA weld metal postweld heat treated to a temper parameter of 32.3(TP-A). From this figure, it is evident that the carbide precipitation has just begun, especially, within the bainite laths.

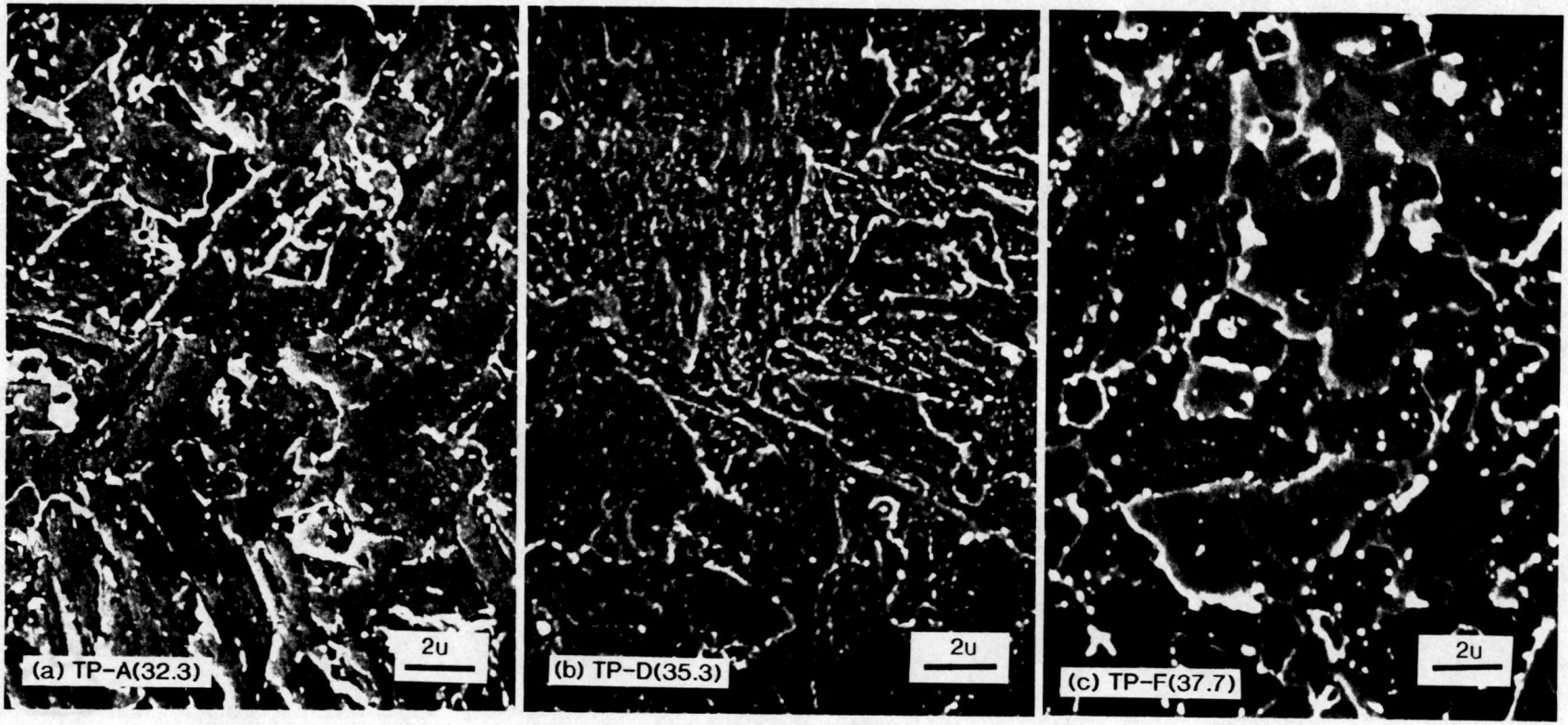

Figure 58. SEM photomicrographs of 2 1/4Cr-1Mo SMA weld metal revealing coarsening of carbides with an increase of the temper parameter, 5000X, 2% nital etch.

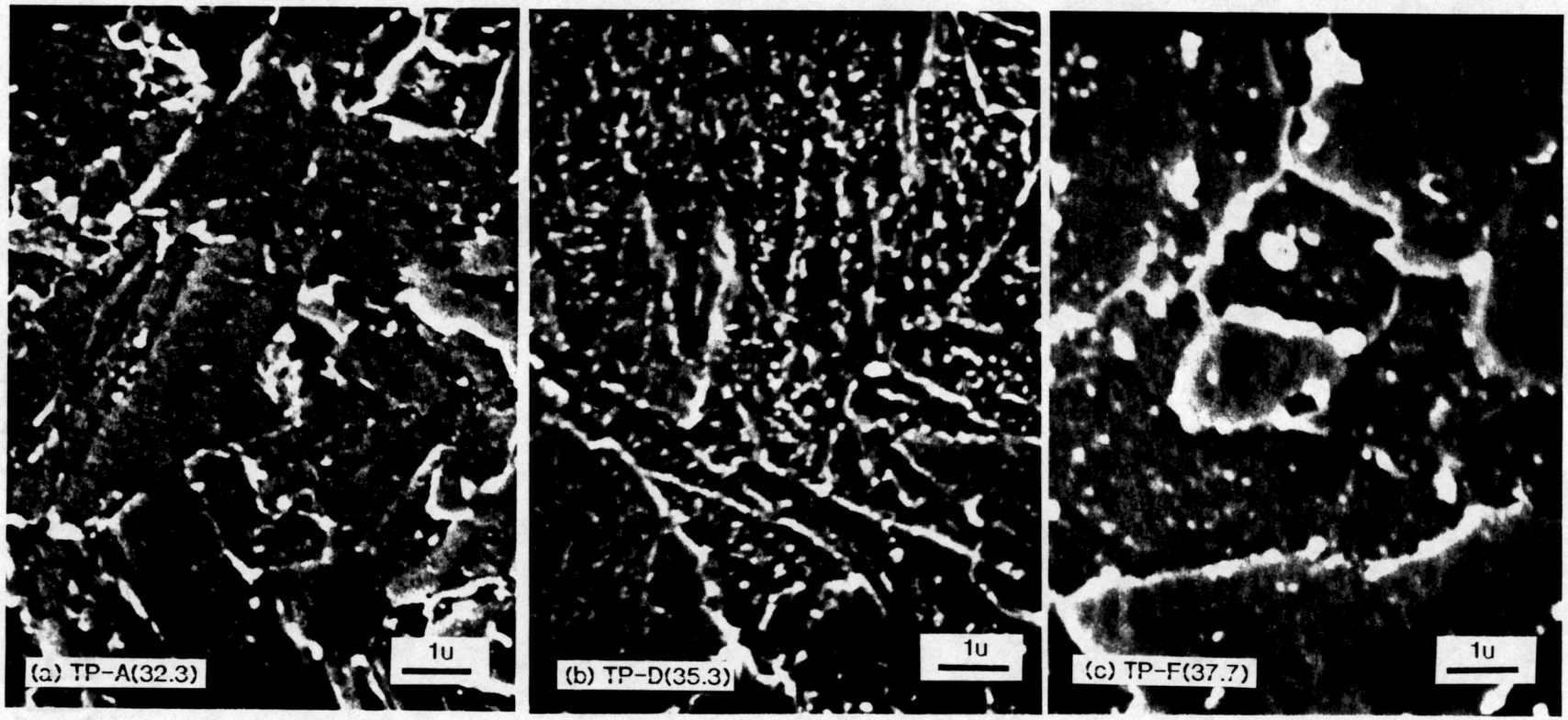

Figure 59. SEM photomicrographs of 2 1/4Cr-1Mo SMA weld metal revealing coarsening of carbides with an increase of the temper parameter, 10,000X, 2% nital etch.

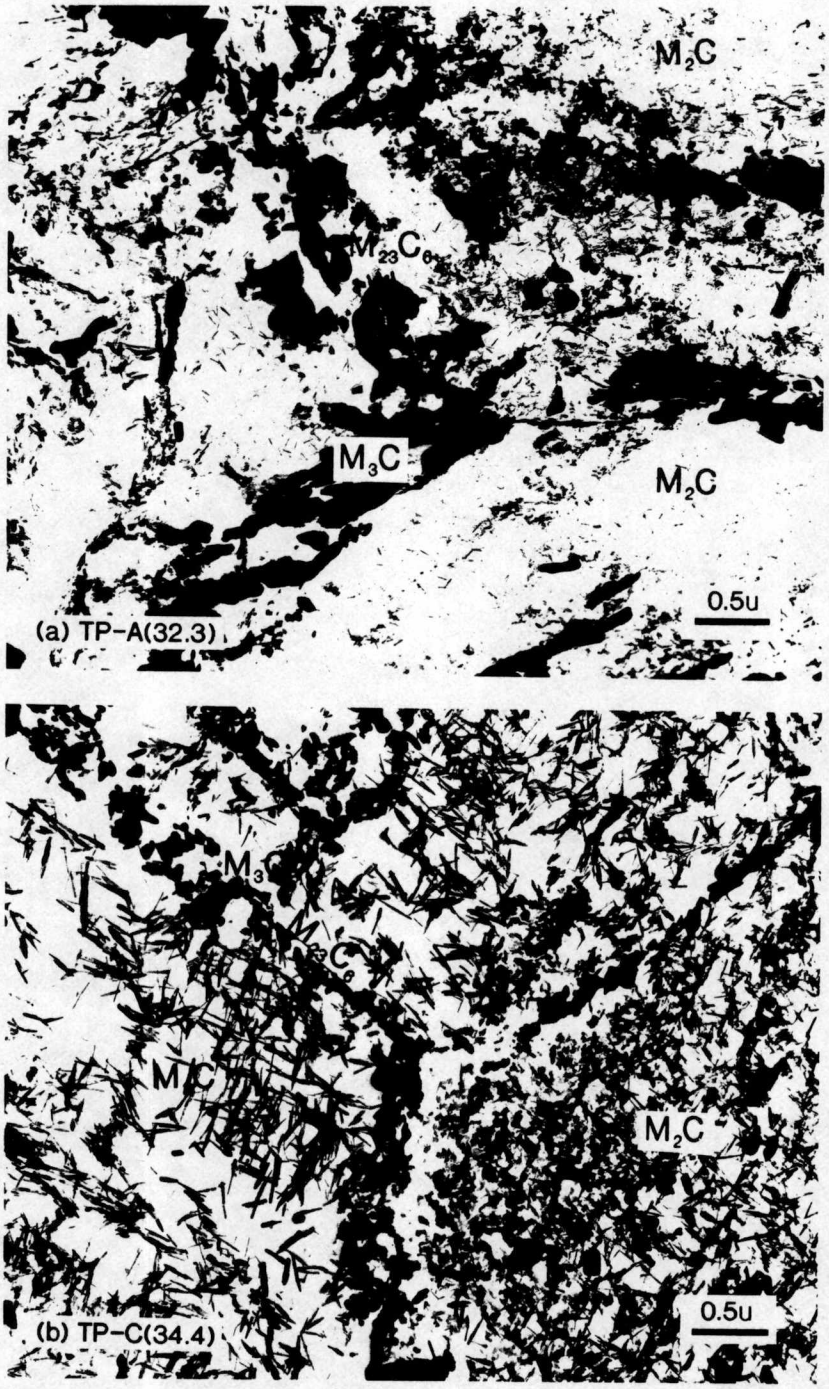

Figure 60. TEM photomicrographs showing the general carbide structure of 2 1/4Cr-1Mo SMA weld metal postweld heat treated to a temper parameter of (a) 32.3(TP-A), (b) 34.4(TP-C), carbon extraction replica, 20,000X.

The grain boundary carbides were identified to be M_3C and $M_{23}C_6$ type and the finer precipitates in the grains were found to be M_2C. Because of the fineness of the carbides, it was not possible to sample a single carbide for microanalysis and hence a small area containing only these fine precipitates was analyzed and found to show carbide composition for the $(Cr,Mo)_2(C,N)$ type. The fine carbides within the grains, coarsened with an increase in the temper parameter 34.4(TP-C) into well defined fine acicular needles as shown in figure 60b. At the temper parameter of 34.4(TP-C), some M_3C type carbides were still found, although the majority of carbides along the grain boundaries were of the $M_{23}C_6$ type. $M_{23}C_6$ type carbides in 2 1/4Cr-1Mo steel have been known to form at the expense of M_3C and M_2C type carbides, their nucleation being either within the M_3C particles or at the M_3C/ferrite interface[18].

Similar behavior was also noticed within the bainite laths and at the lath boundaries as illustrated in figure 61. Figure 61a shows fine acicular precipitates of M_2C in the bainite laths and small globular precipitates of M_3C along the lath boundary for a temper parameter of 32.3(TP-A). Figures 61b and c illustrate growth of both the lath and lath boundary precipitates for temper parameters of 33.4(TP-B) and 34.4(TP-C). Needles of M_2C type carbides grow slowly within the bainite laths as evident from examination of figure 61. Figure 61 also reveals that the lath boundary precipitates grow rapidly to form large precipitates. The coarsening of these M_3C type precipitates (figure 61a) into large $M_{23}C_6$ carbides and some small M_2C type carbides, indicate that the diffusion of solute elements is

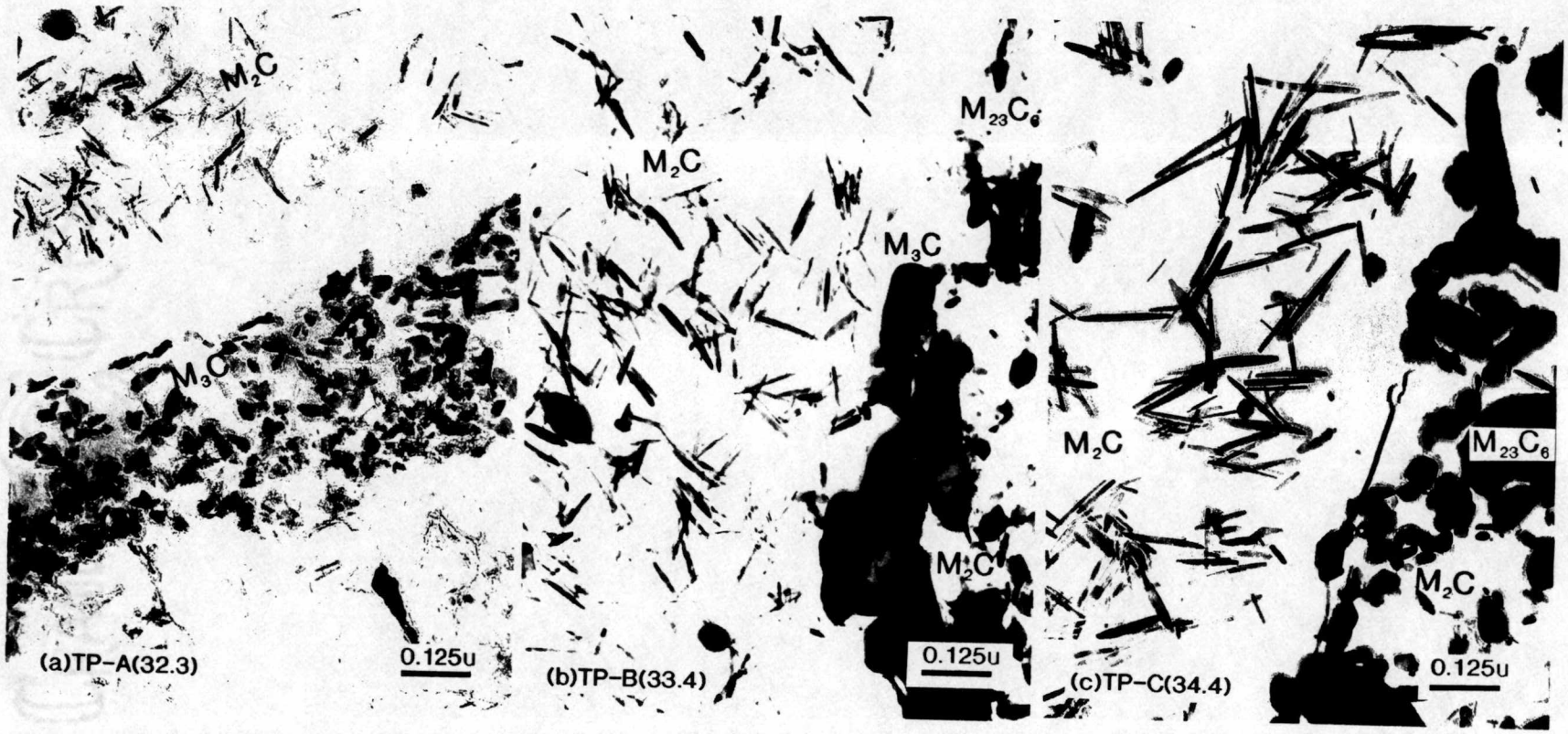

Figure 61. TEM photomicrographs showing the coarsening of carbide precipitates in the bainite laths and lath boundaries of 2 1/4Cr-1Mo SMA weld metal with increase in the severity of tempering, carbon extraction replica, 80,000X.

faster along the boundaries as compared to that within the bainite laths. The acicular M_2C type carbides, within the bainite laths, were found to be very stable (although slight coarsening is apparent) even with an increase in the severity of tempering. This is further illustrated in figure 62 where M_2C carbides were seen to persist even for the highest tempering parameter of 38.7(TP-G). A temper parameter of 38.7 was achieved by tempering at 1350°F for 25 hours which can be said to be equivalent to a service exposure of about 40 years at 950°F (after class 2 heat treatment for 25 hours at 1300°F). In figure 62c it can be seen that M_6C carbides have nucleated and are growing at the expense of the surrounding M_2C carbides.

Fringes of M_2C precipitates were observed in some areas in the initial stages of tempering (TP-A to TP-C). Figure 63 illustrates such fringes of densely packed M_2C carbides. It is anticipated that the austenite in these areas is last to transform or is retained after the weld metal cools to room temperature. Hence, these regions are carbon rich and subsequent tempering results in precipitation of a large number of carbides illustrated in figure 63. The microconstituents in these areas have been termed as M-A constituent by the IIW weld metal classification codes, which constitute a mixture of lath and/or twinned martensite with retained austenite.

Another important feature observed during the TEM study, was the formation of precipitate free zones at the grain boundaries, due to coarsening of the grain boundary precipitates at the expense of precipitates within the grains adjacent to the boundaries. A series of TEM photomicrographs of SMA 2 1/4Cr-1Mo weld metal, postweld heat

Figure 62. TEM photomicrographs showing that the M_2C type carbides in the bainite laths are very stable even with an increase in the severity of tempering, carbon extraction replica, 40,000X.

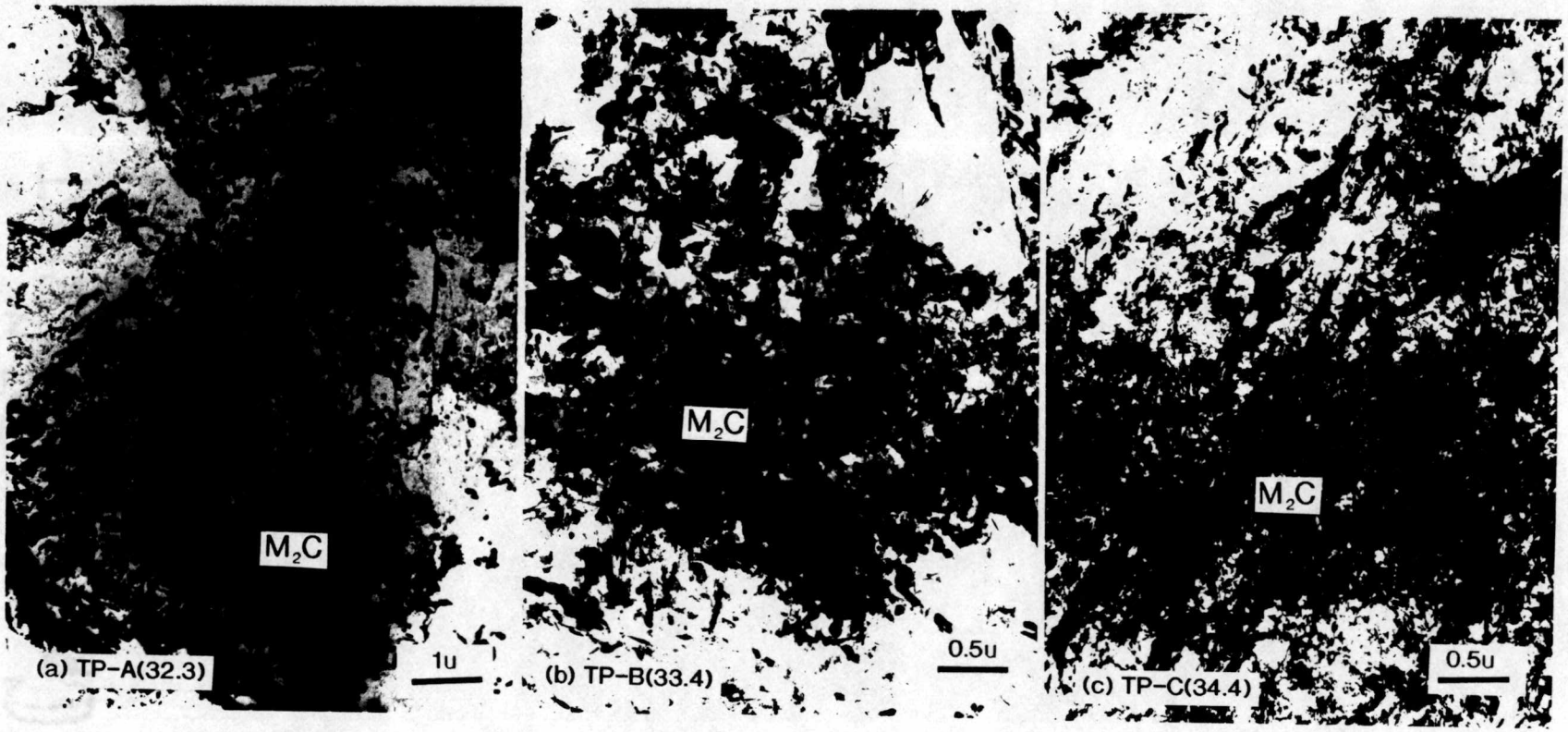

Figure 63. TEM photomicrographs showing fringes of M_2C carbides in regions last to transform, carbon extraction replica, (a) 10,000X, (b) and (c) 20,000X.

treated to different temper parameters (figure 64), reveal the gradual increase in the extent of precipitate free zone upon increase in the severity of tempering. The precipitate free zones are known to reduce creep resistance.

Initially, a fairly uniform dispersion of precipitates exists throughout the microstructure. The tempering conditions, coupled with metallurgical instability causes preferred precipitation of carbides along the grain boundaries. The elements in solid solution, adjacent to the grain boundaries, diffuse to the boundaries which are nucleation sites for precipitates. To maintain solid solution equilibrium in the matrix, small precipitates adjacent to the grain boundaries dissolve. These new solid solution atoms diffuse to the boundaries and precipitate. The process continues, forming a zone depleted of precipitates next to the grain boundaries. When the denuded zones first form they are narrow, but they widen with time either during PWHT or during elevated temperature exposure. The formation of such precipitate free zones result in loss of creep strength. The mechanism of loss of strength associated with formation of such zones can be explained as follows. Initially, when carbides are distributed uniformly, creep strains are transferred across the grain boundary either by shear or grain boundary sliding. The creep strain is hence uniform throughout the material. The occurrence of such precipitate free zones is associated with stress concentrations at the grain triple points. Since the shear strength in this zone is lower than that in either the matrix or grain boundary, most of the deformation occurs within this zone. The

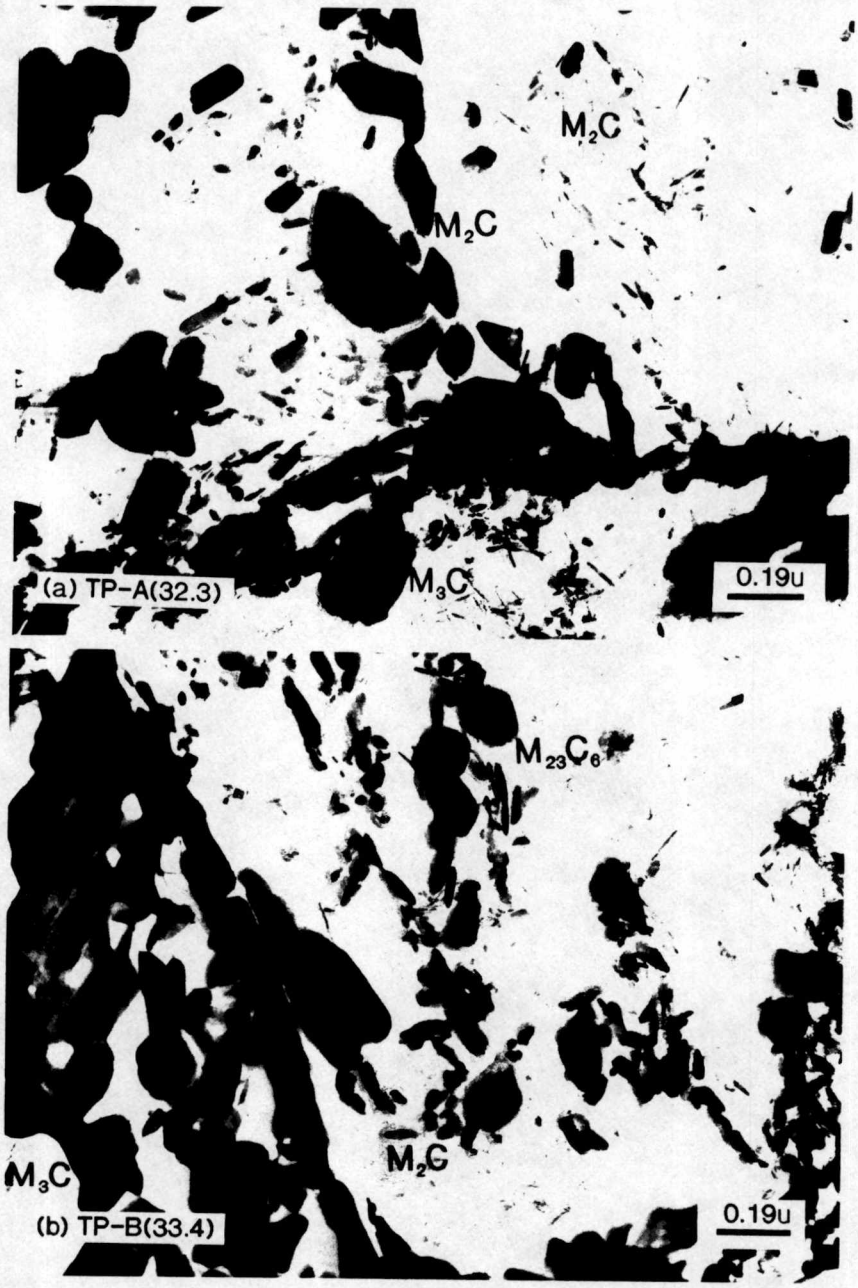

Figure 64. TEM photomicrographs showing precipitate free zones occurring as a result of coarsening of grain boundary pecipitates and dissolution of precipitates adjacent to grain boundaries, carbon extraction replica, (a) TP-A (32.3), (b) TP-B(33.4), 60,000X.

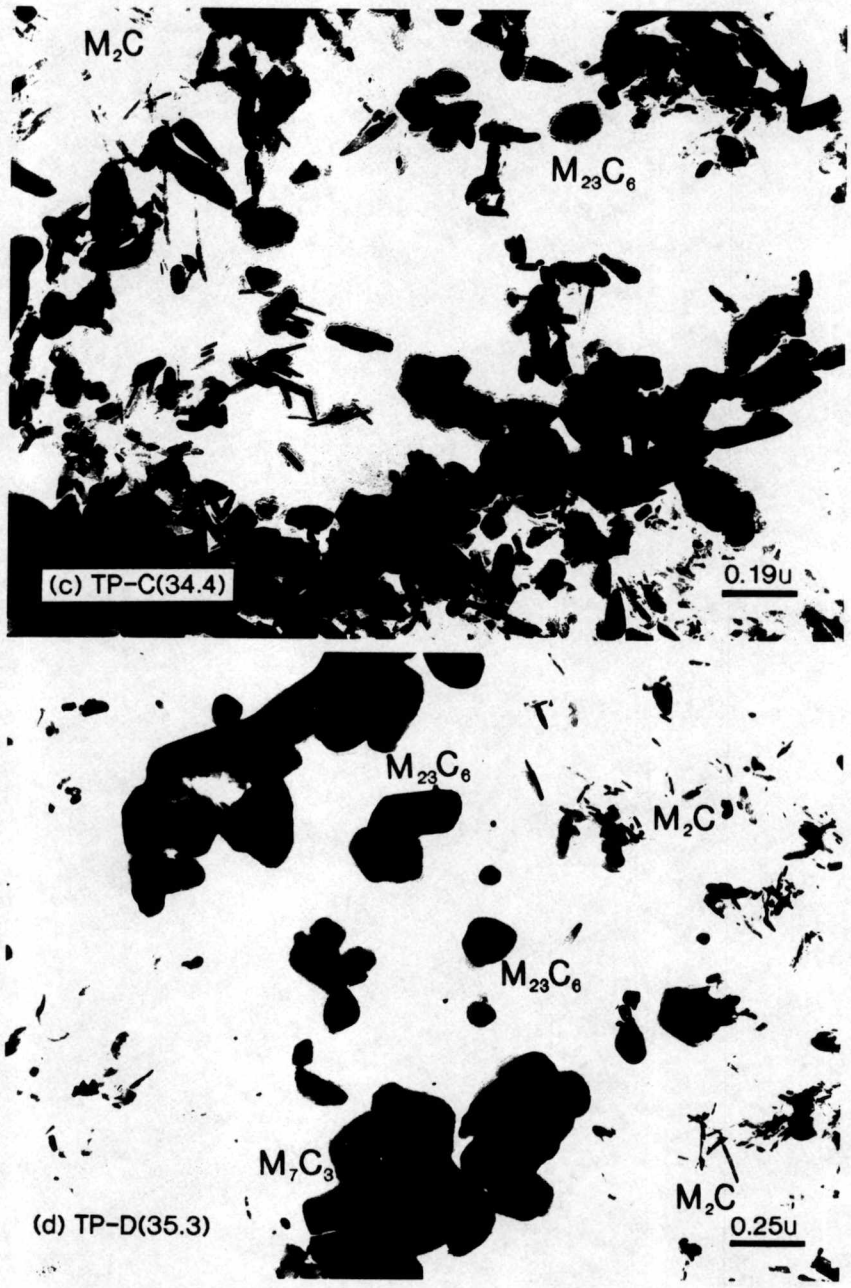

Figure 64. Continued
(c) TP-C(34.4), 60,000X
(d) TP-D(35.3), 40,000X.

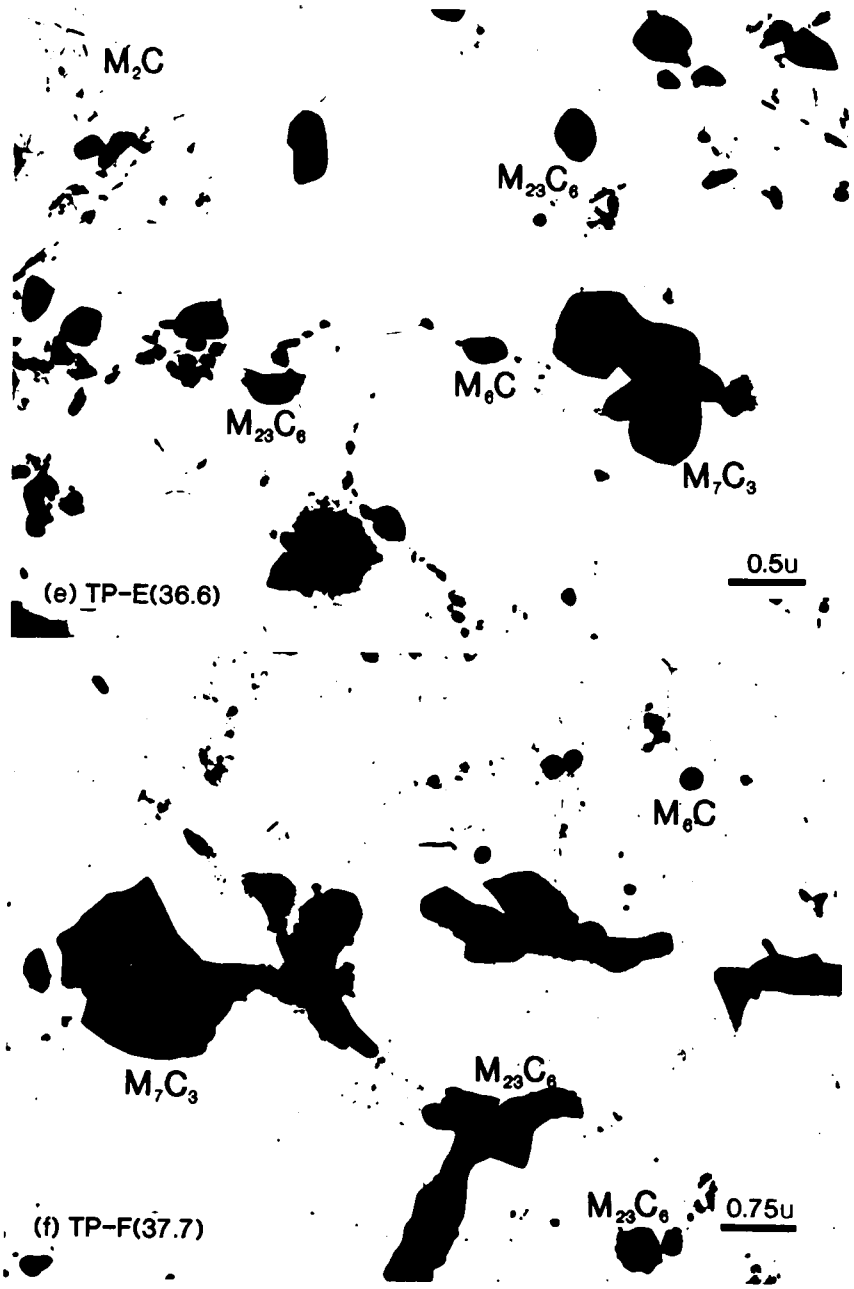

Figure 64. Continued
(e) TP-E(36.6), 20,000X
(f) TP-F(37.7), 15,000X.

Figure 64. Continued
(g) TP-G(38.7), 10,000X.

relative motion of grains sliding past each other is by non-uniform grain boundary sliding, because of unrestricted dislocation movement in this zone, causing a rapid build up of stress at triple points. As time at PWHT or elevated temperature service is increased, the denuded zones become wider causing further loss in strength of the material.

From the present study of the carbide evolution process in SMA 2 1/4Cr-1Mo weld metal, upon tempering, it can be said that the carbide evolution sequence is different at the prior austenite grain boundaries, bainite lath boundaries and within bainite laths. In the bainite laths the carbide evolution process can be illustrated as:

$$M_2C \longrightarrow M_6C$$

Such an evolution sequence of M_2C carbides transforming directly to M_6C carbides, has been found by Baker and Nutting[18] to occur in proeutectoid ferrite grains in 2 1/4Cr-1Mo steel. Since bainite laths are essentially ferritic, the M_2C carbides transform directly to M_6C. The transformation of M_2C type carbides to M_6C carbides requires diffusion of solute elements, especially, molybdenum, silicon and manganese and since these elements form substitutional solid solution in ferrite, their diffusion rates are slow. Hence, the M_2C carbides within the bainite laths are stable and resist degradation even after severe tempering.

The evolution of carbides at the grain boundaries and bainite lath boundaries due to tempering can be given as follows:

$$\left.\begin{matrix} M_3C \\ M_2C \end{matrix}\right\} \longrightarrow \left.\begin{matrix} M_7C_3 \\ M_{23}C_6 \end{matrix}\right\} \longrightarrow M_6C$$

At the grain boundaries and the bainite lath boundaries, the diffusion rate of solute elements is higher (grain boundary diffusion mechanisms). So, a wide variety of carbides have been seen to occur at the boundaries, the type and size changing with an increase in the severity of tempering. The carbide evolution sequence determined from this study, differs slightly from that outlined by Baker and Nutting[18] in quenched and tempered 2 1/4Cr-1Mo steel. In quenched 2 1/4Cr-1Mo steel, the sequence of carbide precipitation studied by Baker and Nutting suggests that M_6C nucleates separately from M_7C_3 and $M_{23}C_6$ whereas, from this study it is clear that M_6C may also form extracting solute elements from both M_7C_3 and $M_{23}C_6$ at the same time or independently away from the other carbides.

4.8 SUMMARY

This study has investigated in detail, the effect of different types of heat treatment (A&T, N&T and PWHT (C1.2)) on the elevated temperature properties of SA weldments. Subcritical postweld heat treatment and its effect on the properties of SMA weld metal has also been studied. Creep test data show the superiority of the N&T heat treated material at 950°F and of A&T heat treated material at 1050°F. PWHT(C1.2) weld metal creep strength is between the A&T and N&T at 950°F and is equal to the N&T at 1050°F. The PWHT(C1.2) weldment, tested in transverse direction, is however weaker due to tempering of the base metal during PWHT.

Subcritical tempering of weld metal to different temper parameters indicates that the hardness, room temperature and 950°F

tensile and yield strength and creep strength, all decrease with an increase in the temper parameter. For the lower temper parameters (32.3 (TP-A) to 34.4 (TP-C)), the creep rupture strength is substantially higher, but appears to approach the same value for longer times (ie.>100,000) hours, but for weld metal with temper parameters greater than 33.4 the rupture strength for 100,000 hour life decreases rapidly. The data from long time tests (10,000 hours) in progress will be helpful in arriving at a definite conclusion in this regard.

Extensive metallography has been conducted to correlate the observed stress rupture behavior to the microstructure of the weld metal, HAZ (especially "soft" zone) and base metal. From this study, it is clear that the elevated temperature strength of 2 1/4Cr-1Mo weld metal depends on the prior heat treatment and service temperature at which the weld is employed. The prior heat treatment determines the microconstituents present in the weld and the size, distribution, type, composition and morphologies of the carbides present in the different microconstituents. The PWHT or service exposure or creep test temperature dictates the rate of coarsening of the carbides in the different microconstituents and hence the rate of loss of strength of the material. The occurrence of precipitate free zones as a result of PWHT and their effects on the stress rupture properties is also described. Different analysis techniques that are used to extrapolate short time stress rupture data to predict long term behavior of the material have also been critically examined. It

was found that log stress/log rupture time technique predicts higher 100,000 hour rupture stresses as compared to Larson-Miller techniques, especially at lower temper parameters.

CHAPTER V

CONCLUSIONS

This investigation was undertaken to determine the elevated temperature properties of 2 1/4Cr-1Mo weldments as a function of heat treatment rendered subsequent to welding. Following conclusions have emerged from this study:

I The study of 2 1/4Cr-1Mo SA weldment heat treated to the A&T, N&T and PWHT(C1.2) conditions reveal that;

1. A "soft" carbon denuded ferritic zone develops along the fusion line, in the heat affected zone of the weld, due to differences in the activity of carbon between the base metal and the weld metal, brought about by chromium differences.
2. The extent of such a ferrite band depends on the type and temperature of postweld heat treatment. This carbon denuded "soft" zone was widest for the A&T heat treatment condition; a few grains wide for the N&T condition and almost nonexistent in the PWHT(C1.2) condition.
3. Tensile testing of all-weld metal specimens revealed that weld metal in N&T condition had higher tensile strength at room temperature and 950^{o}F, followed by the PWHT(C1.2) and A&T materials. However, at 1050^{o}F the PWHT(C1.2) weld metal had higher tensile strength followed by N&T and A&T materials.

4. Tensile strength of base metal was found to be higher than weld metal for the A&T and N&T heat treatment conditions at all test temperatures. In case of PWHT(Cl.2) material, the strength of the weld metal was higher than that of the base metal.
5. Tensile specimens extracted transverse to the weldment did not rupture in the "soft" zone. The transverse specimens ruptured in the weld metal for all the heat treatments and test temperatures.
6. Stress rupture testing of longitudinally oriented all-weld metal specimens showed a superiority of the N&T heat treatment followed by PWHT(Cl.2) and A&T at 950°F.
7. At 1050°F the rupture strength of weld metal is highest for the A&T condition and rupture strength of N&T and PWHT(Cl.2) weld metal is approximately equal but lower than the A&T at 1050°F.
8. The weld metal in A&T and N&T condition contained a mixture of proeutectoid ferrite and bainite. The amount of this proeutectoid constituent is greater in the A&T condition as compared to N&T condition.
9. The PWHT(Cl.2) weld metal was found to contain 100% tempered bainite. SEM examination revealed that the morphology of bainite was mainly massive.
10. SEM observations showed that the carbides in the proeutectoid ferrite grains were finer than the carbides in bainite, in both A&T and N&T conditions.

11. TEM examinations revealed that the carbides were finer in the N&T compared to A&T. PWHT(C1.2) weld metal showed massive carbides and this structure is responsible for the inferior creep rupture behavior.

12. At higher temperatures, M_2C type carbides being more stable in the ferrite of the A&T material compared to the bainitic regions in the N&T, result in the A&T material having superior creep strength to the N&T material. The superiority of N&T at lower temperatures is due to its higher tensile strength because of bainitic structure.

13. Creep rupture properties of the weldment measured transverse to the welding direction, determined by the testing of composite specimens, indicate that the "soft" zone which occurs along the fusion line in the HAZ is resistant to creep rupture. None of the creep rupture specimens fractured in this region.

14. SEM and TEM examination of the "soft" zone in A&T condition revealed presence of fine acicular M_2C or $(Cr,Mo)_2(C,N)$ type carbides in the ferritic matrix. These relatively stable carbides in the ferrite, along with retained free molybdenum in solid solution are responsible for the excellent creep resistance of this zone.

15. Rupture testing of specimens, extracted from the weldment in transverse direction, reveals a superiority for the N&T heat treatment at $950^{o}F$ and for the A&T heat treatment at $1050^{o}F$.

16. The PWHT(C1.2) weldment exhibited poorer properties in transverse direction as compared to A&T and N&T at both the test temperatures. The reason for such behavior is the fact that the base metal was weaker due to the PWHT.
17. The base metal of the PWHT(C1.2) weldment underwent tempering and thus the carbides were coarsened due to this additional PWHT and hence the base metal was weaker than the weld metal. Thus the composite specimens ruptured in the base metal.
18. Creep test specimens in N&T condition rupture in the weld metal at both the test temperatures of 950°F and 1050°F.
19. The N&T material had a finer carbide structure in the base metal than in the weld metal and hence the composite transverse specimens ruptured in the weld metal.
20. The A&T weldment, tested transverse to the welding direction, ruptured in the weld metal at 950°F, in the base metal at 1050°F and again in the weld metal at temperatures between 1125 to 1200°F.
21. The base metal and weld metal microstructure of the A&T weldment was found to be identical. The reason for the shift in the rupture location, from the weld metal at 950°F to base metal at 1050°F and to weld metal again at temperatures between 1125 to 1200°F is not clear.

II The study of SMA 2 1/4Cr-1Mo weld metal postweld heat treated to a range of temper parameters reveal that;

1. The tensile strength and yield strength, tested at room temperature and 950°F, decreases with an increase in the temper parameter. For the lower temper parameters, this decrease is more rapid than at higher temper parameters.
2. Hardness decreases with an increase in the severity of tempering in a manner similar to that observed for tensile behavior.
3. The tensile and yield strength of the weld metal show an excellent linear relationship to hardness. This correlation can be useful for determining tensile properties of PWHT 2 1/4Cr-1Mo weld metal, simply by defining its hardness.
4. The stress rupture strength of weld metal decreases with increase in the temper parameter.
5. The extrapolated stress to cause rupture in 100,000 hours was found to differ depending on the analysis method used. Log stress/log rupture time analyses yielded a higher value of 100,000 hour rupture stress compared to that of Larson-Miller analyses, especially for low temper parameters.
6. The 100,000 hour rupture stress follows a quadratic relationship with the temper parameter, the stress decreases rapidly with an increase in the temper parameter especially for higher temper parameters.
7. Isostress testing resulted in lower extrapolated creep strengths for the PWHT weld metal as compared to the

extrapolated creep strengths determined by Larson-Miller technique.

8. Examination of stress rupture data of SMA and SA weld metal heat treated similarly, revealed that the weld metal deposited by SA welding process has inferior creep rupture properties. The reason for such behavior is believed to be due to the differences in the inclusion type, size and distribution in the weld metal deposited by the two processes.
9. Optical light metallography showed that the prior austenite grain boundaries etch darker than the rest of the microstructure especially at lower temper parameters. TEM examination revealed dense precipitates of M_2C type carbides in these areas. Austenite in these areas is last to transform and hence is either retained or transformed to martensite during cooling. Subsequent tempering results in densely precipitated areas because the austenite last to transform contains higher carbon.
10. SEM examination showed that morphology of bainite in the weld metal was of three forms; massive, granular and lathy.
11. SEM examination also revealed coarsening of carbides in the weld metal upon increase in the severity of tempering.
12. STEM studies revealed that M_2C carbides within the bainite laths were very stable and that the coarsening of these carbides was slow.

13. STEM studies showed that the carbides at the grain boundaries and at the bainite lath boundaries, undergo change more rapidly in size and crystal structure, with an increase in the temper parameter than the interlath carbide.
14. Precipitate free zones adjacent to grain boundaries, near massive carbide precipitates, become wider with an increase in the temper parameter. Occurrence of such zones has been known to have an adverse effect on the creep rupture properties, due to non-ideal plastic flow in these regions.

REFERENCES

LIST OF REFERENCES

1. Klueh, R.L., "Heat Treatment of 2 1/4Cr-1Mo Steel for Breeder Reactor Steam Generators," Nuclear Technology, 57, 1982, pp. 114 - 124.

2. Lautzenheiser, C.E., "Use of Quenched and Tempered 2 1/4Cr-1Mo Steel," Southwest Research Institute Project No. 07-1579, May 1965.

3. Lundin, C.D., Kruse, B.J. and Pendley, M.R., "High Temperature Properties of 2 1/4Cr-1Mo Weld Metal," Welding Research Council Bulletin 277, May 1982.

4. Lundin, C.D., Kelly, S.C., Menon, R. and Kruse, B.J., "Stress Rupture Behavior of Postweld Heat Treated 2 1/4Cr-1Mo Steel Weld Metal," Welding Research Council Bulletin 315, June 1986.

5. Bonta, J.E. and Sikora, O.G., "Fabrication of Heavy-Wall Pressure Vessels," Application of 2 1/4Cr-1Mo Steel for Thick-Wall Pressure Vessels, ASTM STP 755, G.S. Sangdahl and M. Semchyshen, Eds., ASTM, 1982, pp. 255 - 274.

6. Mandich, L.I., Fogleman, E.L. and Gulya, J.A., "Elevated Temperature Properties of Heavy Gauge Cr-Mo Steel Plates," Symposium on Heat Treated Steels for Elevated Temperature Service, ASME, New Orleans, LA, 1966, pp. 45 - 65.

7. Zeisloft, R.H., Leyda, W.E. and Domian, H.A., "Low Carbon 2 1/4Cr-1Mo Steels," Low Carbon and Stabilized 2 1/4% Chromium 1% Molybdenum Steels, ASM, 1970, pp. 37 - 45.

8. Bland, J., "The Arc Welding of 2.25%Cr-1.0%Mo Alloy Steel Pipe," Welding Journal, 35(4), 1956, pp. 181s - 194s.

9. Bynum, J.E., Ellis, F.V. and Roberts, B.W., "Creep and Tensile Properties and Constitutive Equations for a 2 1/4Cr-1Mo Steel," Symposium on Structural Materials for Service at Elevated Temperatures in Nuclear Power Generation, ASME, Houston, TX, 1975, pp. 146 - 166.

10. "Steels for Elevated Temperature Service", United States Steel.

11. Emmanuel, G.N., Leyda, W.E. and Rozic, E.J., "Versatility of 2 1/4Cr1Mo as a Pressure Vessel Material," Symposium on 2-1/4 Chrome 1 Molybdenum Steel in Pressure Vessels and Piping, ASME-MPC, Denver, CO, 1970, pp. 78 - 122.

12. ASTM A387 - 79b, "Standard Specification for Pressure Vessel Plates, Alloy Steel, Chromium - Molybdenum," Annual Book of ASTM Standards, Part 4, 1982, pp. 360 - 362.

13. Grant, N.J. and Choudhuri, A.R., "Creep and Fracture," Deformation and Fracture at Elevated Temperatures, Grant, N.J. and Mullendore, A.W., Eds., The MIT Press, 1964, pp. 79 - 107.

14. Guard, R.W., "Alloying for Creep Resistance," Mechanical Behavior of Materials at Elevated Temperatures, McGraw-Hill, 1961, pp. 79 - 107.

15. Dieter, G.E., "Creep and Struss Rupture," Mechanical Metallurgy, 2nd Edition, McGraw-Hill, 1976, pp. 451 - 489.

16. Reed-Hill, R.E., "Precipitation Hardening," Physical Metallurgy Principles, 2nd Edition, D. Van Nostrand Co., 1973, pp. 358 - 377.

17. Schoeck, G., "Theories of Creep," Mechanical Behavior of Materials at Elevated Temperatures, McGraw-Hill, 1961, pp. 79 - 107.

18. Baker, R.G. and Nutting, J., "The Tempering of 2 1/4Cr-1Mo Steel after Quenching and Normalizing," JISI, 192(7), 1959, pp. 257 - 268.

19. Jones, W.B. and Van Den Avyle, J.A., "Substructure and Strengthening Mechanisms in 2.25Cr-1Mo Steel at Elevated Temperatures," Met. Trans. A, 11A(8), 1980, pp. 1275 - 1286.

20. Wada, T. and Eldis, G.T., "Transformation Characteristics of 2 1/4Cr-1Mo Steel," Application of 2 1/4Cr-1Mo Steel for Thick-Wall Pressure Vessels, ASTM STP 755, G.S. Sangdahl and M. Semchyshen, Eds., ASTM, 1982, pp. 255 - 274.

21. Lundin, C.D., Henning, J.A., Menon, R. and Khan, K.K., "Transformation, Metallurgical Response and Behavior of the Weld Fusion Zone and Heat Affected Zone in Cr-Mo Steels for Fossil Energy Application," Final Technical Report No. ORNL/SUB/81-07685/02&77, Sept. 1987.

22. Sims, J.E. and Fuchs, R., "Influence of Welding Processes on the Mechanical Properties of 2 1/4Cr-1Mo Weld Metals," ASM for Metals Conference, St. Louis, Missouri, 1982.

23. Clark, J.N., "Manual Metal Arc Weld Modelling: Part 1 Effect of Process Parameters on Dimensions of Weld Bead and Heat-Affected Zone," Material Science and Technology, 1, 1985, pp. 1069 - 1080.

24. Clark, J.N., "Manual Metal Arc Weld Modelling: Part 2 Treatment of Multipass Weld," Material Science and Technology, 1, 1985, pp. 1081 - 1089.

25. Clark, J.N., "Manual Metal Arc Weld Modelling: Part 3 Implementation of Two-Layer Heat-Affected Zone Refinement Technique Under Shop Floor Conditions," Material Science and Technology, 1, 1985, pp. 1090 - 1093.

26. Pargeter, R.J. and Dolby, R.E., "Identification and Quantitative Description of Ferritic Steel Weld Metal Microstructures - Interim Report," IIW Doc. No. IX-1323-84, May 1984.

27. "Guidelines for Classification of Ferritic Steel Weld Metal Microstructural Constituents Using the Light Microscope," IIW Doc. No. IX-1377-85, IXJ-102-85, 1985.

28. Oblak, J.M. and Hehemann, R.F., "Structure and Growth of Widmanstatten Ferrite and Bainite," Symposium on Transformation and Hardenability in Steels, Climax Molybdenum Co., 1967, pp. 109 - 132.

29. Pickering, F.B., "The Structure and Properties of Bainite in Steels," Symposium on Transformation and Hardenability in Steels, Climax Molybdenum Co., 1967, pp. 109 - 132.

30. Krauss, G., "Martensite and Bainite," Chapter III, Principles of Heat Treatment of Steel, ASM, May 1985, pp. 43 - 83.

31. Woodhead, J.H. and Quarrel, A.G., "The Role of Carbides in Low-Alloy Creep-Resisting Steels," JISI, 203, 1965, pp. 605 - 620.

32. Roy, P. and Lauritzen, T., "The Relative Strength of Base Metal and Heat-Affected Zone in 2 1/4Cr-1Mo Weldments - A Microstructural Evolution," Welding Journal Research Supplement, 1986, pp. 45s - 47s.

33. Wada, H., "Thermodynamic Properties of Carbides in 2.25Cr-1Mo Steel at 985K," Met. Trans. A, 17A, 1986, pp. 1585 - 1592.

34. Stevens, R.A. and Lonsdale, D., "Isolation, Identification and Quantification by X-Ray Diffraction of Carbide Phases in 2 1/4Cr-1Mo Steel." Journal of Material Science, 20, 1985, pp. 3631 - 3638.

35. Todd, J.A., "The Early Stages of Tempering in a 3Cr -1.5Mo Steel," Scripta Metallurgica, 20, 1986, pp. 269 - 274.

36. Pilling, J. and Ridley, N., "Tempering of 2.25 Pct Cr -1 Pct Mo Low Carbon Steels," Met. Trans. A, 13A, 1982, pp. 557 - 563.

37. Shaw, B.J., "A Study of Carbides Formed in Low Alloy Cr-Mo Steels," Research on Chrome-Moly Steels, R.A. Swift, Editor, ASME, MPC-21, 1984, pp. 117 - 134.

38. Shaw, B.J., "Investigation of Correlation of Carbide Size and Percentage with Mechanical Properties of High Strength Low Alloy Steels," DOE Technical Report Number ORNL/SUB/85-22006/1, 1986.

39. Thomas, R.D., "Welding Technology Assessment for Pressure Vessels and Components for Coal Conversion Processes," Proceeding of the Symposium on the Behavior of Joints in High Temperature Materials, Pettin, Netherlands, 1981, pp. 3631 - 3638.

40. Argent, B.B., Van Niekerk, M.N. and Redfern, G.A., "Creep of Ferritic Steels," JISI, 1970, pp. 830 - 843.

41. Ritchie, R.O., Todd, J.A., Spencer, P.N. and Parker, E.R., "Design of Low Alloy Steels for Thick Walled Pressure Vessels," Final Technical Report No. ORNL/SUB/80-7843/01, June 1985.

42. Klueh, R.L. and Swindeman, R.W., "The Microstructure and mechanical Properties of a Modified 2.25Cr-1Mo Steel," Met. Trans. A, 17A(6), 1986, pp. 1027 - 1034.

43. Goldschmidt, H.J., "The Structure of Carbides in Low Alloy Steels," JISI, 1948, pp. 345 - 362.

44. Kotecki, D.J., Private Communication, Teledyne McKay, Nov. 6, 1984.

45. Klueh, R.L. and Canonico, D.A., "Microstructure and Tensile Properties of 2 1/4Cr-1Mo Steel Weldments with Varying Carbon Contents," Welding Journal Research Supplement, Sept. 1976, pp. 253s - 259s.

46. Klueh, R.L. and Canonico, D.A., "Creep Rupture Properties of 2 1/4Cr-1Mo Steel Weldments with Varying Carbon Contents," Welding Journal Research Supplement, Dec. 1976, pp. 381s - 388s.

47. Campbell, H.C., "Influence of Carbon on Stress Rupture Properties of Cr-Mo Weld Metal," Welding Journal Research Supplement, Feb. 1965, pp. 64s - 71s.

48. Klueh, R.L., "The Effect of Carbon on 2.25Cr-1Mo Steel (1) Microstructure and Tensile Properties," Journal of Nuclear Materials, 54, 1974, pp. 41 - 54.

49. Dittrich, S., Muesch, H.S. and Weber, H.A., "The Effects of Fabrication and Compositional Variables on the Properties of Chrome-Moly Weldments," Part II, Mannesmann, Thyssen Draht AG, Feb. 1987.

50. Komizo, Y., "A Review of Reversible Temper Embrittlement in Cr-Mo Steel Weld metals," IIW Doc. IX-1321-84.

51. "Mechanical Properties of Heavy Section 2 1/4Cr-1Mo Steel Shell Ring Forged From Hollow Ingot," Kawasaki Steel Corporation, December 1982.

52. "Improvement in High Temperature Properties of Heavy Section 2 1/4Cr-1Mo Steel," Kawasaki Steel Corporation, January 1982.

53. Wagner, L.E. and Seth, B.B., "Creep Rupture Behavior of 2 1/4%Cr-1%Mo Weld Metal," Properties of Steel Weldments for Elevated Temperature Pressure Containment Applications, MPC-9, ASME, 1978, pp. 103 - 108.

54. Pilling, J., Ridley, N. and Gooch, D.J., "The Effect of Titanium on Creep Strength in 2.25 Pct Cr-1 Pct Mo Steels," Met. Trans. A, 14A(7), 1983, pp. 1443 - 1449.

55. Gooch, D.J., " Effects of Trace Elements on Creep Strength and Ductility of Low Carbon 2.25Cr-1Mo Steels," Metal Science, 1981, pp. 45 - 54.

56. Viswanathan, R., "Effect of Ti and Ti+B Additions on the Creep Properties of 1.25Cr-0.5Mo Steels," Met. Trans. A, 8A(1), 1977, pp. 57 - 61.

57. Egnell, L., "Mechanical Property and Weldability of a Columbium Stabilized Steel with 2 1/4 % Chrome and 1% Molybdenum for Sodium Cooled Fast Reactor Systems," Low Carbon and Stabilized 2-1/4% Chromium 1% Molybdenum Steels, ASM, 1970, pp. 47 - 55.

58. Husslage, W. and Dortland, W., "Creep Behavior of 2 1/4Cr 1Mo Ni Nb Steel," International Conference on Ferritic Steels for Fast Reactor Steam Generators, British Nuclear Energy Society, London, UK, 1977, pp. 37.1 - 37.5.

59. Thomas, G. and Chen, Y.L., "Structure and Mechanical Properties of Fe-Cr-Mo-C Alloys With and Without Boron," Met. Trans. A, 12A(7), 1981, pp. 933 - 950.

60. Viswanathan, R., "Effect of Sb, P, Sn and B on the Microstructure and Creep Properties of Normalized and Tempered 1.25Cr-0.5Mo Steels, Met. Trans. A, 6A(6), 1975, pp. 1135 - 1141.

61. Tsuboi, J. and Terashima, H., "Review of Strength and Toughness of Ti and Ti-B Microalloyed Deposits," Welding in the World, 21(11/12), 1983, pp. 304 - 316.

62. Mori, N., Homma, H., Wakabayashi, M. and Okita, S., "Mechanical Properties and Metallurgy of Ti-B Bearing Weld Metals," The Forth International Symposium of the Japan Welding Society, Osaka, Nov. 1982, pp. 243 - 248.

63. Manganello, S.J., "Evaluation of Experimental 2-1/4Cr -1Mo-1/2Ni and 3Cr-1Mo-1Ni Steels for 12-inch-wall Pressure Vessels," The Pressure Vessels and Piping Conference, Orlando, Florida, M. Semchyshen, Editor, MPC-18, ASME, 1982, pp. 153 - 177.

64. Pilling, J., Ridley, N. and Gooch, D.J., "The Effect of Phosphorus on Creep in 2.25%Cr-1%Mo Steels," Acta Met., 30, 1982, pp. 1587 - 1595.

65. Cane, B.J. and Fidler, R.S., "The Effect of Microstructure and Grain Size on the Creep and Rupture Properties of 2 1/4Cr1Mo and 9Cr1Mo Steels," International Conference on Ferritic Steels for Fast Reactor Steam Generators, British Nuclear Energy Society, London, UK, 1977, pp. 31.1 - 31.5.

66. Kar, R.J. and Todd, J.A., "Alloy Modification of Thick-Section 2 1/4Cr-1Mo Steel," Application of 2 1/4Cr-1Mo Steel for Thick-Wall Pressure Vessels, ASTM STP 755, G.S. Sangdahl and M. Semchyshen, Eds., ASTM, 1982, pp. 228 - 252.

67. Middleton, C.J., "Reheat Cavity Nucleation and Nucleation control in Bainitic Creep-Resisting Low -Alloy Steels: Roles of Manganese Sulphide, Residual, and Sulfur Stabilizing Elements," Metal Science, 1981, pp. 154 - 167.

68. Hojo, I., Yamamoto, S., Masaie, N. and Okuda, N., "Improvement of Notch Toughness by Nitrogen Addition in 2 1/4Cr-1Mo Weld Metal," IIW/IIS Doc. No. II-1045 -85.

69. Viswanathan, R. and Dooley, R.B., "Creep Life Assessment Techniques for Fossil Power Plant Boiler Pressure Parts," International Conference on Creep, Tokyo, 1986, pp. 349 - 359.

70. Weber, H.A., Muesch, H.S. and Dittrich, S., "Evaluating the Properties of Welded Utility Steam Components Before and After Exposure," Part 1, Mannesmann, Thyssen Draht AG, 1987.

71. Jaske, C.E., "Material Ageing and Prediction of Remaining Service Life," PVP Conference Tutorial Notes, ASME, Knoxville, 1987.

72. Ishiguro, T., Murakami, Y., Ohnishi, K. and Watanabe, J., "A 2 1/4Cr-1Mo Pressure Vessel Steel With Improved Creep Rupture Strength," Application of 2 1/4Cr-1Mo Steel for Thick Wall Pressure Vessel, ASTM STP 755, G.S. Sangdahl and M. Semchyshen, Eds., 1982, pp. 129 - 147.

73. Wada, T. and Biss, V.A., "Restoration of Elevated Temperature Tensile Strength in 2.25Cr-1Mo Steel," Met. Trans. A, 14A(5), 1983, pp. 845 - 855.

74. Wada, T., "Changes in Microstructure and Tensile Strength of Cr-Mo Steels after Long Term Service Exposure," Unusual Techniques and New Applications on Metallography, ASM Metals Congress, St. Louis, Missouri, 1982, pp. 91 - 100.

75. Smith, G.V., "The Strength of 2 1/4Cr-1Mo Steel at Elevated Temperatures," Symposium on 2-1/4Chrome 1Molybdenum Steels in Pressure Vessels and Piping, ASME-MPC, Denver, CO, 1970, pp. 1 - 26.

76. Murphy, M.C. and Branch, G.D., "Metallurgical Changes in 2.25CrMo Steels During Creep-Rupture Test," JISI, 209, 1971, pp. 546 - 561.

77. Batte, A.D. and Murphy, M.C., "Creep Rupture Properties of 2 1/4CrMo Weld Deposits," Welding Journal, 1973, pp. 261s - 267s.

78. Nutting, J., "The Metallography of Creep-Resistant Alloys," ISI Special Report No. 70, 1961, pp. 147 - 165.

79. D'Angelo, D., Regis, V., Franzoni, U. and Rossi, M.A., "Relaibility of Quantitative Metallography Approach for Material Evolution Assessment," BTF Special Issue, 1984, pp. 126 - 130.

80. Svensson, L.E. and Dunlop, G.L., "Growth of Intergranular Creep Cavities," International Metals Review, 1981, No. 2, pp. 109 - 131.

81. DeWitte, M. and Stubbe, J., "Experiences with Remanent Life Evaluation Testing," Proc. of Conf. on High Temperature Alloys for Gas Turbines and Other Applications, Liege, Belgium, 6-9 Oct., 1986, pp. 1571 - 1584.

82. Bendick, W. and Weber, H., "Metallurgical Investigations on Creep-Exposed Components for a Better Assessment of Service Behavior in Power stations," Proc. of Conf. on High Temperature Alloys for Gas Turbines and Other Applications, Liege, Belgium, 6-9 Oct., 1986, pp. 1595 - 1604.

83. Hildebrandt, U.W., Schneider, K., Persch, H. and Willems, H., "The Potential of NDT-Methods in Predicting the Residual Lifetime of Turbine Components," Proc. of Conf. on High Temperature Alloys for Gas Turbines and Other Applications, Liege, Belgium, 6-9 Oct., 1986, pp. 1649 - 1670.

84. Kimura, K., Fujiyama, K., Ishii, F. and Muramatsu, M., "Effect of Material Degradation on Creep Properties and Life Estimation," Proceedings of the International Conference on Creep, April 14-18, 1986, Tokyo, pp. 343 - 348.

85. Sklenicka, V. and Cadek, J., "Fracture Criteria and Prediction of Creep Life," Proc. of Conf. on High Temperature Alloys for Gas Turbines and Other Applications, Liege, Belgium, 6-9 Oct., 1986, pp. 1585 - 1594.

86. Neubauer, B. and Wedel, U., "Restlife Estimation of Creeping Components by Means of Replicas," ASME International Conference on Advances in Life Prediction Methods, April 18-20, 1983, pp. 307 - 313.

87. Neubauer, B., "Creep Damage Evolution in Power Plants," Creep and Fracture of Engineering Materials and Structures, B. Wilshire and D.R.J. Owen, Eds., Proc. of Conf., Swansea, UK, 24-27 March, 1981, pp. 1217 - 1226.

88. Needham, N.G. and Cane, B.J., "Creep Strain and Rupture Predictions by Cavitational Assessment in 2 1/4Cr1Mo Steel Weldments," Proceedings of the International Conference on Creep, April 14-18, 1986, Tokyo, pp. 65 - 73.

89. Neubauer, B., "Criteria for Prolonging the Safe Operations of Structures Through the Assessment of the Onset of Creep Damage Using Non Destructive Metallographic Measurements," Creep and Fracture of Engineering Materials and Structures, B. Wilshire and D.R.J. Owen, Eds., Proc. of Conf., Swansea, UK, 24-27 March, 1981, pp. 617 - 627.

90. Cane, B.J., "Creep Fracture of Dispersion Strengthened Low Alloy Ferritic Steels," Acta Metallurgica, 29, 1981, pp. 1581 - 1591.

91. Coffin, L.F. and Goldhoff, R.M., "Predictive Testing in Elevated Temperature Fatigue and Creep: Status and Problems," Testing for Prediction of Material Performance in Structures and Components, ASTM STP 515, ASTM, 1972, pp. 22 - 74.

92. Prager, M., "Understanding Materials Behavior Through the Application of Modern Parametric Analysis Techniques," Proceedings of the International Conference on Creep, April 14-18, 1986, Tokyo, pp. 39 - 46.

93. Booker, M.K. and Booker, B.L.P., "New Methods for Analysis of Materials Strength Data for the ASME Boiler and Pressure Vessel Code," Use of Computers in Managing Materials Property Data, MPC-14, ASME, pp. 31 - 64.

94. Le May, I. and da Silveira, T.L., "Creep Damage Assessment in Petrochemical Plants," Proceedings of the International Conference on Creep, April 14-18, 1986, Tokyo, pp. 361 - 366.

95. Roberts, B.W., Ellis, F.V. and Bynum, J.E., "Remaining Creep or Stress Rupture Life Under Nonsteady Temperature and Stress," Journal of Engineering Materials and Technology, 101, 1979, pp. 331 - 336.

96. Borggreen, K. and Huntley, P., "Corrections to the Constant Stress, Augmented Temperature Extrapolation Method due to Oxidation of Subsize Creep Specimens," Paper Presented at the Second International Conference on Creep and Fracture of Engineering Materials and Structures.

97. Stubbe, J. and van Melsen, C., "Practical Applications of a Short-Term Creep Test Method for Evaluation of the Restlife," International Symposium on Prediction of Residual Lifetime of Constructions Operating at High Temperature, Hague, 1977.

98. Melton, K.N., "The Isostress Extrapolation of Creep Rupture Data," Materials Science and Engineering, 59, 1983, pp. 143 - 149.

99. John, A.W., Draper, H.M. and Williamson, J., "Some Long Time Evidence Supporting the Constant Stress, Accelerated Temperature Method of Extrapolating Creep-Rupture Data," Arch. Eisenhuttenwes, 48, 1977, pp. 581 - 583.

100. Cane, B.J. and Brear, J.M., "A Probabilistic Approach to Condition Assessment and Life Extension - The Requirement for Materials Parameter Data," EPRI Conf. on Life Extension and Assessment of Fossil Plants, June 2-4, 1986, Washington, DC.

101. Maruyama, K. and Oikawa, H., "A New Predictive Method of Long-Term Creep Curve and Rupture Life," Proceedings of the International Conference on Creep, April 14-18, 1986, Tokyo, pp. 373 - 378.

102. Lonsdale, D. and Flewitt, E.J., "Statistical Considerations for Accelerated Test Program Design to Optimize Data Extrapolation," Materials Science and Engineering, 69, 1985, pp. L15 - L20.

103. Borggreen, K. and Huntley, P., "Some Environmental Effects on Creep Testing and Extrapolation Using Minor Specimens," Proc. of Conf. on High Temperature Alloys for Gas Turbines and Other Applications, Liege, Belgium, 6-9 Oct., 1986, pp. 1295 - 1303.

104. Guttman, V. and Schutze, M., "Interaction of Corrosion and Mechanical Properties," Proc. of Conf. on High Temperature Alloys for Gas Turbines and Other Applications, Liege, Belgium, 6-9 Oct., 1986, pp. 293 - 326.

105. Emerson, R.W. and Hutchinson, W.R., "Welded Joints Between Dissimilar Metals in High Temperature Service," Welding Journal Research Supplement, March 1952, pp. 126s - 141s.

106. Thielsch, H., "Stainless Steel Weld Deposits on Mild and Alloy Steels," Welding Journal Research Supplement, Jan. 1952, pp. 126s - 141s.

107. Scheil, M.A., "Migration of Chromium and Carbon in a Weld in Type 502," Metal Progress, Vol. 64, Sept. 1953, pp. 108 - 110.

108. Christoffel, R.J. and Curran, R.M., "Carbon Migration in Welded Joints at Elevated Temperatures," Welding Journal Research Supplement, Sept. 1956, pp. 157s - 168s.

109. Emerson, R.W., Jackson, R.W. and Dauber, C.A., "Transition Jointa Between Austenitic and Ferritic Steel Piping for High Temperature Steam Service," Welding Journal Research Supplement, Sept. 1962, pp. 385s - 393s.

110. Eckel, J.F., "Diffusion Across Dissimilar Metal Joints," Welding Journal Research Supplement, April 1964, pp. 170s - 178s.

111. Mitchell, M.D., Offer, H.P. and Ring, P.J., "Carbon Migration in Transition Joint Welds," General Electric Report No. GEFR-00398, Sept. 1978.

112. Lundin, C.D., "Dissimilar Metal Welds - Transition Joints Literature Review," Welding Journal Research Supplement, Feb. 1982, pp. 58s - 63s.

113. Lundin, C.D., "Progress/Coordination Report - Gallatin Unit 2 - Hot Reheat Steam Piping," Unpublished Report to TVA-Chattanooga, August 1987.

114. Lundin, C.D., Yang, D. and Khan, K.K., "Carbon Migration in Cr-Mo Weldments - Effect on Metallurgical Structure and Mechanical Properties," Report of Research Conducted under 1987 WRC Grant-in-Aid to University of Tennessee, Knoxville, Jan. 1988.

115. Robinson, V.S., Pense, A.W. and Stout, R.D., "The Creep Rupture Properties of Pressure Vessel Steels," Welding Journal Research Supplement, Dec. 1964, pp. 531s - 540s.

116. deBarbadillo, J.J., Pense, A.W. and Stout, R.D., "The Creep Rupture Properties of Pressure Vessel Steels - Part II," Welding Journal Research Supplement, Aug. 1966, pp. 357s - 367s.

117. Steiner, C.J.P., deBarbadillo, J.J., Pense, A.W. and Stout, R.D., "The Creep Rupture Properties of Pressure Vessel Steels - Part III," Welding Journal Research Supplement, Apr. 1968, pp. 145s - 154s.

118. Rogers, P., Phelps, B. and Murphy, M.C., "The Creep-Rupture Properties of 2 1/4Cr-1Mo Submerged-Arc Weld Metal," Proceedings of the Conference on Welding Creep-Resistant Steels, 17-18 Feb. 1970, The Welding Institute, pp. 136 - 143.

119. Abdel-Latif, A.M., Corbett, J.M. and Taplin, D.M.R., "Analysis of Carbides Formed During Accelerated Aging of 2.25Cr-1Mo Steel," Metal Science, Vol. 16, Feb. 1982, pp. 90 - 96.

120. Swift, R.A. and Rogers, H.C., "Stydy of Creep Embrittlement of 2 1/4Cr-1Mo Steel Weld Metals," Welding Journal Research Supplement, July 1976, pp. 188s - 198s.

VITA

The author was born in Pune, India on July 17, 1960. He attended high school in his hometown, Barrackpore, and graduated from Central School in 1977. He entered the Indian Institute of Technology, Kharagpur for his undergraduate studies. He received B.Tech(Hons.) degree in Metallurgical Engineering in May 1982. After completing undergraduate studies he worked for TELCO a major automobile company in India for four years. It was then the author was inspired to continue his education. Study towards a M.S. degree in Metallurgical Engineering at the University of Tennessee, Knoxville began in September 1986. This M.S. degree was awarded in December 1988. The author is continuing his study at the University of Tennessee to pursue a Ph.D. program in metallurgical Engineering.

The author is a member of the American Welding Society.